

KATHOLIEKE UNIVERSITEIT LEUVEN
FACULTEIT TOEGEPASTE WETENSCHAPPEN
DEPARTEMENT ELECTROTECHNIEK
AFDELING ESAT
Kardinaal Mercierlaan 94 — 3001 Leuven (Heverlee)

Virtual Engineering for Design and Control of Continuously Variable Transmissions

Promotoren :
Prof. Dr. Ir. B. DE MOOR
Prof. Dr. Ir. J. VANDEWALLE

Proefschrift voorgedragen tot
het behalen van het doctoraat
in de toegepaste wetenschappen

door

Paul VANVUCHELEN

6 mei 1997



KATHOLIEKE UNIVERSITEIT LEUVEN
FACULTEIT TOEGEPASTE WETENSCHAPPEN
DEPARTEMENT ELECTROTECHNIEK
AFDELING ESAT
Kardinaal Mercierlaan 94 — 3001 Leuven (Heverlee)

Virtual Engineering for Design and Control of Continuously Variable Transmissions

Jury :
Prof. Dr. Ir. E. Aernoudt, voorzitter
Prof. Dr. Ir. B. De Moor, promotor
Prof. Dr. Ir. J. Vandewalle, promotor
Prof. Dr. Ir. J. De Schutter
Prof. Dr. Ir. R. Belmans
Prof. Dr. Ir. P.P.J. van den Bosch (TU Eindhoven, NL)
Ir. R. Buckinx (VCST-VT), toegevoegd lid

Proefschrift voorgedragen tot
het behalen van het doctoraat
in de toegepaste wetenschappen

door

Paul VANVUCHELEN

UDC : 681.51

6 mei 1997

© Copyright by Katholieke Universiteit Leuven
Zonder voorafgaandelijke toestemming van de auteur en de promotor is overnemen, copiëren, gebruiken of realiseren van deze uitgave of gedeelten ervan verboden.
Voor aanvragen tot of informatie i.v.m. het overnemen en/of gebruik en/of realisatie van gedeelten van dit werk, wendt U tot de K.U.Leuven, Faculteit Toegepaste Wetenschappen, Dept. Elektrotechniek, Onderzoeksgroep SISTA, Kardinaal Mercierlaan 94, 3001 Heverlee-Leuven, België.
Voorafgaandelijke toestemming is eveneens vereist voor het aanwenden van de in dit proefschrift vermelde (originele) methoden, schakelingen en programma's voor industrieel of commercieel nut.

D/1997/7515/09

ISBN 90-5682-074-5

Voorwoord

Aan het einde van dit doctoraat neem ik graag de gelegenheid te baat om iedereen te bedanken voor zijn of haar steun en inspiratie.

In de eerste plaats wil ik mijn promotor Professor Bart de Moor bedanken. Zijn enthousiasme en oprechte verwondering bij het bekijken van de allereerste klep-simulaties op basis van bondgraafmodellen hebben mij de kracht van fysisch modelleren doen beseffen. De lijnrechte tegenstellingen tussen 'zijn' identificatie-modellen en 'mijn' fysische modellen waren dan ook telkens weer een dankbaar onderwerp voor discussie. Uit zijn lessen en seminaries onthoud ik vooral dat de boodschapper grotendeels het effect van een boodschap bepaalt: door zijn uitstraling op het podium werd regeltechniek een feest.

Zijn betogen over de financiële aspecten van onderzoeksprojecten werkten echter even aanstekelijk als zijn lessen regeltechniek: hij toonde mij de weg in het labyrint van de overheidsfinanciering en hij stimuleerde mij bij het aanvragen van verschillende industriële projecten. Op dergelijke momenten droomden wij ook van ondernemerschap en van een eigen bedrijfje, dat de echte vragen van de industrie met de modernste ingenieurstechnieken zou aanpakken. Ongeveer een jaar geleden werd uiteindelijk de spin-off Intelligent Systems Modelling and Control N.V. opgericht, een brug tussen de universiteit en de industrie.

Als mechatronica-student van het eerste uur, op zoek naar een afstudeerwerk met praktische toepassingen, kwam ik na vele omzwervingen terecht bij mijn promotor Professor Joos Vandewalle. Uit één van zijn vele documentatie-kasten kwam een eindwerkvoorstel bij het toenmalige Volvo Car Sint-Truiden tevoorschijn. Na dit eindwerk gaf hij mij de kans om een, naar zijn zeggen, 'horizontaal' doctoraat binnen de groep SISTA aan te vatten. De meerkosten tengevolge van dit 'horizontale' karakter nam hij steeds voor zijn rekening. Van hem kreeg ik bovendien de gelegenheid om mijn horizon te verruimen via buitenlandse cursussen en lesopdrachten.

Professor Joris De Schutter bedank ik voor zijn deelname aan mijn leescomité

en voor het grondig nalezen van deze tekst. In zijn cursus over toegepaste kinematica en dynamica maakte ik kennis met toegepaste fysische modellering.

Professor Ronnie Belmans wil ik bedanken als jury-lid, maar vooral ook voor alle kennis en medewerking die ik van hem en zijn laboratorium-personeel heb mogen ontvangen, bij het bouwen van de testopstelling voor CVTs in de kelders van ESAT.

Professor Paul Van den Bosch wil ik als lid van mijn jury eveneens bedanken voor zijn interesse en voor het in mij gestelde vertrouwen tijdens de begeleiding van één van zijn Erasmus-afstudeerders.

Ingenieur Ronnie Buckinx wil ik als lid van mijn jury, maar ook als projectleider van het huidige IWT-project bedanken voor de steun, medewerking en collegialiteit die ik in al die jaren mocht ervaren. Zijn geloof in 'modelgebaseerd werken' motiveerde mij om dit onderzoeksproject uit te voeren.

Vervolgens wil ik ook een aantal medewerkers van VCST-VT in Sint-Truiden bedanken. Jaak Vandermaesen dank ik voor het in mij gestelde vertrouwen. Als manager toonde hij mij dat persoonlijk contact en communicatie het welslagen van vernieuwingen binnen R&D-afdelingen bepalen. Peter Aberson, Dirk Reniers, Gert-Jan Vogelaar, Stijn Helsen, Peter Vandemoortele en Marc Thijs dank ik voor hun medewerking bij het formuleren van problemen, het zoeken naar informatie en het beoordelen van oplossingen en voor hun hulp bij het begeleiden van mijn 17 eindwerkstudenten.

Mijn ISMC-collega Christiaan Moons dank ik in de eerste plaats voor het realiseren van de proefstand, maar ook voor zijn geduldige uiteenzettingen over hardware en zijn verwoede maar vergeefse pogingen om mij met alle software van ESAT vertrouwd te maken. Mijn ISMC-collega Peter Van Overschee dank ik voor zijn hulp bij het oplossen van numerieke problemen, voor de talrijke discussies over het verschil tussen theorie en praktijk en voor de Latex-hulp bij het tot stand komen van deze tekst. Mijn thesismaatje Wim Minten bedank ik voor de prettige samenwerking tijdens en na ons eindwerk, voor de urenlange babbels over fysisch modelleren en voor de overtuiging en vakkennis waarmee hij mij de geheimen van bondgrafen heeft bijgebracht. Nog steeds laat de bondgraaffilosofie mij toe om een fysisch proces gestructureerd en correct te modelleren. Alle overige collega's van SISTA bedank ik voor de prettige werksfeer en voor de plezierige activiteiten buitenuit.

Mijn CVT-eindwerkstudenten Wim, Joris, Peter, Jan, Gert, Frank, Koen, Jan, Geert, Rudy, Phillipe, Dirk, Patricia, Roel, Anje, Jan en Kris wil ik eveneens bedanken voor hun inzet en enthousiasme bij het ontrafelen van het CVT-kluwen.

Het IWT en VCST zou ik willen bedanken voor het in mij gestelde vertrouwen en voor de bijhorende financiële steun: dankzij twee IWT-projecten in samenwerk-

ing met VCST Sint-Truiden heb ik steeds in optimale omstandigheden kunnen werken.

Mijn vroegere wiskunde-leraar Mathieu Caenen bedank ik omdat hij mij steeds aangemoedigd heeft om de ingenieursstudies aan te vatten. Mijnheer Caenen, wiskunde is inderdaad mooi.

Mijn ouders en broer bedank ik voor het onvoorwaardelijke vertrouwen dat zij steeds in mij gehad hebben, vóór, tijdens en na mijn studies. Bedankt voor de dagelijkse trips naar Leuven tijdens de examens, bedankt voor het geduld en de aanmoedigingen in moeilijke momenten, bedankt voor alles. Ook mijn schoonouders dank ik voor hun steun.

Tenslotte bedank ik mijn echtgenote Ine, voor haar geduld, haar begrip, haar steun en haar aanmoedigingen, maar bovenal voor haar liefde voor mij en onze twee peuters Gilles en Nathalie. Zonder hen zou ik niet zijn wie ik nu ben, niet staan waar ik nu sta. Ik draag deze thesis dan ook op aan mijn gezin.

Paul Vanvuchelen
Kinrooi, Mei 1997

Abstract

This thesis focusses on the *development and application of virtual engineering techniques for design and control of Continuously Variable Transmissions.* The major contributions are the following:

1. Physical modeling techniques are used to obtain generic models of the environment, the car, the drive train, the engine, the various types of couplings, the push-belt variator and the wide variety of valve-bodies.

   The characteristic behavior of each component as well as the interactions between components are described in detail. This leads to highly non-linear, multi-variable system equations, that are useful for both simulation-based analysis and design.
   Analytical linearization is used to derive linearized equations from the physical descriptions. These equations are physically parameterized and are useful for analytical analysis and design.

2. Specific experiments have been defined and conducted, to generate model calibration data. Design-of-experiments-techniques are used to increase the reliability of the experiments and to reduce the number of experiments.

   The generic models are tuned for a wide range of applications. The following applications have been considered:

   - **Cars**: Rover Metro, Rover 216, Rover 416, X, Y, Volvo 440 and Volvo 850. Preliminary work has been done for Korean car manufacturers.
   - **Combustion engines**: Volvo engines (B18U-1800 cc, N2P20-2000 cc) and Rover engines (7 types).
   - **Coupling elements**: a wet multi-plate clutch (P811) and a torque convertor (Daikin YT220).
   - **Push-belt variators**: all important VCST variators (VT-1, VT-2, VT-3) and their application-specific variants.

- **Valve-bodies**: VCSTs hydro-mechanical controlled valve-body (VT1-H) and some of their electro-hydraulical controlled valve-bodies (VT1-E, EVT2, VTF). These valve-body models include the gear pump, the regulator and servo valves, the pulley and clutch pistons and the control system (actuators, sensors and intelligence).

3. The derived models have been used for design and optimization of the valves, the variator and the control system, for a wide variety of car-engine-coupling combinations.

   In this context, effective performance indices, based on customer's specifications and on experimental results are defined. Specific attention is paid to fuel consumption, dynamic car performance (accelerations, speed, hill-climbing), and vertical and longitudinal drive comfort.

4. Model-based controllers were designed, implemented and validated if possible.

   Model-based optimization of the actual digital control algorithms (PID and (non-linear) static feedforward) has been done extensively. To analyse and validate these controllers, a computer-controlled test-rig has been constructed.

   Advanced model-based digital control algorithms are developped also. At this moment, these algorithms are being implemented and validated on the 'upgraded' power test-rig at VCST. Implementation in cars will only be possible when the electronic control unit (ECU) is no longer a cost constraint for series production.

   All derived controllers fully exploit the derived physical models. Feedback linearization theory and linear control theory are combined to design the controllers.

5. The virtual engineering framework has been implemented in Matlab and Simulink, in the tailor-made toolbox VIRTUES (VIRTUal Engineering Software). In this toolbox, the models and the proposed controllers are implemented. Dedicated techniques for model calibration, system analysis and optimizationbased parameter design are implemented also.
   Currently, a graphical user interface and a CAD-database are being added.

Contents

Voorwoord i

Abstract v

Notation xvii

1 Introduction and Motivation 1
- 1.1 Virtual engineering for mechatronic design . . . 2
  - 1.1.1 A special attitude for mechatronics . . . 2
  - 1.1.2 Virtual engineering . . . 3
- 1.2 A glimpse on CVTs . . . 7
  - 1.2.1 Changing gears: an historical overview . . . 7
  - 1.2.2 Functional description of a CVT . . . 11
  - 1.2.3 Virtual engineering of CVTs . . . 20
- 1.3 Overview and contributions . . . 21
  - 1.3.1 Chapter by chapter overview . . . 21
  - 1.3.2 Contributions . . . 23

2 Modeling Vehicle Motion 27
- 2.1 Introduction . . . 28
- 2.2 Resistances to car motion . . . 28
  - 2.2.1 Roll resistance . . . 28
  - 2.2.2 Air drag and lift . . . 30
- 2.3 Disturbances for car motion . . . 30
  - 2.3.1 Wind dynamics . . . 31
  - 2.3.2 Road profile noise . . . 33
- 2.4 Car modeling . . . 36
  - 2.4.1 A car model to describe longitudinal and vertical motion 39
  - 2.4.2 A linearized model for comfort analysis . . . 42
  - 2.4.3 A reduced model for longitudinal motion control . . . 45
- 2.5 Modeling of industrial applications . . . 46

3 Comfort and Performance **47**
3.1 Introduction 47
3.2 Car performance and fuel economy 49
3.2.1 A benchmark test for CVT-equipped cars 49
3.2.2 Dynamic performance 50
3.2.3 Fuel economy 52
3.3 Drive comfort 54
3.3.1 The human sensitivity filters 55
3.3.2 Comfort indices 58
3.3.3 An integrated car-comfort model 59
3.4 A sample of results and conclusions 60

4 Drive Train Modeling and Control **71**
4.1 Description of the drive train 72
4.2 Drive train component models 75
4.2.1 The combustion engine 75
4.2.2 The wet multi-plate clutch 76
4.2.3 The torque converter 80
4.2.4 The gear pump 83
4.2.5 The push-belt variator 86
4.2.6 The pinion gear 87
4.2.7 The drive axle 87
4.3 Drive train modeling 88
4.3.1 A physical model of the drive train 89
4.3.2 A reduced model for clutch control 92
4.3.3 A reduced model for variator control 93
4.4 Drive train control 93
4.4.1 Drive train management via variogram control 94
4.4.2 An algorithm for control in clutch mode 98
4.4.3 An algorithm for control in variator mode 100
4.5 A sample of results and conclusions 101

5 Modeling and Control of the Push Belt Variator **107**
5.1 Introduction 107
5.2 Modeling of the push-belt variator 108
5.2.1 Geometric relations 108
5.2.2 Kinematic relations 110
5.2.3 Static flow and pressure requirements 111
5.2.4 Dynamic flow and pressure requirements 115
5.2.5 Efficiency 125
5.3 Variator control 129
5.3.1 Outer control 130

5.3.2 Inner controllers for pressure and flow steering 131

6 Valves and mechanisms for piston control 139
6.1 Introduction 139
6.2 A configuration for variator control 141
6.2.1 The variator pistons 144
6.2.2 The used transmission oil 145
6.2.3 The gear pump 146
6.3 Typical spool valves for piston control 147
6.3.1 A double stage flow valve for piston control 149
6.3.2 A flow valve with pressure feedback for piston control . . 157
6.4 Control systems 164
6.4.1 Hydro-mechanical control 164
6.4.2 Electro-hydraulic control 166

7 VIRTUES: VIRTUal Engineering Software 169
7.1 Objectives 169
7.2 VIRTUES: Virtual Engineering Software 170
7.2.1 The model descriptions of VIRTUES 171
7.2.2 The VIRTUES database 171
7.2.3 The graphical user interface of VIRTUES 172
7.3 Conclusions 177

8 A Test-Rig for Valve Body Analysis and Control 179
8.1 Introduction 179
8.2 Objectives 180
8.3 Steered inputs and measured outputs 180
8.4 Test-rig lay-out 181
8.4.1 The induction motor 183
8.4.2 The variator 183
8.4.3 The cooling unit 184
8.4.4 The data acquisition and control system 184

9 Conclusions and open problems 187
9.1 Conclusions 187
9.2 Open problems 189

A Parameter tuning using numerical optimization 191
A.1 Practical parameter tuning problems 191
A.2 Mathematical formulation 192
A.3 A practical approach 195
A.4 An illustrative example 196

Bibliography 201

Nederlandse Samenvatting 212

List of Figures

1.1 A typical virtual engineering cycle 5
1.2 The Variomatic from DAF 9
1.3 A modern belt-type Continuously Variable Transmission 16
1.4 The metal push-belt of Hub Van Doorne 17
1.5 Shifting of the CVT 18
1.6 Valve-body of an hydro-mechanically controlled transmission . . 19
1.7 Organization of the thesis 22

2.1 A simple model for roll resistance 29
2.2 Experimental roll resistance coefficients 29
2.3 The air drag coefficient and the air lift coefficient 31
2.4 Experimentally determined wind spectrum 33
2.5 Measured and modeled wind spectra 34
2.6 Experimentally determined road spectrum 35
2.7 Different car models for different purposes 36
2.8 Functional model of the car 37
2.9 Relations between fixed points on the car body 40

3.1 Experimentally determined torque-speed curves (engine B18U) . 49
3.2 Experimentally determined fuel consumption curves (engine B18U) 50
3.3 The desired car speed profile for the Urban cycle 53
3.4 The desired car speed profile for the Highway cycle 53
3.5 The desired car speed profile for the ECE-cycle 54
3.6 The human sensitivity for longitudinal comfort 57
3.7 The human sensitivity for transversal comfort 58
3.8 Influence of the control unit and control strategy for a Rover 216, engine 1.6K16MPI, VT1 variator, wet multi-plate clutch (P811) (simulation) 64
3.9 Influence of the control unit and control strategy for a Rover 216, with engine 1.6K16MPI, VT1 variator, wet multi-plate clutch (P811) (experiment) 65

3.10 Influence of the control unit and control strategy for a Rover 216, with engine 1.6K16MPI, VT1 variator, wet multi-plate clutch (P811) (experiment) 66
3.11 Variator optimization: influence of OD and FD on the consumed fuel at constant car speeds, for a Volvo 850, with engine N2-P20 and a VT1-E variator and a wet multi-plate clutch (P811) (simulation) 67
3.12 Plate clutch versus torque converter for a Rover 216, with engine 1.6K16MPI and a VT1-H variator (simulation) 68
3.13 Plate clutch versus torque converter for a Volvo 850, with engine N2-P20 and a VT1-E variator (simulation) 69

4.1 Functional model of the drive train 72
4.2 A functional model of the drive train 74
4.3 Experimental torque time constant $\tau_e(\dot{\theta}_e)$ 76
4.4 An example of a wet multi-plate clutch 77
4.5 A cross section and a longitudinal section of the wet multi-plate clutch 78
4.6 Experimentally determined clutch friction coefficient μ_{cl} for Esso EZL 799 and Lubrizol oil 78
4.7 A functional model for clutch piston displacement 80
4.8 The experimentally determined force-displacement characteristic of the VT1 clutch plate package 81
4.9 Cross section of a modern torque converter 82
4.10 Experimentally determined torque ratio $M_{tc}(s_{N,tc})$ as a function of speed ratio $s_{N,tc}$, for a Daikin YT220 torque converter 83
4.11 The experimentally determined capacity factor $S_{tc}(s_{N,tc})$ as a function of the speed ratio $s_{N,tc}$, for a Daikin YT220 torque converter 84
4.12 A modern push-belt variator 85
4.13 Functional model of a push-belt variator 86
4.14 The experimentally determined torque-speed characteristic and the optimal operating line for sport mode, for a B18U engine . . 95
4.15 The experimentally determined fuel consumption characteristic and the optimal operating line for economy mode for a B18U engine 96
4.16 An economy variogram for a B18U engine 97
4.17 A scheme for variogram control 97
4.18 Feedback linearization and model reference CVT control 99
4.19 Influence of the control unit and control strategy for a Rover 216, engine 1.6K16MPI, VT1 variator, wet multi-plate clutch (P811) (simulation) 102

4.20 Influence of the control unit and control strategy for a Rover 216, with engine 1.6K16MPI, VT1-H variator, wet multi-plate clutch (P811) (experiment) 103
4.21 Influence of the control unit and control strategy for a Rover 216, with engine 1.6K16MPI, VT1-F variator, wet multi-plate clutch (P811) (experiment) 104
4.22 Plate clutch versus torque converter for a Rover 216, with engine 1.6K16MPI and a VT1-H variator (simulation) 105

5.1 The geometry of a metal V-belt variator 109
5.2 The running radii R_s and R_p as a function of the ratio i_v 110
5.3 The oil flows Q_p and Q_s to obtain a rate of ratio change equal to $\frac{di_v}{dt} = -0.5\text{s}^{-1}$ 111
5.4 Forces on the belt and the pulleys 113
5.5 The experimentally determined force ratio $\frac{K_p}{K_s}$ as a function of the variator ratio i_v, for different primary speeds (VT1-variator), at $T_p = 40$ Nm 114
5.6 The experimentally determined force ratio $\frac{K_p}{K_s}$ as a function of the variator ratio i_v, for different primary torques (VT1-variator), at a primary speed of 2000 rpm 115
5.7 A physical model to describe shifting of the push-belt variator around Medium 117
5.8 Response of a flow steered variator 121
5.9 Response of a pressure steered variator 122
5.10 Response of a pressure-flow steered variator 123
5.11 Matlab/Simulink implementation of the experimental variator shifting model 124
5.12 A static neural network to fit the variator efficiency map 126
5.13 The predicted variator efficiency η_v as a function of the primary torque T_p, for an hydraulical (VT1-H) and an electronical (VT1-E) controlled drive train 127
5.14 Predicted relations between loss torque, variator ratio, secondary pressure and primary speed, for a primary torque of 35 Nm (simulation) 128
5.15 Two stage variator control 129
5.16 A single-piston model to design inner control algorithms 131
5.17 Two configurations to realize a flow into a piston 133
5.18 Feedback linearization and model reference piston control 135
5.19 Performance of an inner loop for pressure control, based on linear control and feedback linearization (VT1-variator, NO-configuration) 136
5.20 Performance of an inner loop for speed control, based on linear control and feedback linearization (VT1-variator, NO-configuration) 137

6.1 A configuration for variator control (pp-configuration, VT1-E) . 142
6.2 A configuration for variator control (pQ-configuration, VT1-H) . 143
6.3 A functional model of a single variator piston 144
6.4 The experimental mass density and kinematic viscosity of Esso EZL 799 146
6.5 A double stage flow valve for piston control 149
6.6 Orifices at the servo pilot and the main pilot of a double stage flow valve 150
6.7 Static characteristics of a double stage flow valve 154
6.8 Dynamic characteristics of a double stage flow valve 155
6.9 Influence of the feedback gain $w_{sv,2}$ on the dynamic characteristics of the double stage flow valve 156
6.10 A flow valve with pressure feedback for piston control 157
6.11 Orifice for a flow valve with pressure feedback 159
6.12 Static characteristics of a flow valve with pressure feedback (experiment versus simulation). 161
6.13 Dynamic characteristics of a flow valve with pressure feedback (experiment versus simulation) 162
6.14 Influence of included air on the dynamic characteristics of a flow valve with pressure feedback (simulation) 163
6.15 Components in a control scheme 164
6.16 Experimentally obtained pitot pressure parabola, for a VT1-H variator 166
6.17 Experimentally obatined servo pressure as a function of applied duty cycle, for a Bosch 3/2 PWM valve 168

7.1 Hierarchical Simulink block scheme of the drive train 174
7.2 Specific component file of a B18U combustion engine 175
7.3 Specific component file of a VT-175 variator 176

8.1 Functional description of the test rig 182
8.2 Photograph of the test-rig (ESAT-SISTA, K.U.Leuven) 183
8.3 Interface of CVT-Log program 186

A.1 A 1DOF configuration with a control law $K(s)$ to be designed . . 196
A.2 Step responses with a PI-controller: the initial design and non-inferior designs for various weights 198
A.3 The trade-off curve for the classical PI-parametrization 199
A.4 Trade-off curves for the classical parametrizations and the modern parametrization 200

List of Tables

2.1 Typical values of the parameters that determine the coefficients C_x and C_z 30
2.2 Disturbances for car motion 32
2.3 Important parameters of the car model and typical values 38

3.1 A design benchmark for a CVT-equipped passenger car 51
3.2 Dynamic performance VT1-H versus VT1-F (Rover 216, engine 1.6K16MPI) 61
3.3 CVT benchmark test (Rover 216, engine 1.6K16MPI, variator VT1-E) 63

4.1 Parameters to describe an ideal clutch 79
4.2 Friction coefficient parameters, for different types of oil (Esso EZL 799 and Lubrizol) and operating conditions 79
4.3 Additional parameters of a non-ideal clutch 80
4.4 Drive train parameters of a Volvo 480, equipped with a VT1-H transmission, Esso EZL 799 oil, 12 mm gear pump, wet multi-plate clutch, variator and pinion 89
4.5 The proposed control strategy for drive train control 98

5.1 Important CVT-parameters (VT1) 109
5.2 Parameters and typical values for the simplified variator model (around Medium) 118
5.3 Piston and load related parameters 132

6.1 Piston and load related parameters 145
6.2 Important oil characteristics 145
6.3 Pump flow parameters (12 mm gear pump) 147
6.4 Double stage flow valve parameters 153
6.5 Pressure feedback flow valve parameters 158

8.1 Measurement range, accuracy and bandwidth of the test-rig sensing equipment 181

A.1 PI-designs on the trade-off boundary 198
A.2 Four different control laws to realize closed-loop performance . . 200
A.3 Designs on the trade-off boundary, for four different control laws 200

Notation

Symbol	Property	Units
F	Force.	(N)
M	Torque.	(Nm)
N	Rotation speed.	$(\frac{rad}{s})$
p	Pressure.	$(Pa,\ bar)$
P	Instantaneous power.	(W)
Q	Volume flow.	$(\frac{m^3}{s})$
s_x	Translational slip speed.	$(\frac{m}{s})$
s_θ	Rotational slip speed.	$(\frac{rad}{s},\ rpm)$
t	Time.	(s)
T	Temperature.	$(^oF,\ ^oC)$
v	Translational speed.	$(\frac{m}{s},\ \frac{km}{h},\ mph)$
x, z	Horizontal, vertical position.	(m)
θ	Angular position.	(rad)
a	Section, orifice.	$(m^2,\ mm^2)$
A	Surface.	(m^2)
b	Translational damping.	$(\frac{N}{m/s})$
c	Torsional stiffness.	$(\frac{Nm}{rad})$
d	Torsional damping.	$(\frac{Nm}{rad/s})$
i	Transmission ratio.	$(-)$
I	Rotation inertia.	(kgm^2)
k	Translational stiffness.	$(\frac{N}{m})$

L	Distance, length.	(m)
m	Mass.	$(kg,\ g)$
r	Radius.	$(m,\ mm)$
R	Running radius.	$(m,\ mm)$
β, γ, δ	Angle.	$(rad,\ degr)$
η	Efficiency.	$(-)$
μ	Friction coefficient.	$(-)$
ρ	Mass density.	$(\frac{kg}{m^3})$
ν	Kinematic viscosity.	$(\frac{m^2}{s})$
τ	Time constant of a linear first order system.	$(s,\ ms)$
ζ	Damping ratio of a linear second order system.	$(-)$
ω_n	Natural frequency of a linear second order system.	$(\frac{rad}{s},\ Hz)$
t_d	Time delay.	$(s,\ ms)$

Symbol	Description
A, B ,C ,D	State space representation of a linear dynamic system.
M, R, K, N	Mass-damper-spring representation of a linear dynamic system.
X, U, Y	States, inputs and outputs of a state space model.
Z, W	States and inputs of a mass-damper-spring model.
σ	Variance of a Gaussian white noise signal.
$n_{\bar{m},\sigma}(t)$	Gaussian white noise signal, mean m, variance σ.
$\triangle L$	Period of harmonic space vectors.
$\triangle T$	Period of harmonic time vectors.
ω	Time-based frequency.
Ω	Space-based frequency.
ξ	Noisy part of a vector.
$P_{\xi(t)}(\omega)$	Time-based spectrum of $\xi(t)$.
$P_{\xi(x)}(\Omega)$	Space-based spectrum of $\xi(x)$.

$\bar{x}(t)$	Mean value of a time signal $x(t)$.
$\dot{x}(t)$	First derivative of time signal $x(t)$.
$\ddot{x}(t)$	Second derivative of time signal $x(t)$.
$\sqrt[\pm]{\lvert x\rvert}$	$\sqrt{\lvert x\rvert}\text{sign}(x)$.

Subscript	Related to
a	Driving axle.
air	Air around the car.
b	Back wheels.
$brake$	Brake.
c	Car body.
cl	Wet multi-plate clutch.
cp	Controlled piston.
cv	Control valve.
dl	Drive-line.
ds	Double stage flow valve.
dyn	Dynamical property.
e	Combustion engine.
f	Front wheels.
FD	Final drive reduction.
gp	Gear pump.
lk	Oil leakage.
oil	Transmission oil.
p	Primary art of the variator.
pc	Internal compensated pressure valve.
r	Road characteristics.
s	Secondary part of the variator.
sf	Safety considerations.
ss	Single stage flow valve.
$stat$	Static property.
tc	Torque converter.

up	Uncompensated pressure valve.
v	Variator.
w	Wind that acts on the car.
x	Longitudinal property.
z	Transversal property.
0	Initial condition.

Abreviation	Description
AT	Automatic Transmission.
CAD	Computer Aided Design.
CVT	Continuously Variable Transmission.
DOE	Design Of Experiments.
DOF	Degrees Of Freedom.
ECU	Electronic Control Unit.
I/O	Input/Output.
LOW	The highest transmission ratio (low).
MT	Manual Transmission.
MEDIUM	A transmission ratio of 1 (medium).
OD	The lowest transmission ratio (overdrive).
PID	Proportional-Integral-Derivative control.
PWM	Pulse Width Modulated.
VCST	Vehicle Components, Systems and Transmissions N.V. (before Volvo Car Sint-Truiden N.V.).
VIRTUES	VIRTUal Engineering Software.
cog	Center Of Gravity.
pp	Pressure-Pressure control of a CVT.
pQ	Pressure-Flow control of a CVT.

Chapter 1

Introduction and Motivation

" Mechatronics is a combination of mature technologies.
It is the clever combination of methodologies, technologies
and application knowledge that brings success,
not basic research."
Jacob Buur from Lyngby Institute for Engineering Design, Denmark
at the first Conference on Mechatronics,
Tampere, Finland, February 1994.

In this Chapter, we summarize our main contributions. In Section 1.1, we discuss different aspects of mechatronics. From this, we show that a virtual engineering framework is natural within mechatronics and that it leads to excellent tools for development of mechatronic products. In Section 1.2, we start with a short overview of the developments in changing gears. We also describe the basic properties of a Continuously Variable Transmission. Notes on the organization of this book and a Chapter by Chapter overview can be found in Section 1.3.

1.1 Virtual engineering for mechatronic design

1.1.1 A special attitude for mechatronics

Mechatronics has become a catch-word, and the fast penetration of this word in Europe and in the USA has indicated a growing awareness of the competitive potential of combining mechanics, electronics and computer sciences.

Although a generally accepted definition of mechatronic products does not exist, one can get an idea of the elements of such a definition by enumerating some typical mechatronic products such as a video recorder, a CD-player, a Xerox copier, a printer, a robot, a CNC-machine or an electronically controlled car. In [Buu 92], Buur gives the following definition of mechatronics:

> *Mechatronics is a technology which combines mechanics with electronics and information technology to form both functional interaction and spatial integration in components, modules, products and systems.*

It points out two important aspects of mechatronics:

- The functional interaction which must occur between different technologies.
- The spatial integration of subsystems in a single physical unit.

This implies that an acceptable mechatronic design integrates and fully exploits components and modules from different technologies. To implement mechatronics in practice, different needs must be fulfilled:

- The need for competitive strategies

  The mechatronics business is a field of fast and constant changes: shifts in technologies, in markets, in buyer's attitudes and in competition. A mechatronics company will only survive if it is constantly on the watch for new developments and if its organization is geared for frequent upheavals in marketing, research and manufacturing.

  Fast product development is one of the key factors to increase manoeuvrability and speed of reaction in the fast moving competitive environment. Of course, the development projects can not be shortened ad libitum. There is a relation between the development time and the achievable innovative change in the product.

- The need for interdisciplinarity

  It is in the nature of mechatronics that design requires wide, interdisciplinary knowledge of several areas of technology, e.g. mechanics, hydraulics, pneumatics, electronics and software. Within a project team, this knowledge may be achieved in two ways. One is to educate all designers with a general knowledge, the other is to put together specialists and to encourage communication and cooperation within the team.

  Without interdisciplinary knowledge, it may be possible to suggest a mechatronic product concept, but it is certainly not possible to realize it or to create a full range of alternative concepts and to evaluate those in a total context in order to choose the best. Interdisciplinary education and intensive communication and cooperation are required both.

- The need for design methodology and tools

  The field of mechatronics design is very young and there is hardly any support from design research for the central task of creating a mechatronic product.

  A key point in mechatronics design methodology research is to develop tools which support the designer in allocating technologies to the functions of the product (=dividing the product into modules), and that allow the designer to translate the functions of the modules into objective specifications.

  A second point is to establish product models in a common 'language', that can deal with mixed concepts. The product models can be used for evaluation of alternatives in a total context. The product models address all important technological issues and application specific knowledge.

  A third point is to develop tools that link dedicated experimental results to the product models, in order to tune the models towards reality.

From this, one might conclude that mechatronics needs indeed a special attitude: it is not simply a question of pooling the design skills of mechanical, electronics and software engineers.

1.1.2 Virtual engineering

The interest in mechatronics arises from the awareness of its competitive potentials. Speed and reliability in product development are important factors when dealing with the constant changes in technology, markets, buyer's attitudes and competitors. When doing product development, two approaches are possible:

- A classical prototyping approach

  A physical prototype of the product is the key element in this approach. In many cases, an earlier version of the product or a competitor's product is used as a starting point. Based on experiments with the prototype, the designers use prior knowledge and experience to iterate towards a new product.

  In this approach, effort and time are mainly used for:

  - Construction and adaptation of the prototype
  - Preparation and execution of experiments
  - Conditioning and maintenance of the prototype
  - Analysis of the obtained data and product iteration

- A model-based approach

  A mathematical model of the product is the key element in this approach. In many cases, a model of an existing product is used as a starting point. Based on simulations with the product model, the designers use dedicated tools to iterate towards a new product.

  In this approach, effort and time are mainly used for:

  - Modeling, calibration and implementation of the model
  - Simulation
  - Product optimization

In the proposed virtual engineering framework, we tried to combine the best of both worlds:

> *Based on physical knowledge and on dedicated experiments, an accurate mathematical description with physical parameters (the model) is constructed. In this way, the real system (the prototype) might be replaced by the virtual system (the mathematical model). Simulations are used instead of real-life experiments, to analyze and to optimize the system. User-specific knowledge is combined with powerful optimization tools to ensure fast iteration.*

In practice, a virtual engineering cycle goes through the following stages (see figure 1.1):

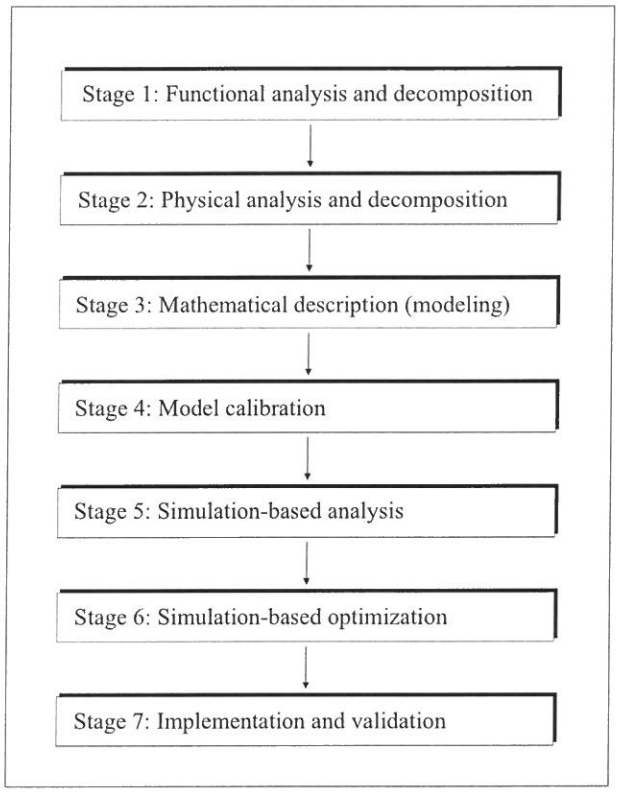

Figure 1.1 *A typical virtual engineering cycle*

1. Functional analysis and decomposition of the product

   In this stage, the operation of the product is analyzed in detail. The product is decomposed into different functional modules. The functionality of each module is implemented by combining different components.

2. Physical analysis and inventarization of each module

   The physical operation of each module is analyzed in detail. For each module, a preliminary list of important physical phenomena and components is created, based on data sheets, technical drawings and experimental results. The physical inputs and outputs of each module are defined also.

3. Mathematical description of the product and its modules

   First, a mathematical description of the product is derived. Basically, the interactions between the different functional modules are described. To

avoid causality problems afterwards, the inputs and outputs as determined in stage 2 must be carefully examined.

Next, a detailed mathematical description of the physical operation of each module is derived. The characteristic equations that describe each phenomenon or component can be found in the literature. The parameter values are determined from technical drawings, data sheets and experimental results. Each module is described by a set of mathematical equations with physical inputs, outputs and parameters.

4. Calibration of the product model

   For each module, preliminary simulations are compared with experimental results. If the simulations are accurate enough, no further calibration is required. If not, additional experiments are done, to complete the list of important phenomena (in the case of a structural error) or to adapt one or more physical parameters (in the case of a parametric error). This is repeated for each module. Once the descriptions of all modules are calibrated, they are integrated into the product model. The product model is now ready for analysis and design.

5. Simulation-based analysis of the product and its modules

   Extensive simulation is used to compute static and dynamic characteristics of each module and of the product itself. Sensitivity analysis and tolerance analysis are done also.

6. Simulation-based optimization of the product and its modules

   Optimization tools are used to iterate on the physical parameters of the modules, to meet user-defined performance specifications. If a set of specifications is given, trade-off surfaces for a given module or for the complete product can be computed. These trade-off surfaces represent the limits-of-performance of the considered module or product.

7. Validation

   The optimized product is constructed and experiments are used to validate the followed approach.

Following this procedure, a wide variety of industrial engineering problems can be solved:

- Analysis and sizing of physical systems (see [BE 91], [WAB 91]).
- Tolerance optimization of physical systems (see [Roel 91], [BS], [Styb 91]).

- Tuning of analog or digital controllers (e.g. [LC 90], [WN 93], [MFMV 91]).

To compare alternative concepts, the approach must be repeated for each concept. Comparison of the trade-off surfaces allows evaluation in a total context, since these surfaces take into account all user-defined performance specifications (see [BB 91], [FP 85], [Grace 89], [Toiv 84], [YA 90], [ZA 73]).

Although not mentioned as specific stages in the cycle, one should notice that the implementation of all physical equations and the development and implementation of application-specific analysis and optimization tools are time-consuming activities that require specific skills, techniques and algorithms (see [FMc 68], [GM 89], [PM 76], [Sim 96], [PMS 84], [ST 90]).

The effort spent on virtual engineering depends on the knowledge that is present in the design team. In practice, an optimal mix of application knowledge and mathematical concepts is required. A so-called 'virtual engineer' definitely needs the following skills:

- Knowledge of the application: product, used technologies, specifications, problems, possible experiments.
- Knowledge of physical modeling concepts and techniques.
- Knowledge of simulation and optimization concepts and techniques.
- Ability to program in dedicated packages like Matlab [Mlab] or Xmath [Xmath 96].

Since the application presented in this book is not widely spread, the next section starts with an historical background. It also explains the basic properties of the application and motivates the use of virtual engineering.

1.2 A glimpse on CVTs

1.2.1 Changing gears: an historical overview

Every car has a transmission. It is the collection of gears, clutches and other devices that connects the engine to the final drive. The modern automatic transmission is so transparent that the driver needs to pay little attention to this very complex piece of machinery. Yet it was not always the case (see [Got 91] for a complete overview).

In the early days, the lack of an acceptably "user friendly" transmission was a major factor in limiting sales and use of the motor car. The development of an easy-to-use transmission was the keystone to make mobility possible for everybody.

While the basic configuration of the engine was decided upon long before 1930, transmission design continued to evolve. The operation and configuration of most automatic transmissions are based on the following four major components which had been developed during a period of some fifteen years (1945-1960):

- The torque converter is a three-element unit consisting of impeller, turbine and stator. The stator is connected to the output shaft and serves to redirect the fluid flow from the driven turbine to the driving impeller for torque multiplication. When torque multiplication is not required, the stator free-wheels with the turbine and the torque converter acts as a fluid coupling (for details, see e.g. [Hur 94]).

- The friction clutch in automatic transmissions is mostly used to engage different elements of the gear train. Only in applications with restricted power, it replaces the torque converter (for details, see e.g. [Bak 92]).

- The planetary gear train is used to accelerate a vehicle with the performance requirements of today's automobiles. The engagement element (torque converter or multi-plate clutch) needs to be augmented by an automatically operated ratio-changing mechanism (usually a gear box) to yield acceptable performance.

- Control units effect the automatic operation of the gear box insuring smooth execution of shifts at appropriate vehicle speeds and loads. All transmissions developed prior to 1975 used hydraulics for both actuation and control. After 1975, many units incorporated some degree of electronic control and used hydraulics for control as well as actuation. The Chrysler A-604, introduced in 1978, was the first electronically controlled transmission in the world using hydraulics exclusively for actuation.

From the '60s through the '70s, the big manufacturers settled on a fairly standard design. Innovations and developments focused largely on cost reduction and shift quality. Only private industry spent time and effort for the development of alternative types of transmissions. In 1955, the Dutch car company DAF began production of a variable cone pulley transmission known as the Variomatic (see figure 1.2). This transmission is the predecessor of modern belt-type Continuously Variable Transmissions.

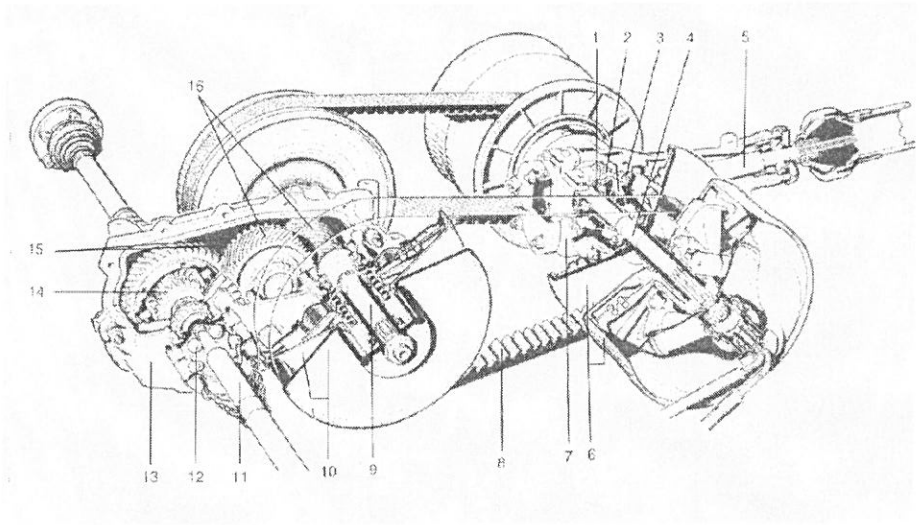

Figure 1.2 *The Variomatic from DAF, one of the fore-runners of the modern belt-type Continuously Variable Transmission. Pinion (3), driving shaft (5), primary pulleys (6), rubber V-belt (8), secondary shaft (9), secondary pulleys (10), driven shaft (11) and final drive reduction (16) can be observed (Source: [MS92]).*

In the '70s, the industry was faced with pressures for increased fuel economy and cleaner air. Transmissions, the basic design of which appeared to be stagnated since the early '60s, became an object of intensive research and development. Three-speed automatics shared the market with four- and five-speed automatics, while CVT transmissions were being developed for use in the '90s. Hydraulics were demoted from control and actuation functions to purely actuation, controlled by electronics.

Specific attention was paid to the contribution from the transmission to overall vehicle fuel consumption. In practice, this contribution is twofold:

- Presence of inherent losses

  The transmission has inherent power and thus fuel consuming features. Some of these losses are due to inefficiencies such as slip in the torque converter or friction in bearings, while other losses are those from parasitic energy consumers such as pumps required for the operation of the transmission.

- Limited ratio range

  The gear ratio affects the speed at which the engine runs. In general, lower engine speeds for the same output power result in higher engine efficiency. The greater the ratio range of the transmission, the greater the potential for reduced engine speeds.

To take this into account, lock-up torque converters were developed to reduce the torque converter losses, intelligent control units were designed to reduce the pump pressures and the ratio range of most transmissions was increased.

> *In the '70s, the role of the transmission changed from that of a slave to the demands made upon the engine, to an integral part of the engine control strategy.*
>
> *Although the current generation of classical automatic transmissions is refined and reconfigured, the industry and the government are well aware that more significant changes are required. CVTs and electronic controls hold promise of even greater fuel economy.*

The advantages of Continuously Variable Transmissions fall into three categories:

- Improved drive-ability and passenger comfort due to the lack of shifting and the corresponding uneven vehicle acceleration.
- Improved vehicle performance and fuel economy, because a CVT allows an engine to run at his most effective point with respect to torque production, power production or fuel consumption, virtually independent of vehicle speed (see [Sun 88], [NSS 90] and [Gie 89]).
- Minimum manufacturing cost for a drive train which will maximize fleet average fuel economy. A CVT is cost-effective due to its ability to optimize the fuel economy of a range of vehicles using the same transmission.

Today, some very novel and unique variable transmission configurations are being evaluated (see figure 1.3). Although the Variomatic, equipped with a rubber belt, has specific advantages over a metal belt (no need for lubrication and a higher coefficient of friction (0.4 opposed to 0.1) which reduces axial forces and thus pump pressures), the restricted durability and the high inherent power losses made it disappear. Advantages of the metal belt over the rubber belt are the power capacity and efficiency, the compactness and the fact that the entire unit runs in lubricant, thus protecting it while ensuring predictable operating conditions.

The most successful metal belt, developed by Huub Van Doorne, is a segmented belt with no connection between the segments, thereby transmitting power by compression (see figure 1.4, for details see [MS 92] and [Roo 91]). In 1987, it was put into production for passenger cars. It was equipped with hydraulic controls for both the wet multi-plate clutch and the variator. Based on this transmission, various manufacturers developed alternative CVTs with hydraulic controls (VT1H (VCST), CTX (Ford),).

The first electronic controls appeared with Subaru's ECVT, which was equipped with an electro-magnetic powder clutch controlled by a micro-processor. Shifting was still performed by hydraulic actuation and controls. In '95, Honda presented the Multimatic, a full electronically controlled CVT that uses hydraulics only for actuation.

Since engine and drive train controls evolve (see e.g. [COYVBJF 84], [DH 95], [FM 92], [GS 95], [LRWK 93], [NSS 90], [Spijk 94]), the potential benefits of the CVT increase when compared to conventional fixed ratio, stepped transmissions. Electronic engine controls will allow variable engine emissions, fuel consumption and output characteristics such as those afforded by variable valve timing and air/fuel ratio control. Engine and transmission controls will become integrated, such that the engine and transmission are treated as a single prime mover system. When this occurs, only a CVT can provide the precise, independent coupling of engine speed and torque output with drive wheel requirements which allow an optimized combination of performance, fuel consumption and emissions.

1.2.2 Functional description of a CVT

Although most material is valid for other CVTs, it is important to notice that the following description is based on the VT-1 transmission developed at VCST-VT in Sint-Truiden (see [Rov 92]).

Basics of CVT operation

The transmission uses a fixed length steel drive belt and two adjustable V-shaped pulleys to transmit the drive power and to vary the gear ratio.

The primary pulley, driven by the engine, is connected by the belt to the secondary pulley which drives the wheels. Both pulleys have one fixed half, and one mobile half which is splined to its shaft and attached to a hydraulic chamber, which controls its position.

The gear ratio is varied by moving the mobile half of the primary pulley towards or away from its fixed half, which increases or reduces the radius that the belt

is forced to follow around the pulley (see figure 1.5).
When the primary pulley mobile half is moved away from its fixed half, the drive belt is allowed to sit 'into' the pulley, providing a small belt diameter on the primary pulley. The secondary halves will be positioned at this stage, forcing the belt to follow a large diameter. This combination will provide a high gear ratio, suitable for pulling away from rest, i.e. high engine speed/low vehicle speed.
To provide a lower gear ratio, suitable for higher speed driving and cruising, i.e. low engine speed/high vehicle speed, the primary pulley mobile half is forced towards its fixed partner, which makes the belt follow a larger diameter on the primary pulley. Because the belt is of fixed length and will not stretch, this movement results in it being pulled into the secondary pulley, forcing its mobile half away from its fixed half, and providing a lower gear ratio.

The transmission control unit automatically and continuously adjusts the position of the primary pulley mobile half, to ensure the most suitable gear ratio is supplied for the prevailing driving conditions. It's this continuous adjustment which provides the smooth step-less change in gear ratio.

Driving a CVT equipped car

Driving a vehicle equipped with a CVT will initially feel strange to those used to a more conventional automatic gear box. Although the vehicle speed and rate of acceleration is as usual, controlled by movement of the throttle pedal, there is no fixed connection between the engine speed and the vehicle speed.

The selector lever has five available positions:

- Park (P) locks the transmission and must only be engaged when the vehicle is stationary with the hand brake applied.
- Reverse (R) provides reverse drive in a high gear ratio and is the only position where the transmission does not vary the gear ratio.
- In Neutral (N), no power is transmitted to the front wheels. It should be used when the vehicle is stationary with the engine running.
- Drive (D) is used for normal driving and provides forward power to the front wheels. When accelerating in D, an immediate increase in engine speed will precede a more gradual increase in vehicle speed. The gear ratio will be automatically and continuously varied in a smooth and step-less manner, always providing a ratio that matches the driving condition.
- Low (L) is also used to drive forward. The gear ratio will again be varied, although ratio up-changes will be delayed until a higher vehicle speed is

achieved. Increased engine braking is also offered in L, making it suitable for towing, hilly or sporty driving conditions.

Maximum vehicle speed can be obtained in D and in L. The vehicle will creep forward when the brakes are released while the engine is idling and either D or L is selected. Creep in the reverse direction will occur when R is selected.

Transmission components

The transmission is composed of a number of components which can be classified into three main sections. The first group consists of all elements which provide mechanical torque flow through the transmission. The elements in the second group are associated with the actuation and control unit, and enable the transmission to transmit torque, control the clutches and vary the gear ratio, to correspond with load conditions and the drivers requirement. The third group consists of components which connect the transmission to other vehicle subsystems.

- Group 1: elements which provide mechanical torque flow through the transmission.
  - Input shaft and epicyclic gear train
    Engine torque enters the transmission via a torsional damper which is bolted to the engine flywheel and splined to the input shaft. The input shaft transmits power to the planet gears. The epicyclic gear train enables the transmission to deliver driving torque to the drive shafts in two directions.
  - Forward and reverse clutches
    Both multi-plate clutches are composed of three double-sided friction plates, each sandwiched by a steel plate. They are designed to provide a smooth take up of drive, and also allow the vehicle to be held stationary while a drive gear is engaged.
  - Torque converter
    A torque converter with lock-up facilities might be added in cases where severe comfort specifications and high initial accelerations are required simultaneously.
  - Pulleys and steel belt
    Two V-shaped pulleys and a steel belt are used to transmit torque and are the heart of the transmission. Each pulley consists of one fixed half and one axially slidable half, both have 11° sloping sides.

The two movable sheaves are each connected to a hydraulic chamber which is used to control its position. These are diagonally opposed to each other in order to reduce misalignment of the belt as the gear ratio changes. Ball splines on each pulley prevent the mobile halves from rotating independently to their fixed partners.

A 24mm wide push-type steel drive belt is used to transfer torque between the two pulleys. It's assembled from more than 300 randomly selected stainless steel segments which vary in thickness to reduce belt operating noise. The flanks of each segment are tapered to match the pulley cone angle. A dimple and hollow feature helps keeping each segment engaged with its two neighboring segments. The belt is further aligned and guided by two bands, each of which is composed of ten steel straps (see figure 1.4).

The belt is tightly gripped by the halves of both pulleys. As driving torque is delivered to the primary pulley, the segments are forced against one another, creating a continuous strut which transmits force to the secondary pulley in compression, rather than in tension. The speed at which the secondary pulley revolves is determined by the gear ratio, i.e. the combined position of the drive belt on the pulleys.

- Pinion gear

  The pinion gear provides a two step reduction between the secondary pulley and the crown wheel. The reduction must be large enough to provide good vehicle performance.

- Differential unit

  Torque delivered to the crown wheel is distributed to the drive shafts via a conventional gear differential.

- Group 2: elements associated with the actuation and control unit.

  - Oil pump

    The oil pump is an external gear pump, driven at engine speed. Pressurized fluid is supplied by the pump, to the hydraulic unit, and is used for actuation of the transmission as well as for lubrication purposes.

  - Valve body and control unit

    Basically, the valve body (see figure 1.6) is used to regulate the pulley positions (gear ratio) and the clutch engagement. It does this using spool valves which respond to a variety of inputs.

    Basically, there are five inputs to the control unit: drive mode, engine speed, primary pulley speed, transmission ratio and throttle position.

These inputs are used by the control unit to regulate four output pressures: secondary pressure, primary pressure and forward and reverse clutch pressure.

Although actuation will always be performed hydraulically, three types of control are possible:

* Hydro-mechanical control: the valve-body and the control unit are integrated in a single component. The control inputs are generated by mechanical (kick-down cable, sensing shoe on the primary pulley, selector lever) and hydraulic (pitot systems) assemblies and are directly fed to the valve-body. This type of control is said to be analog, since no sampling is involved.
* Electro-mechanical control: the valve-body is additionally equipped with electro-mechanical actuators (stepper motors or linear motors) that steer the position of the spool valves. The control unit is an ECU (electronic control unit, consisting of a processor and I/O facilities). All previously defined control inputs are measured by dedicated sensors. Pressure sensors generate additional control inputs and allow to construct inner and outer control loops (master-slave). This type of control is said to be digital, since sampling is done by the ECU.
* Electro-hydraulic control: the valve body is additionally equipped with electro-hydraulic actuators (PWM valves) that steer one of the forces on the spool valves. The control unit is again an ECU. All previously defined control inputs are measured by dedicated sensors. Pressure sensors generate additional control inputs and allow to construct inner and outer control loops (master-slave). This type of control is also digital.

The secondary valve is used to control the secondary piston, while the primary valve is used to control the primary piston. The clutch valve controls the engagement of the clutch.

- Group 3: connections to other vehicle subsystems.
  - Selector mechanism to change between P, R, N, D and L-position.
  - Oil cooling facilities to restrict the oil temperature ($< 120\ ^oC$).

Additional aspects of the CVT will be addressed in detail in specific chapters of this book.

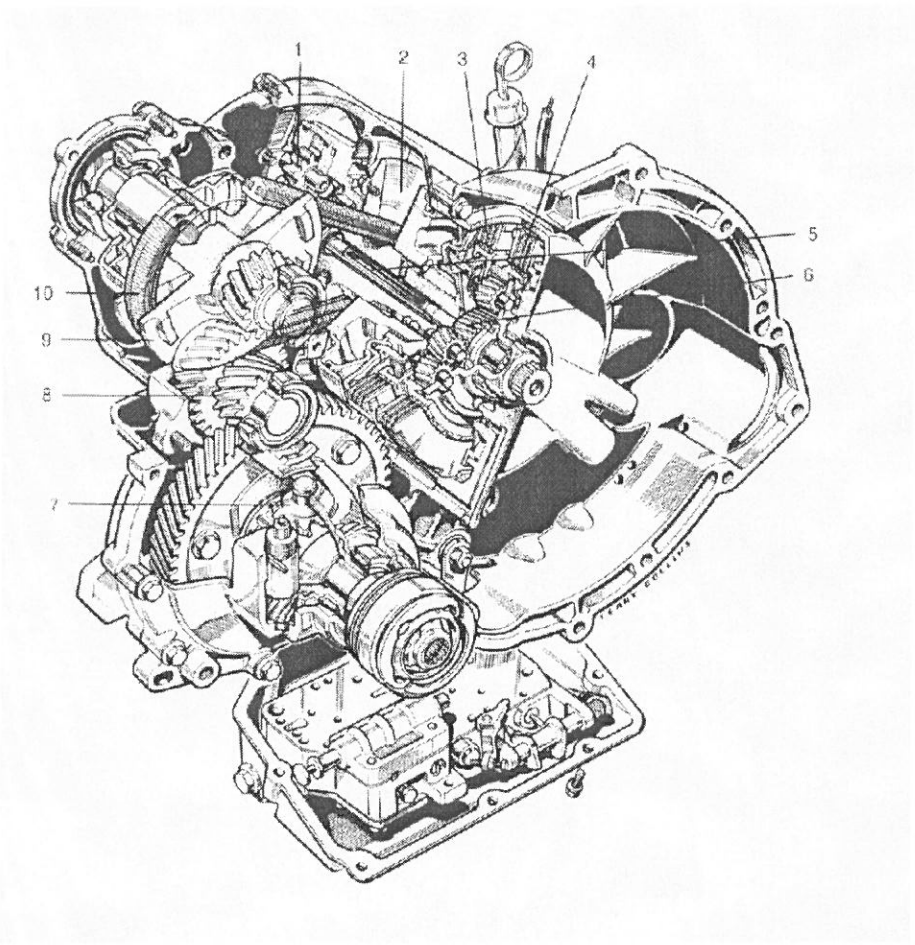

Figure 1.3 *A modern belt-type Continuously Variable Transmission. Different components can be observed: oil pump (1), primary pulleys (2), forward clutch (3), backward clutch (4), pump shaft (5), planetary set (6), differential gears (7), final drive reduction (8), secondary pulleys (9) and metal push-belt (10) (Source: [MS 92]).*

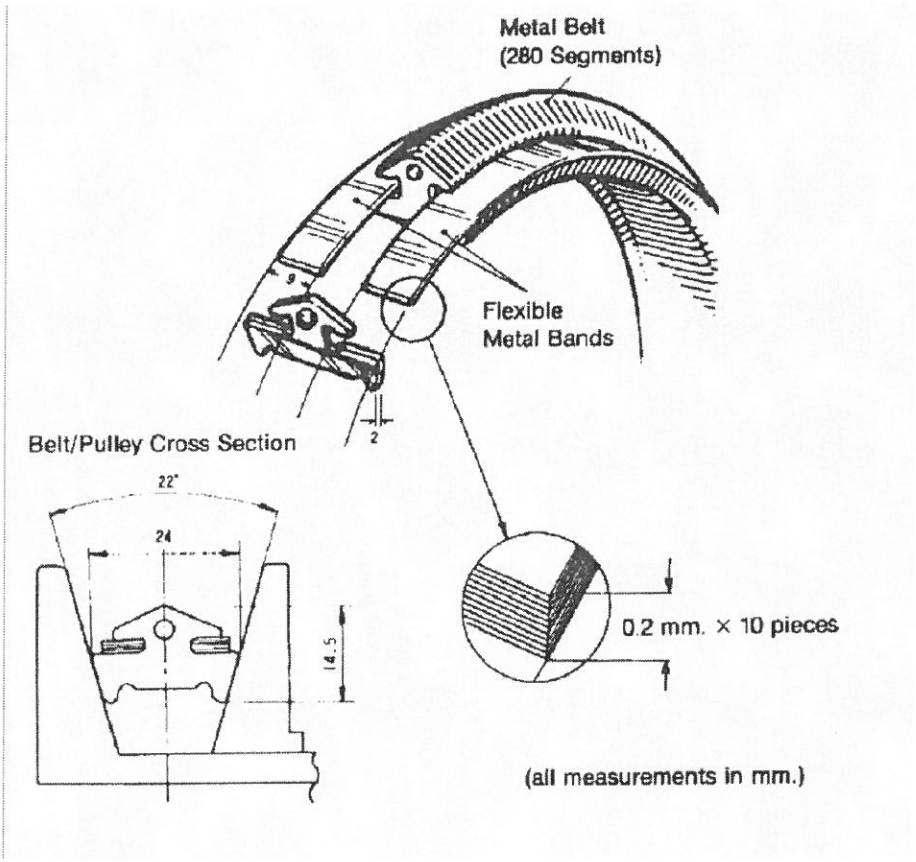

Figure 1.4 *The metal push-belt of Hub Van Doorne. This belt is used in almost all today's push-belt variator (Source: [MS 92]).*

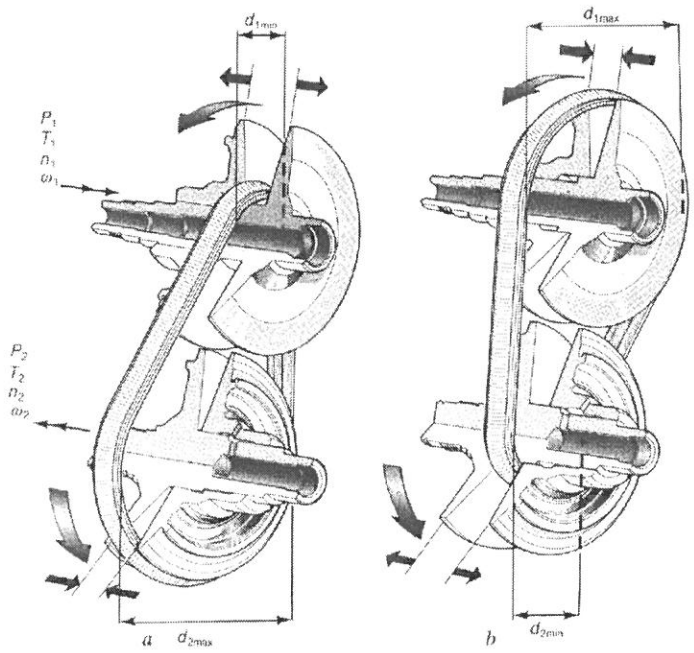

Figure 1.5 *Shifting of the CVT: pulley and belt positions corresponding to maximal ratio (LOW) (a) and a minimal ratio (OD) (b).*

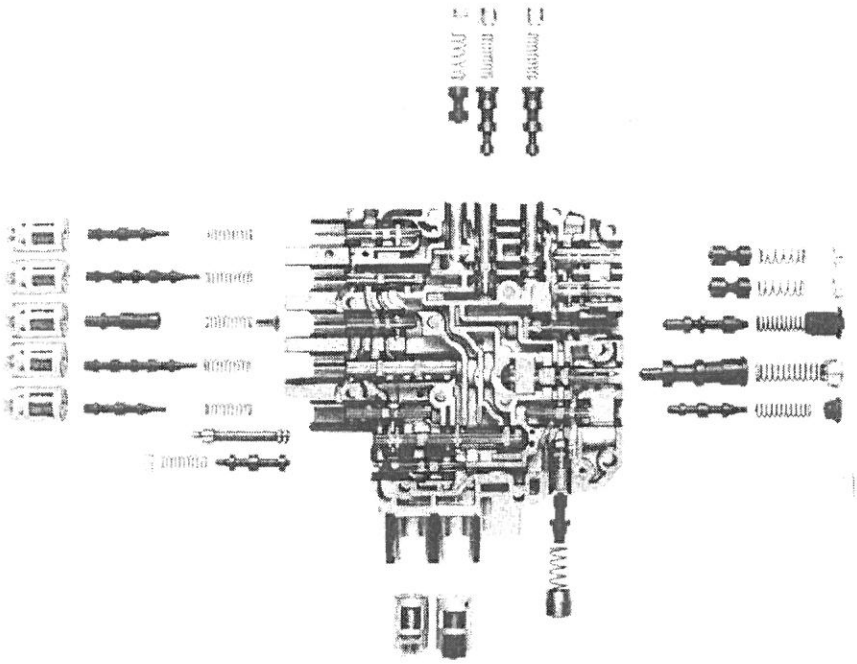

Figure 1.6 *Valve-body of an hydro-mechanically controlled transmission (Source: [MS 92]).*

1.2.3 Virtual engineering of CVTs

In the beginning of the '90s, the increased specifications with respect to performance, comfort and fuel economy forced the CVT designers to look for alternatives: couplings, valves and control mechanisms needed to be (re)designed, electronic control strategies had to be investigated and transmission control became the key element in drive train management.

This change from an hydraulic to a mechatronic system, required fundamental insights in the physical operation of the system. Furthermore, with the introduction of electronic control, additional experience and skills, apart from hydraulic engineering were required to make these new products.

Managers as well as engineers were aware that the classical prototyping approach was no longer a time- and cost effective way to compare alternatives and to generate high quality products. An urgent need for physical models and computer-aided analysis and design techniques was expressed.

In effect, the virtual engineering approach advocates the efficient evaluation of a large number of candidate designs under an effective control of the designer. It makes extensive use of computation and physical models.

The five key areas where further innovation and development is required for more effective, extensive and successful application of the approach are summarized here (see [Ng 93]):

- Effective parameterizations are required, to ensure that the true system lies in the model set.
- Effective performance indices are required and must be derived from clients specifications.
- Efficient analysis and design methods are required, to allow the evaluation of multiple alternatives and to reduce development times (see [Pha 89], [PMS 84],[BB 91]).
- Human-computer interface facilities are required, to allow the designer to control the process and to present the information in a clear and attractive way (see [FWKT 89], [PSWN 85],[Roel 91]).
- Database facilities are required, to allow the user to work with models of various complexity, with experimental results and with engineering design data.

1.3 Overview and contributions

1.3.1 Chapter by chapter overview

When confronted with a sizeable amount of research material and results, there are different ways of organizing it:

- A first possible organization is to present the theory behind modeling, optimization and control. The advantage of this organization is that theorems, definitions and proofs can be presented as research results. In this case, the application (the CVT) serves as a showcase, that fits in a general mathematical frame. The disadvantage however is that the reader might think he found the ultimate solution to all his engineering problems, because no application-oriented knowledge seems to be required.
- In the second application-oriented organization the reader is slowly introduced to the application and has the time to assimilate it. The advantage of this organization is that the reader understands all aspects of the application and of the virtual engineering approach, and that he sees the consequences of the approach with respect to required time, effort and skills. The disadvantage however is that no neat mathematical proofs can be given. However, we think the advantage of increased understanding of both the application and the approach is a good reason to select the second organization

The Chapters of this thesis are organized as follows (see figure 1.7):

- Chapter 1: Introduction and motivation

  contains an introduction and motivation for mechatronic product design. It is shown that a virtual engineering approach is required to obtain quality products in a cost and time effective way. Next, the origin and the operation of the Continuously Variable Transmission are described, and its potentials with respect to performance, comfort and fuel economy are shown. Finally, the important issues for development of a virtual engineering framework are discussed.
- Chapter 2: A system's approach to vehicle motion

  starts with a description of the physical interactions between the car and the environment. Experimental results from different car manufacturers are compared. Next, a physical car model for longitudinal and transversal motion is derived (9 DOF). For analysis of comfort, this model is linearized

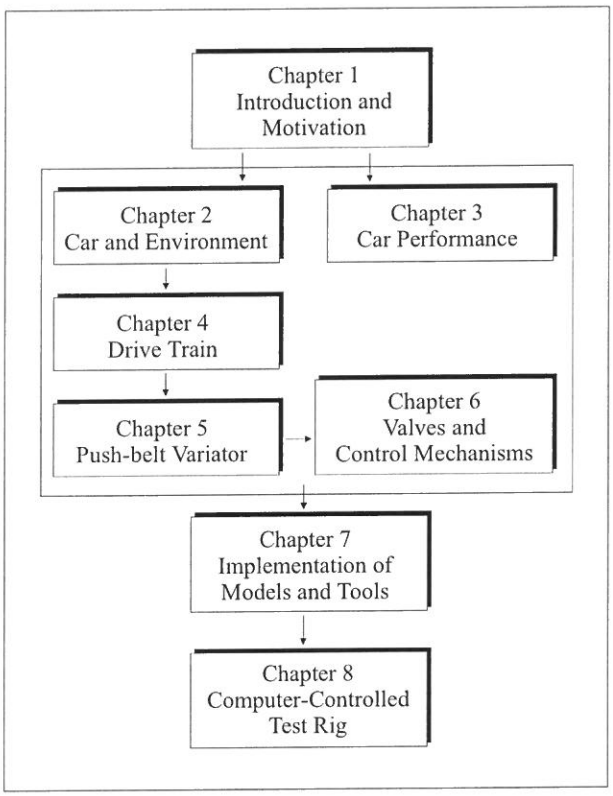

Figure 1.7 *Organization of the thesis.*

using singular perturbation techniques. For longitudinal motion control, the car model is only reduced (1 DOF), but not linearized.

- Chapter 3: Performance, fuel economy and comfort

  treats the different specifications that are imposed on today's cars. Based on specifications from various car manufacturers, a CVT challenge is defined. Special attention is given to acceleration, efficiency and comfort.

- Chapter 4: Drive train modeling and control

  treats the physical interactions between the drive train components. Based on idealized components, a model of the drive train is constructed. Reduced models for coupling mode and variator mode are derived for control purposes. Based on these models, a drive train control algorithm based on feedback linearization is obtained.

- Chapter 5: Modeling and control of the push-belt variator

  starts with the derivation of a reduced variator model, to compare the two basic control alternatives (pressure-pressure versus pressure-flow control). Next, the non-ideal characteristics of the variator are considered. Geometrical and kinematic properties and flow and pressure requirements are combined to analyze how hydraulics and mechanics interact, and to model the non-ideal variator. The efficiency of the variator is discussed also, and is used to point out the advantages of electronic control for drive train management. Finally, we present two strategies to realize shifting while avoiding belt slip, and we derive the required outer and inner controllers.

- Chapter 6: Hydraulic valves and mechanisms for piston control

  treats the modeling, analysis and optimization of typical hydraulic valves and mechanisms that are used in CVT control. First, two typical valves are discussed in detail: a double-stage flow valve and a pressure valve with hydraulic feedback. Next, the different control mechanisms for hydraulic piston control are treated: hydro-mechanical control, electro-mechanical control and electro-hydraulic control.

- Chapter 7: Implementation of models and techniques

  treats the implementation of all developed models and techniques. First, the philosophy behind the software is explained, next the software itself is discussed in detail.

- Chapter 8: A test rig for CVT valve bodies

  treats the computer-controlled test-rig for analysis and validation of valve-bodies and control mechanisms. First, the philosophy behind the test-rig is explained, next the used hardware and software are discussed in detail.

1.3.2 Contributions

Since this book is the result of an intensive cooperation between the author and at least 25 other people, either engineers from VCST or colleagues and graduate students from different faculties and universities, it is important to point out that this thesis is a result of joint research. Although initiated in the author's master's thesis (see [VD *et al* 96]), most of the work has been done within two research projects, sponsored by the IWT and VCST:

- IWT-project 92/064, *A development system for electronically controlled Continuously Variable Transmissions.* Leuven/Sint-Truiden, 1992-1994.

- IWT-project 95/0117, *Feasibility analysis and implementation of a framework for design and control of Continuously Variable Transmissions.* Leuven/Sint-Truiden, 1995-1997.

Within this context, the author had the opportunity to guide 17 master students. This work resulted in 12 master's theses (referred to as [VD *et al* 96]). Multiple details that are omitted in this book are carefully derived and explained in the theses.

Other experiments and results on modeling, design and control are described in detail in [MVD 93], [VDM 93], [VDRV 93], [VMD 94], [EVV 95], [VMMD 95], [MVMD 95], [MMVD 95], [MV 96], [Van 96a], [Van 96b], [Van 96c], [Van 96d], [Van 96e], [VVo 96a], [VVo 96b], [VVo 96c], [VVo 96d], [Van 97], [VV 96a], [VV 96b], [VV 96c], [VV 96d] and [VVM 96].

The contributions to design and control of CVTs are the following[1]:

1. Physical modeling techniques are used to obtain generic models of the environment, the car, the drive train, the engine, the various types of couplings, the push-belt variator and the wide variety of valve-bodies (see [MVD 93], [VDRV 93], [MMVD 95], [VMMD 95], [MV 96], [VD *et al* 96]).

   The characteristic behavior of each component as well as the interactions between components are described in detail. This leads to highly non-linear, multi-variable system equations, that are useful for both simulation-based analysis and design.
   Based on singular perturbation techniques, linearized equations are derived from the physical descriptions. These equations are physically parameterized and are useful for analytical analysis and design.

   The bond graph technique was very useful when dealing with specific modeling problems (stick-slip, causality, input and output assignment (see [VD *et al* 96])).

2. Specific experiments have been defined and conducted, to generate model calibration data (see [Van 96c], [Van 96d], [Van 96e], [VV 96a], [VV 96b], [VV 96c], [VV 96d] and [VVM 96]). Design-of-experiments-techniques are used to increase the reliability of the experiments and to reduce the number of experiments.

   The generic models are tuned for a wide range of applications. The applications that have been considered are (see [Van 96a]):

[1] The major contributions of this thesis are situated at the level of the coordination of the research project and its researchers, the organization of the sizeable amount of information and results in a single book and the development of a general engineering approach towards model-based design and control of CVTs.

- **Cars**: Rover Metro, Rover 216, Rover 416, X, Y, Volvo 440 and Volvo 850. Preliminary work has been done for Korean car manufacturers.
- **Combustion engines**: Volvo engines (B18U-1800 cc, N2-P20-2000 cc) and Rover engines (7 types).
- **Coupling elements**: a wet multi-plate clutch (P811) and a torque convertor (Daikin YT220).
- **Push-belt variators**: all important VCST variators (VT-175, VT-200, VT-3) and their application-specific variants.
- **Valve-bodies**: VCSTs hydro-mechanical controlled valve-body (VT1-H) and some of their electro-hydraulical controlled valve-bodies (VT1-E, EVT2, VTF). Valve-body models include the gear pump, the regulator and servo valves, the pulley and clutch pistons and the control system (actuators, sensors and intelligence).

3. The derived models have been used for design and optimization of the valves, the variator and the control system, for a wide variety of car-engine-coupling combinations (see [VVo 96a], [VVo 96b], [VVo 96c], [VVo 96d], [VD *et al* 96] for examples).

   In this context, effective performance indices, based on customer's specifications and on experimental results are defined. Specific attention is paid to fuel consumption, dynamic car performance (accelerations, speed, hill-climbing), and vertical and longitudinal drive comfort (see [Van 96b]).

4. Model-based controllers were designed, implemented and validated (if possible).

   Model-based optimization of the actual digital control algorithms (PID and (non-linear) static feedforward) has been done extensively (VT1E, EVT2, VT1F).
   To analyse and validate these controllers, a computer-controlled test-rig has been constructed (see [VMD 94], [MVMD 95], [VD *et al* 96]). Some results on fuzzy control of the valve-body for EVT2 were obtained also, (see [EVV 95]), to analyse the advantages and disadvantages of fuzzy control over gain-scheduled PID-control.

   Advanced model-based digital control algorithms are developped also. At this moment, these algorithms are being implemented and validated on the 'upgraded' power test-rig at VCST. Implementation in cars will only be possible when the electronic control unit (ECU) is no longer a cost constraint for series production.

   All derived controllers fully exploit the derived physical models. Feedback linearization theory and linear control theory are combined to design the controllers.

5. The virtual engineering framework has been implemented in Matlab and Simulink, in a tailor-made toolbox VIRTUES (VIRTUal Engineering Software) (see [Van 96a]). In this toolbox, the models and the proposed controllers are implemented. Dedicated techniques for model calibration, system analysis and optimization-based parameter design are implemented also.
   Currently, a graphical user interface and a CAD-database are being added (see [Van 97]).

It should be noticed that the project has been executed in cooperation with an industrial partner. For reasons of confidentiality, not all results are shown explicitly. For the same reason, parameters and simulation results are sometimes scaled or omitted. However, this book contains all information, required to explain the developped approach[2].

[2]This constraint may be unacceptable for the pure scientist, whose scientific beliefs may be shocked by such a non-disclosure agreement and who may argue that the essential requirements of scientific research - namely full experimental details to guarantee complete reproducibility by independent third parties - are not respected. This scientist may contact the author or VCST for additional information.

Chapter 2

Modeling Vehicle Motion

In this Chapter, we analyze the car and its physical interaction with the environment in detail. In Section 2.2, we describe the major resistances for car motion. First, the roll resistance of a car is discussed. Experimental results show that the roll characteristics mainly depend on car speed, and little on car design. Next, we analyze the effect of the surrounding air. At high car speeds, the air resistance becomes important for longitudinal motion. Lift effects due to air drag are of less importance. Wind tunnel experiments show that the distance between the car bottom and the road and the frontal surface of the car are key elements to reduce the effect of air drag and air lift. In Section 2.3, we model the stochastic disturbances that act on the car. Based on measured wind spectra, the wind dynamics are modeled by a simple linear system. To model the noise in the road profile, we use available road spectra. At constant car speeds, we proof that road profile noise may be produced by an integrator, driven by Gaussian white noise. In Section 2.4, we finally model the car. Since CVT-equipped cars are shifting continuously, both transversal and longitudinal accelerations are important for comfort and must be included in a single model. For comfort evaluation, we linearize this model using singular perturbations. For longitudinal motion control, the original model is physically reduced, but not linearized. These generic models (known equations, parameters depend on the application) are tuned (fully or partially) for 7 different industrial applications (Rover, Volvo, MG, Renault, Daewoo, Daihatsu and Hyundai).

2.1 Introduction

When dealing with car modeling (and system modeling in general), a wide variety of methods is described in the literature. The selected method mainly depends on the properties of the system under consideration and on the objectives and preferences of the modeller.

Although parameter estimation techniques are succesfully applied in car and drive train modelling (see [Lju 87], [SM 93], [MD 93]), we prefer to use physical modeling techniques to model the car and its interactions (see [Mit 84], [KL 93], [Fun 95], [Granda 90], [Granda 91], [Rau 92]).

This allows us to create generic models, with physical parameters that depend on the application. The model parameters can be obtained from car manufacturer's data-sheets and from rather familiar experiments that every car manufacturer is willing and able to do.

In a context of tuning transmission characteristics towards car and engine characteristics, it is advantageous that only data-sheets and a few experiments are required to tune the car model for a new application.

2.2 Resistances to car motion

Driving a car at a constant speed requires energy. Although part of this energy is consumed by the drive train components (friction in bearings, pump losses, slip in a coupling, transmission losses), most of the energy is required to overcome roll resistance, air resistance and gravity forces.

2.2.1 Roll resistance

Roll resistance is caused by the dissimilarity in tire deformation (see [Mit 84], [KL 93], [Dub 90] and the references therein), as shown in figure 2.1. At a constant longitudinal car speed v_c and a wheel rotation speed N, the relation between the roll resistance force F_x and the vertical force F_z is given by:

$$F_x = -f_r F_z \tag{2.1}$$

The force F_x is assumed to apply as a force on the wheel, delivering a negative torque $F_x r$ to the wheels. The roll resistance coefficient f_r mainly depends

on the tire characteristics. It remains constant at low car speeds, but changes drastically when car speed increases. Curves from the literature (see [KL 93]) and own experimental results are shown in figure 2.2.

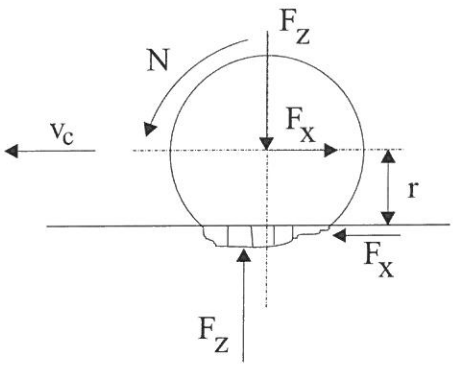

Figure 2.1 *Roll resistance: forces on a non-driven wheel, at a constant car speed v_c and a wheel rotation speed N.*

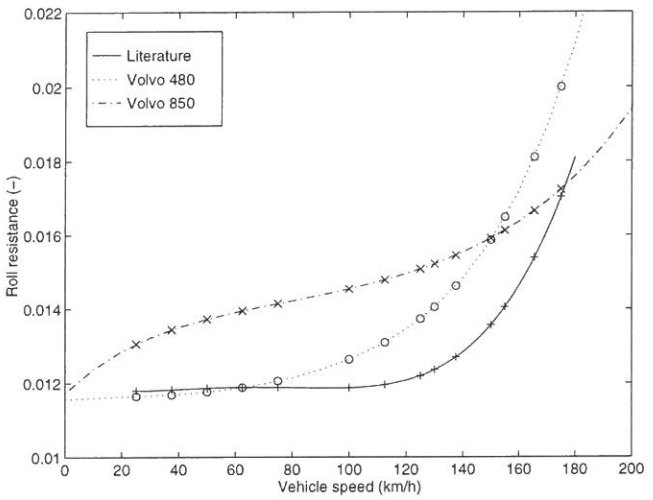

Figure 2.2 *Experimental roll resistance coefficients f_r, as a function of car speed v_c, for different cars (Source: VCST).*

2.2.2 Air drag and lift

In practice, especially at higher car speeds, air resistance forces become even more important than roll resistance forces (see [Mit 84], [KL 93]). At a constant car speed v_c and a wind speed v_w (assume the same reference direction), the horizontal and vertical forces due to car motion and air flow are given by:

$$W_x = \frac{f_x A_c \rho_{air}}{2}(v_c + v_w)^2 = C_x(v_c + v_w)^2 \quad (2.2)$$

$$W_z = \frac{f_z A_c \rho_{air}}{2}(v_c + v_w)^2 = C_z(v_c + v_w)^2 \quad (2.3)$$

These forces are assumed to apply on the center of gravity of the car. The air drag coefficient f_x and the lift coefficient f_z depend on the free height e_c between the road and the car bottom (see figure 2.3 for some characteristics from [KL 93]). Experiments in wind tunnels are required to obtain these characteristics. Typical values of all the parameters that effect air resistance forces are given in table 2.1.

Parameters	Meaning	Value	Units
f_x	Air drag coefficient	0.35	-
f_z	Air lift coefficient	0.5	-
A_c	Frontal surface of the car	1.9	m^2
ρ_{air}	Density of air	1.23	kg/m^3

Table 2.1 *Typical values of the parameters that determine the coefficients C_x and C_z (car speed v_c in km/h).*

2.3 Disturbances for car motion

Longitudinal and transversal accelerations of a car body are the result of the interplay between the driver (via throttle and brake pedal), the road (via the road profile, obstacles and slopes) and the environment (wind, tunnels). Some of these accelerations are explicitly desired by the driver, while others are considered to be disturbing. The influence of the steering wheel is neglected, since only motions in the XZ-plane are considered in this thesis. Table 2.2 shows the different disturbances for car motion.

In the next subsections, the road noise and the wind dynamics (which are stochastic disturbances) will be described in detail. Experimental data from

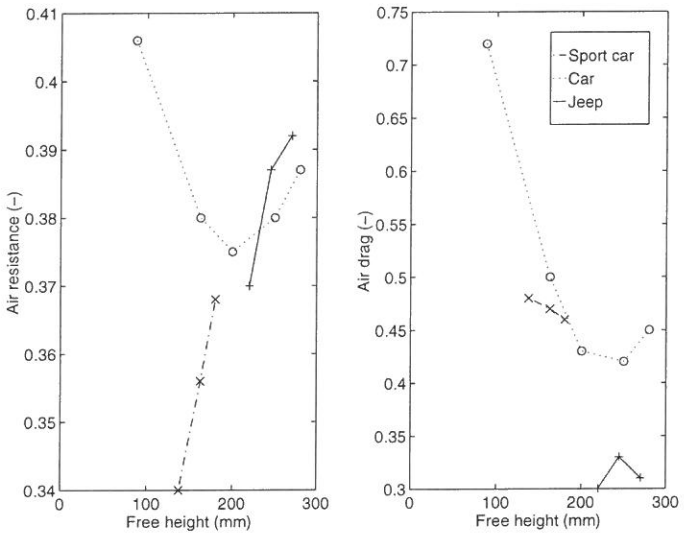

Figure 2.3 *The air drag coefficient f_x and the air lift coefficient f_z as a function of the free height e_c between the road and the car bottom, for three types of cars. A low drag and high lift coefficient guarantee highest dynamic performance (Source: [KL 93]).*

the literature (see [Dub 90], [Mit 84], [DDVDB 91]) will be used to model these disturbances by white noise driven linear dynamic systems.

2.3.1 Wind dynamics

The frequency contents of the wind can be determined experimentally (see [DDVDB 91], [Dub 90]). Figure 2.4 shows the spectrum of the wind, for nominal wind speeds and for extreme wind speeds[1].

It can be seen from this figure that there are high frequency components present, probably due to turbulence in the air. The gap between the high frequency contents (over 10 cycles/hour) and the low frequency contents (below 0.1 cycles/hour) is quite wide. The amplitude of the high frequency contents depends on the mean wind speed $\bar{v}_w$. For car applications, only the high frequency contents are important. In that case, the wind can be modeled approximately by:

[1] Due to the stochastic character of the wind, both in time and in place, reproduction of these characteristics is hard and time-consuming. Therefore, we used available experimental data.

Source		Applies on	Type of disturbance
Car			
	Drive train	Car	Deterministic
	Unbalance	Car, suspension	Deterministic
Road			
	Obstacles	Suspension	Deterministic
	Wave profile	Suspension	Deterministic
	Noise	Suspension	Stochastic
Environment			
	Wind dynamics	Car	Stochastic
	Tunnels	Car	Deterministic

Table 2.2 *Disturbances for car motion.*

$$v_w = \bar{v}_w + \xi_w(t) \tag{2.4}$$

with the noisy part of the wind $\xi_w(t)$ generated by a linear dynamic system, driven by a Gaussian white noise signal $n_w(t) = n_{0,\bar{v}_w}(t)$:

$$\dot{\mathrm{X}}_w = \mathrm{A}_w\mathrm{X}_w + \mathrm{B}_w n_w \tag{2.5}$$

$$\xi_w = \mathrm{C}_w\mathrm{X}_w + \mathrm{D}_w n_w \tag{2.6}$$

The matrices A_w, B_w, C_w and D_w can easily be computed from the experimental results, using a continuous-time frequency domain identification technique (see [VDM 96]). Figure 2.5 compares the modeled and the measured spectra of the wind.

$$\mathrm{A}_w = \begin{pmatrix} -0.6729 & -0.051 & -0.0021 \\ 1 & 0 & 0 \\ 0 & 1 & 0 \end{pmatrix}$$

$$\mathrm{B}_w = \begin{pmatrix} 1 \\ 0 \\ 0 \end{pmatrix}$$

$$\mathrm{C}_w = \begin{pmatrix} 2.0219 & 0.1894 & 0.0032 \end{pmatrix}$$

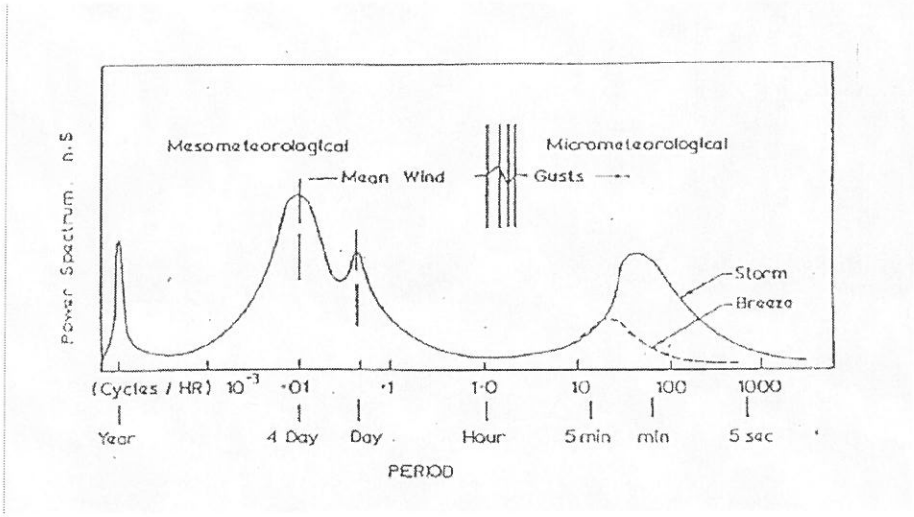

Figure 2.4 *Experimentally determined spectrum of the wind (Source: [DDVDB 91]).*

$$D_w = 0.0402$$

2.3.2 Road profile noise

For different types of road materials, the spectrum of the road profile $\xi_r(x)$ can be determined experimentally[2] (see [Dub 90], [Mit 84]).

Define the spatial frequency Ω as:

$$\Omega = \frac{2\pi}{\triangle L} \text{ (rad/m)} \tag{2.7}$$

with $\triangle L$ being the road period. From figure 2.6, it follows that for the frequency range $10^{-3} \leq \Omega \leq 1$ (rad/cm), the road spectrum $P_{\xi_r(x)}(\Omega)$ can be described by:

[2]Due to the stochastic character of the road, reproduction of these characteristics is hard and time-consuming. Therefore, we used available experimental data.

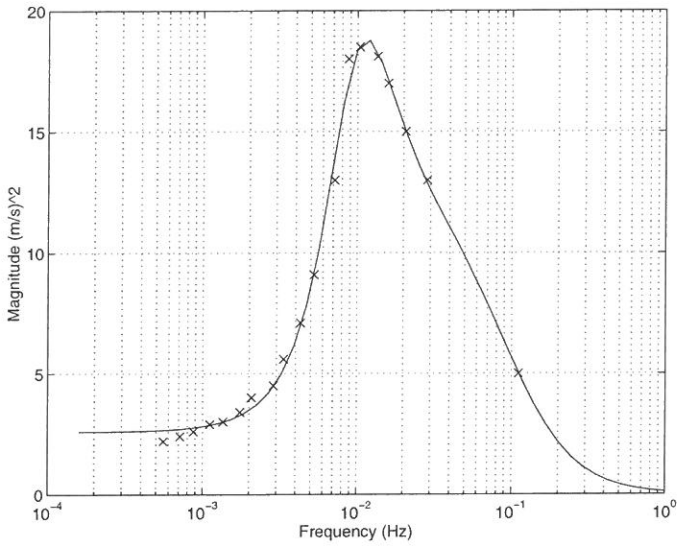

Figure 2.5 *Measured and modeled wind spectra.*

$$P_{\xi_r(x)}(\Omega) = P_0 \left(\frac{\Omega_0^2}{\Omega^2} \right) \tag{2.8}$$

In order to describe the road noise as a time sequence rather than as spatial sequence, the space-based spectrum needs to be used to compute the corresponding time-based spectrum. The relation between the spatial frequency $\Omega = \frac{2\pi}{\triangle L}$ (rad/m) and the time frequency $\omega = \frac{2\pi}{\triangle T}$ (rad/s) is found from the definition of car speed:

$$v_c = \frac{dx}{dt} = \frac{\triangle L}{\triangle T} \tag{2.9}$$

At a constant car speed v_c, it holds that:

$$\omega = v_c \Omega$$

From Parceval's theorem, it follows that:

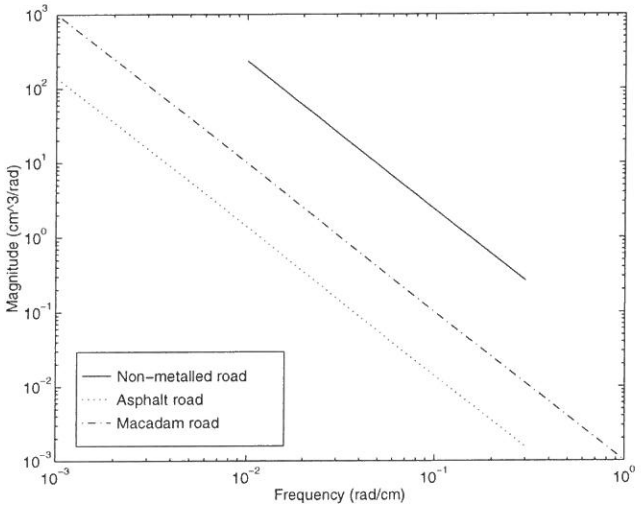

Figure 2.6 *Experimentally determined road spectrum* $P_{\xi_r(x)}(\Omega)$ *(Source: [Dub 90]).*

$$P_{\xi_r(t)}(\omega) = P_{\xi_r(x)}(\Omega)\frac{d\Omega}{d\omega}$$

The spectrum $P_{\xi_r(t)}(\omega)$ is then easily computed as:

$$P_{\xi_r(t)}(\omega) = P_0\frac{\Omega_0^2}{\omega^2}v_c \tag{2.10}$$

This corresponds to the spectrum of the output signal of a single integrator, driven by Gaussian white noise $n_r(t)$ (zero mean, $\sigma_r^2 = P_0\Omega_0^2 v_c$).

In state space representation, this corresponds to:

$$\dot{\mathrm{X}}_r = \mathrm{A}_r\mathrm{X}_r + \mathrm{B}_r n_r \tag{2.11}$$
$$\xi_r = \mathrm{C}_r\mathrm{X}_r + \mathrm{D}_r n_r \tag{2.12}$$

with

$$A_r = 0,\ B_r = 1,\ C_r = 1,\ D_r = 0$$

In practice, the disturbance $\xi_{r,f}(t)$ at the front wheels is also applied at the back wheels, but with a time delay $t_d = \frac{L_b+L_f}{v_c}$ (proportional to the wheel distance $L_b + L_f$). This implies that:

$$\xi_{r,b}(t) = \xi_{r,f}(t - t_d) \tag{2.13}$$

2.4 Car modeling

Since CVT-equipped cars are shifting continuously, both transversal and longitudinal accelerations are important for comfort (see [Ket 91]) and must be computed using one integrated car model. For comfort evaluation, this model is linearized around an operating point. For longitudinal motion control, the car model is physically reduced, but not linearized. An overview is given in figure 2.7.

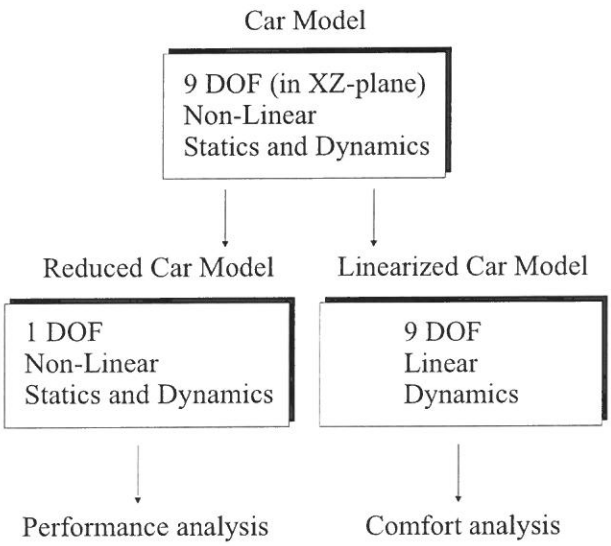

Figure 2.7 *Different car models for different purposes.*

Figure 2.8 shows the functional car model under consideration. The front wheels as well as the back wheels are reduced to equivalent single wheels, to reduce the

model complexity. Transversal (Z) and longitudinal (X) translation and rotation in the XZ-plane are considered only. Translations of the car body, the front wheel drive and suspension and the back wheel drive and suspension are considered. Rotations of the car body, the front and the back wheels are considered also[3]. The considered system has 9 degrees of freedom (9 DOF).

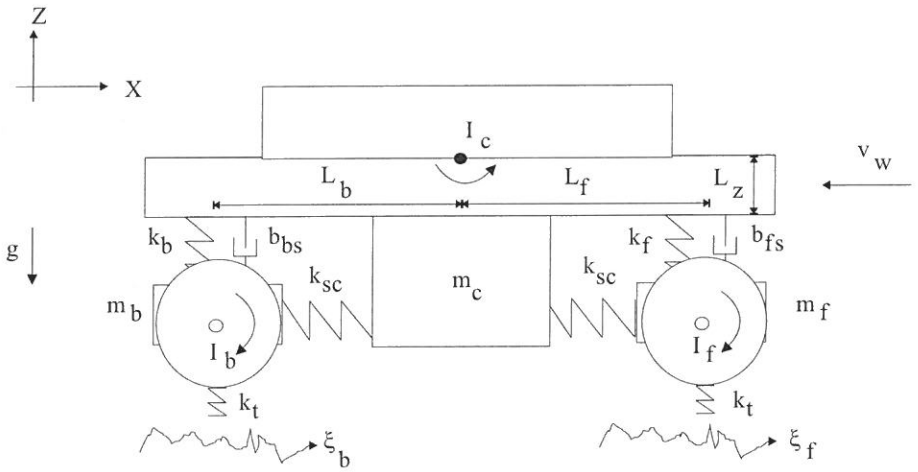

Figure 2.8 *Functional model of the car. Only motion in the XZ-plane is considered.*

Before deriving the equations that describe the car movement, an overview of all important phenomena is given (for details, see [KL 93], [Mit 84], [Granda 90]). All important parameters and their typical values are listed in table 2.3.

- The car body is modeled as a mass for translation and as an inertia for rotation.
- The stiffness and viscous damping of each suspension is modeled.
- The wheels and axles are modeled as masses for translation and as inertias for rotation. The stiffness of the tires is assumed to be linear. The damping for wheel slip is assumed to be proportional to the relative slip at each wheel. By assuming this, the complex tyre-road interaction can be described easily (see [KL 93], [Pac 76]).
- The horizontal stiffness of the connection between the wheels and the car

[3]The X-axis is assumed to remain parallel to the mean road slope. Only car body rotations relative to this slope are considered.

body is taken into account. In practice, this connection is almost infinitely stiff.

- The driving torque M_{fw} is applied at the front wheels (all CVT equipped cars use front wheel drive).

- The air resistance (air resistance W_x, air drag W_z, and assume a wind speed $v_w = \bar{v}_w + \xi_w$), the roll resistance and the road slope (assume a slope angle θ_r) generate load forces. The road noise ξ_r is taken into account also.

	Meaning	Value	Units
m_b	Mass of back wheels and axle	50	kg
m_f	Mass of front wheels and axle	70	kg
m_c	Mass of car body and passengers	1450	kg
I_b	Inertia of back wheels and axle	1.6	kgm^2
I_f	Inertia of front wheels and axle	1.6	kgm^2
I_c	Inertia of car body with passengers	1500	kgm^2
k_b	Stiffness of back suspension	27000	N/m
k_f	Stiffness of front suspension	30000	N/m
k_t	Stiffness of tires	250000	N/m
k_{sc}	Hor. stiffness of wheel-to-body connection	800000	N/m
b_{bs}	Viscous damping of back suspension	2820	Ns/m
b_{fs}	Viscous damping of front suspension	3230	Ns/m
L_b	Hor. distance between back suspension and cog	1.3	m
L_f	Hor. distance between front suspension and cog	1.1	m
L_z	Vert. distance between suspension connection and cog	0.1	m
r	Dynamic radius of the wheels	0.3	m
C_x	Roll coefficient	0.5	Ns^2/m^2
C_z	Lift coefficient	0.5	Ns^2/m^2
b_{bw}	Slip coefficient at back wheels	128000	N
b_{fw}	Slip coefficient at front wheels	128000	N
g	Nominal gravity constant on earth	9.81	m/s^2
f_r	Nominal roll resistance	0.012	-

Table 2.3 *Important parameters of the car model and typical values.*

2.4.1 A car model to describe longitudinal and vertical motion

From the torque and force balances of the car body, the following equations can be obtained:

$$\begin{aligned} I_c\ddot{\theta}_c &= M_{fw} + k_{sc}(x_f - x_2)c_3 - k_{sc}(x_1 - x_b)c_1 + k_f(z_f - z_2)c_4 + \\ &\quad b_{fs}(\dot{z}_f - \dot{z}_2)c_4 - k_b(z_b - z_1)c_2 - b_{bs}(\dot{z}_b - \dot{z}_1)c_2 \qquad (2.14) \\ m_c\ddot{x}_c &= k_{sc}(x_f - x_2) - k_{sc}(x_1 - x_b) - W_x - m_c g\sin\theta_r \qquad (2.15) \\ m_c\ddot{z}_c &= k_b(z_b - z_1) + b_{bs}(\dot{z}_b - \dot{z}_1) + k_f(z_f - z_2) \\ &\quad + b_{fs}(\dot{z}_f - \dot{z}_2) - m_c g\cos\theta_r + W_z \qquad (2.16) \end{aligned}$$

Expressions for the coefficients (c_1, c_2, c_3, c_4) and for the coordinates (x_1, z_1) and (x_2, z_2) are computed further in this section. From the torque balance on the back wheels and axle, and the force balances of the back wheels and suspension, the following equations are obtained:

$$\begin{aligned} I_b\ddot{\theta}_b &= -F_{bw}r - k_t(\xi_b - z_b)f_r r \qquad (2.17) \\ m_b\ddot{x}_b &= F_{bw} + k_{sc}(x_1 - x_b) - m_b g\sin\theta_r \qquad (2.18) \\ m_b\ddot{z}_b &= k_t(\xi_b - z_b) - k_b(z_b - z_1) - b_{bs}(\dot{z}_b - \dot{z}_1) - m_b g\cos\theta_r \qquad (2.19) \end{aligned}$$

From the torque balance on the front wheels and axle, and the force balances of the front wheels and suspension, the following equations are obtained:

$$\begin{aligned} I_f\ddot{\theta}_f &= -F_{fw}r - k_t(\xi_f - z_f)f_r r + M_{fw} \qquad (2.20) \\ m_f\ddot{x}_f &= F_{fw} - k_{sc}(x_f - x_2) - m_f g\sin\theta_r \qquad (2.21) \\ m_f\ddot{z}_f &= k_t(\xi_f - z_f) - k_f(z_f - z_2) - b_{fs}(\dot{z}_f - \dot{z}_2) - m_f g\cos\theta_r \qquad (2.22) \end{aligned}$$

The tire-road interaction at the front and the back wheels is modeled by a damping for wheel slip. To describe this effect more accurate, complex models are available in the literature (see [Pac 76], [KL 93]). In this book, damping is assumed to be proportional to the relative slip at each wheel:

$$F_{bw} = b_{bw}\frac{r\dot{\theta}_b - \dot{x}_b}{\dot{x}_b} \qquad (2.23)$$

$$F_{fw} = b_{fw}\frac{r\dot{\theta}_f - \dot{x}_f}{\dot{x}_f} \tag{2.24}$$

The wind forces W_x and W_z are given by:

$$W_x = C_x(\dot{x}_c + v_w)^2 \tag{2.25}$$
$$W_z = C_z(\dot{x}_c + v_w)^2 \tag{2.26}$$

The absolute coordinates (x_1, z_1) and (x_2, z_2), corresponding to fixed points on the car body (i.e. the points where the suspension forces apply) are related to the car body coordinates (x_c, z_c, θ_c) by geometrical relations (see figure 2.9). The coefficients (c_1, c_2, c_3, c_4) can easily be obtained.

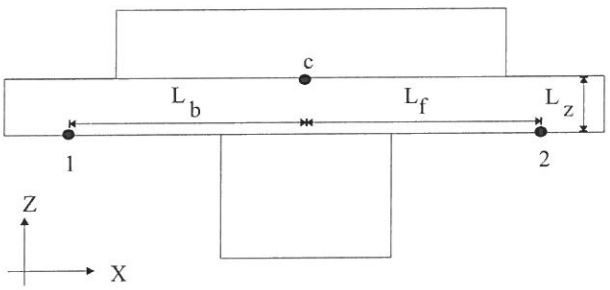

Figure 2.9 *Relations between fixed points on the car body.*

The absolute coordinates (x_1, z_1) and (x_2, z_2), corresponding to fixed points on the car body, are given by:

$$\begin{aligned} x_1 &= x_c - L_1\cos(\alpha_1 + \theta_c) \\ z_1 &= z_c - L_1\sin(\alpha_1 + \theta_c) \\ x_2 &= x_c + L_2\cos(\alpha_2 - \theta_c) \\ z_2 &= z_c - L_2\sin(\alpha_2 - \theta_c) \end{aligned}$$

with L_1, L_2, α_1 and α_2 given by:

$$L_1 = \sqrt{L_z^2 + L_b^2}$$

$$
\begin{aligned}
L_2 &= \sqrt{L_z^2 + L_f^2} \\
\alpha_1 &= \arctan \frac{L_z}{L_b} \\
\alpha_2 &= \arctan \frac{L_z}{L_f}
\end{aligned}
$$

The finite differences, required for model linearization, can easily be computed:

$$
\begin{aligned}
dx_1 &= dx_c + (L_z \cos\theta_c + L_b \sin\theta_c) d\theta_c \\
dz_1 &= dz_c + (L_z \sin\theta_c - L_b \cos\theta_c) d\theta_c \\
dx_2 &= dx_c + (L_z \cos\theta_c - L_f \sin\theta_c) d\theta_c \\
dz_2 &= dz_c + (L_z \sin\theta_c + L_f \cos\theta_c) d\theta_c
\end{aligned}
$$

The coefficients c_1, c_2, c_3 and c_4 are obtained from geometry also:

$$
\begin{aligned}
c_1 &= L_z \cos\theta_c + L_b \sin\theta_c \\
c_2 &= -L_z \sin\theta_c + L_b \cos\theta_c \\
c_3 &= L_z \cos\theta_c - L_f \sin\theta_c \\
c_4 &= L_z \sin\theta_c + L_f \cos\theta_c
\end{aligned}
$$

For $\theta_c \approx 0$, the finite difference equations reduce to:

$$
\begin{aligned}
dx_1 &= dx_c + L_z d\theta_c && (2.27) \\
dz_1 &= dz_c - L_b d\theta_c && (2.28) \\
dx_2 &= dx_c + L_z d\theta_c && (2.29) \\
dz_2 &= dz_c + L_f d\theta_c && (2.30)
\end{aligned}
$$

and the coefficients are given by:

$$
\begin{aligned}
c_1 &= L_z && (2.31) \\
c_2 &= L_b && (2.32) \\
c_3 &= L_z && (2.33) \\
c_4 &= L_f && (2.34)
\end{aligned}
$$

2.4.2 A linearized model for comfort analysis

To analyze the influence of deterministic inputs (basically changes in the applied torque M_{fw}) on transversal and longitudinal comfort, the full non-linear model is used to perform time-domain simulations. However, to analyze the influence of stochastic disturbances (road profile and wind dynamics) on transversal and longitudinal comfort, a linearized model is required to generate the frequency response characteristics (see [Mit 84], [KL 93]).

At a nominal longitudinal car speed v_c and a mean wind speed $\bar{v}_w$, linearization around an operating point Y_0 of the earlier derived non-linear equations and recombination of the terms finally results in the following description:

$$\mathrm{M}_c\ddot{\mathrm{Y}} + \mathrm{R}_c\dot{\mathrm{Y}} + \mathrm{K}_c\mathrm{Y} = \mathrm{N}_c\mathrm{W} \tag{2.35}$$

with the vector Y and the input vector W defined as:

$$\mathrm{Y} = \begin{pmatrix} \triangle\theta_c & \triangle x_c & \triangle z_c & \triangle\theta_b & \triangle x_b & \triangle z_b & \triangle\theta_f & \triangle x_f & \triangle z_f \end{pmatrix}'$$

$$\mathrm{W} = \begin{pmatrix} \xi_b & \xi_f & \xi_w & \triangle\theta_r & \triangle M_{fw} \end{pmatrix}'$$

The operating point Y_0 is computed from the nominal working conditions and the non-linear model, and is given by:

$$\mathrm{Y}_0 = \begin{pmatrix} \theta_{c,0} & x_{c,0} & z_{c,0} & \theta_{b,0} & x_{b,0} & z_{b,0} & \theta_{f,0} & x_{f,0} & z_{f,0} \end{pmatrix}'$$

The matrices M_c, R_c, K_c and N_c are given on the next page:

$$\mathrm{M}_c = \begin{pmatrix} I_c & 0 & 0 & 0 & 0 & 0 & 0 & 0 & 0 \\ 0 & m_c & 0 & 0 & 0 & 0 & 0 & 0 & 0 \\ 0 & 0 & m_c & 0 & 0 & 0 & 0 & 0 & 0 \\ 0 & 0 & 0 & I_b & 0 & 0 & 0 & 0 & 0 \\ 0 & 0 & 0 & 0 & m_b & 0 & 0 & 0 & 0 \\ 0 & 0 & 0 & 0 & 0 & m_b & 0 & 0 & 0 \\ 0 & 0 & 0 & 0 & 0 & 0 & I_f & 0 & 0 \\ 0 & 0 & 0 & 0 & 0 & 0 & 0 & m_f & 0 \\ 0 & 0 & 0 & 0 & 0 & 0 & 0 & 0 & m_f \end{pmatrix}$$

$$
\mathrm{R}_c = \begin{pmatrix}
b_{bs}L_b^2 + b_{fs}L_f^2 & 0 & -b_{bs}L_b + b_{fs}L_f & 0 & 0 \\
0 & 2C_x(v_c + \bar{v}_w) & 0 & 0 & 0 \\
-b_{bs}L_b + b_{fs}L_f & -2C_z(v_c + \bar{v}_w) & b_{bs} + b_{fs} & 0 & 0 \\
0 & 0 & 0 & \frac{r^2 b_{bw}}{v_c} & -\frac{r b_{bw}}{v_c} \\
0 & 0 & 0 & -\frac{r b_{bw}}{v_c} & \frac{b_{bw}}{v_c} \\
b_{bs}L_b & 0 & -b_{bs} & 0 & 0 \\
0 & 0 & 0 & 0 & 0 \\
0 & 0 & 0 & 0 & 0 \\
-b_{fs}L_f & 0 & -b_{fs} & 0 & 0
\end{pmatrix} \cdots
$$

$$
\cdots \begin{pmatrix}
b_{bs}L_b & 0 & 0 & -b_{fs}L_f \\
0 & 0 & 0 & 0 \\
-b_{bs} & 0 & 0 & -b_{fs} \\
0 & 0 & 0 & 0 \\
0 & 0 & 0 & 0 \\
b_{bs} & 0 & 0 & 0 \\
0 & \frac{r^2 b_{fw}}{v_c} & -\frac{r b_{fw}}{v_c} & 0 \\
0 & -\frac{r b_{fw}}{v_c} & \frac{b_{fw}}{v_c} & 0 \\
0 & 0 & 0 & b_{fs}
\end{pmatrix}
$$

$$
\mathrm{K}_c = \begin{pmatrix}
k_b L_b^2 + k_f L_f^2 + 2k_{sc} L_z^2 & 2k_{sc}L_z & -k_b L_b + k_f L_f & 0 & -k_{sc}L_z \\
2k_{sc}L_z & 2k_{sc} & 0 & 0 & -k_{sc} \\
k_f L_f - k_b L_b & 0 & k_b + k_f & 0 & 0 \\
0 & 0 & 0 & 0 & 0 \\
-k_{sc}L_z & -k_{sc} & 0 & 0 & k_{sc} \\
k_b L_b & 0 & -k_b & 0 & 0 \\
0 & 0 & 0 & 0 & 0 \\
-k_{sc}L_z & -k_{sc} & 0 & 0 & 0 \\
-k_f L_f & 0 & -k_f & 0 & 0
\end{pmatrix} \cdots
$$

$$
\cdots \begin{pmatrix}
k_b L_b & 0 & -k_{sc}L_z & -k_f L_f \\
0 & 0 & -k_{sc} & 0 \\
-k_b & 0 & 0 & -k_f \\
-k_t f_r r & 0 & 0 & 0 \\
0 & 0 & 0 & 0 \\
k_b + k_t & 0 & 0 & 0 \\
0 & 0 & 0 & -k_t f_r r \\
0 & 0 & k_{sc} & 0 \\
0 & 0 & 0 & k_f + k_t
\end{pmatrix}
$$

$$\mathrm{N}_c = \begin{pmatrix} 0 & 0 & 0 & 0 & 1 \\ 0 & 0 & -2C_x(v_c + \bar{v}_w) & -m_c g & 0 \\ 0 & 0 & 2C_z(v_c + \bar{v}_w) & 0 & 0 \\ -k_t f_r r & 0 & 0 & 0 & 0 \\ 0 & 0 & 0 & -m_b g & 0 \\ k_t & 0 & 0 & 0 & 0 \\ 0 & -k_t f_r r & 0 & 0 & 1 \\ 0 & 0 & 0 & -m_f g & 0 \\ 0 & k_t & 0 & 0 & 0 \end{pmatrix}$$

To analyze the vertical and longitudinal comfort of the car, accelerations, being states of the model, need to be computed. This is easily done by taking the time derivative of the matrix differential equation 2.35. Define the state vector X_c as:

$$\mathrm{X}_c = \begin{pmatrix} \dot{\mathrm{Y}} \\ \ddot{\mathrm{Y}} \end{pmatrix}$$

and the input vector U_c as:

$$\mathrm{U}_c = \dot{\mathrm{W}}$$

The state space representation of the system is now given by:

$$\dot{\mathrm{X}}_c = \mathrm{A}_c\mathrm{X}_c + \mathrm{B}_c\mathrm{U}_c \tag{2.36}$$

with the matrices A_c and B_c given by:

$$\mathrm{A}_c = \begin{pmatrix} 0 & I \\ -\mathrm{M}_c^{-1}\mathrm{K}_c & -\mathrm{M}_c^{-1}\mathrm{R}_c \end{pmatrix}$$

$$\mathrm{B}_c = \begin{pmatrix} 0 \\ \mathrm{M}_c^{-1}\mathrm{N}_c \end{pmatrix}$$

Note that the time derivatives of the road profiles $\xi_{r,b}(t)$ and $\xi_{r,f}(t)$ become time shifted white noise sequences.

2.4.3 A reduced model for longitudinal motion control

For drive train control, the earlier derived non-linear 9 DOF model is far too complex. For longitudinal motion control, only longitudinal motion of the car needs to be described (see [NSS 90], [Spijk 94], [GS 95], [LRWK 93]).

Assume a stiff connection between the wheels and the car body ($\ddot{x}_c = \ddot{x}_b = \ddot{x}_f$) and no transversal motion ($\ddot{z}_c = \ddot{z}_b = \ddot{z}_f = 0$). Define the total mass $m_{tot} = m_c + m_b + m_f$. By summing the force equations 2.15, 2.18, 2.21, and 2.16, 2.19, 2.22, the following equations are obtained:

$$\begin{aligned} m_{tot}\ddot{x}_c &= F_{bw} + F_{fw} - W_x - m_{tot}g\sin\theta_r & (2.37)\\ 0 &= k_t(\xi_b - z_b) + k_t(\xi_f - z_f) + W_z - m_{tot}g\cos\theta_r & (2.38) \end{aligned}$$

After summing equations 2.17 and 2.20, and assuming equal wheel speeds ($\dot{\theta}_b = \dot{\theta}_f$), it follows that:

$$(I_c + I_b)\ddot{\theta}_f = -(F_{bw} + F_{fw})r - k_t(\xi_b - z_b)f_r r - k_t(\xi_f - z_f)f_r r + M_{fw} \quad (2.39)$$

Assuming no wheel slip ($r\dot{\theta}_f = \dot{x}_f$), the equations 2.37, 2.38 and 2.39 can be combined in a single equation (1 DOF):

$$I_{tot}\ddot{\theta}_f = M_{fw} - r(W_x - f_r W_z) - m_{tot}gr(\sin\theta_r + f_r\cos\theta_r) \quad (2.40)$$

with I_{tot} the total inertia for rotation $I_{tot} = I_b + I_f + m_{tot}r^2$. If no wind is assumed ($W_x = C_x\dot{x}_c^2, W_z = C_z\dot{z}_c^2$), the final equation becomes:

$$I_{tot}\ddot{\theta}_f = M_{fw} - R_{tot}\dot{\theta}_f^2 - T_{ext} \quad (2.41)$$

with:

$$\begin{aligned} T_{ext} &= m_{tot}gr(\sin\theta_r + f_r\cos\theta_r) & (2.42)\\ R_{tot} &= r^3(C_x - f_r C_z) & (2.43) \end{aligned}$$

2.5 Modeling of industrial applications

Based on manufacturer's data, the parameters given in table 2.3 are determined for a wide range of applications (Rover Metro, Rover 216, Rover 416, MGF, Renault Clio, MGF, Volvo 480, Volvo 850). Although sizes, masses and tyres change over the different applications, all simulations in this book are done with the parameters of table 2.3 for confidentiality reasons.

In Chapter 4, these models will be used for simulation of car motion and for longitudinal motion control. Notice that only vibrations below 25 Hz can be studied with this model. For higher frequencies, the deformation of the coach-work comes into play and a finite element model is required (see [KL 93], [Mit 84]).

Chapter 3

Comfort and Performance

In this Chapter, we treat the different specifications that are imposed on today's passenger cars. In Section 3.2, the specifications for performance and fuel economy are discussed. Based on specifications of various car manufacturers (Rover, Volvo and Chrysler) and on our experiences, a CVT benchmark test is defined. Next, it is shown how all defined indices can be computed from simulation results. In Section 3.3, we discuss a possible approach to deal with car comfort. Since comfort is related to accelerations, caused by stochastic or deterministic disturbances, it is intuitively right to use acceleration signals for comfort evaluation. From experimental results of human's sensitivity for longitudinal and transversal accelerations, two human sensitivity models are constructed. Section 3.4 shows a sample of results and conclusions.

3.1 Introduction

Performance, fuel economy and comfort of a CVT-equipped car depend on the characteristics of the following components (see [COYVBJF 84], [FM 92], [Gie 89], [Ket 91], [Rek 90], [Roo 91] and [Spijk 94]):

- The combustion engine

  For CVT equipped cars, integrated engine-transmission control allows to optimize to either performance, fuel economy or comfort. In practice, an acceptable trade-off is chosen. Two engine characteristics are of major importance (see [CA 94], [Hey 88]):

  - The *torque-speed characteristic* $T_e(N_e, \alpha_{th})$ relates the delivered static engine torque T_e to the engine rotation speed N_e and the throttle position α_{th} (see figure 3.1)
  - The *fuel consumption characteristic* $\Phi_e(T_e, N_e)$ relates the consumed fuel Φ_e to the delivered engine torque T_e and the engine rotation speed N_e (see figure 3.2).

- The coupling device

  Two possible alternatives will be discussed:

  - The *wet multi-plate clutch* has small inherent power losses, but requires an accurate control system to avoid comfort losses at engagement and at low speeds (see [Bak 92], [Gie 89], [Hur 94]).
  - The *torque converter* has larger inherent power losses due to permanent slip, but provides drive-away acceleration by torque multiplication at engagement and comfort due to inherent viscous damping. If a lock-up facility is added, the power losses are reduced significantly (see [Hur 94]).

- The variator and pinion gear

  In practice, the following parameters (exact definitions are given in Chapter 4) determine the performance of the variator and pinion:

  - The maximum (LOW) and minimum (OD, overdrive) ratio of the variator.
  - The gear ratio (FD) of the pinion.
  - The maximal torque that can be transmitted.
  - The push-belt properties (see [Roo 91]).

  The inherent power losses in the variator, due to friction between components, depend on the point of operation (see [Dev 93], [MLB 94], [Rek 90] and [Sun 88]) and are strongly related to the quality of the drive train control unit.

- The drive train control unit

  The power consumed by the oil pump and the power losses in the variator (fuel economy), the shifting quality (comfort) and the shifting speed (performance) are all determined by the quality of the drive train control unit (see [Gie 89], [Dev 93], [MLB 94], [NSS 90]).

- The car characteristics $(C_x, C_z, m_{tot}, I_{tot}), r, f_r(v_c))$ also determine comfort, performance and fuel consumption. Customers accept that fuel consumption is exchanged for performance and comfort, when car size increases.
- The environmental conditions (wind and road) are important also.

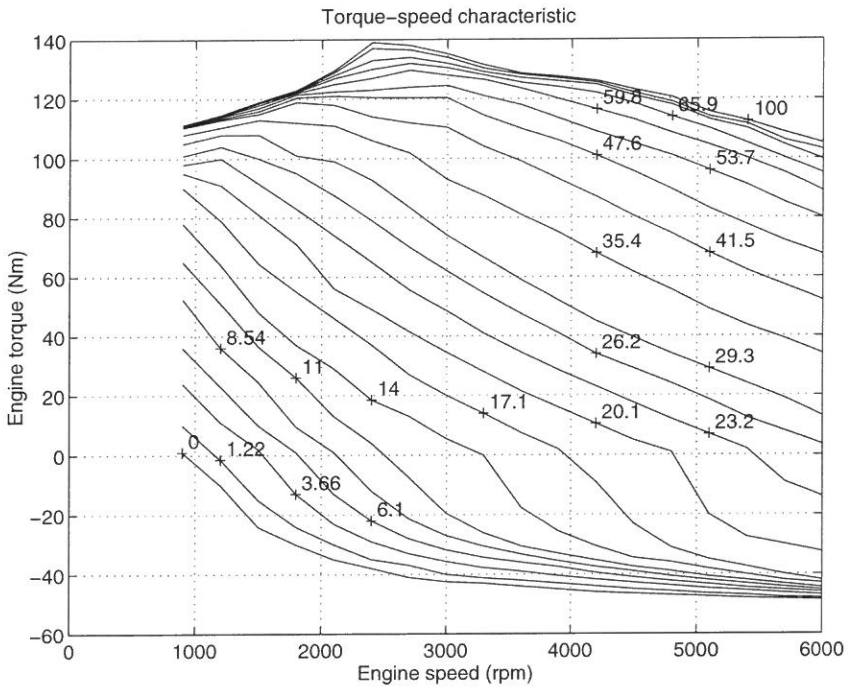

Figure 3.1 *Experimentally determined torque-speed curves (engine B18U). Lines of constant throttle position (%) are shown (Source: VCST).*

3.2 Car performance and fuel economy

3.2.1 A benchmark test for CVT-equipped cars

Comfort and fuel economy of a car are strongly related to the considered application (engine-transmission-car combination). However, since the specifications

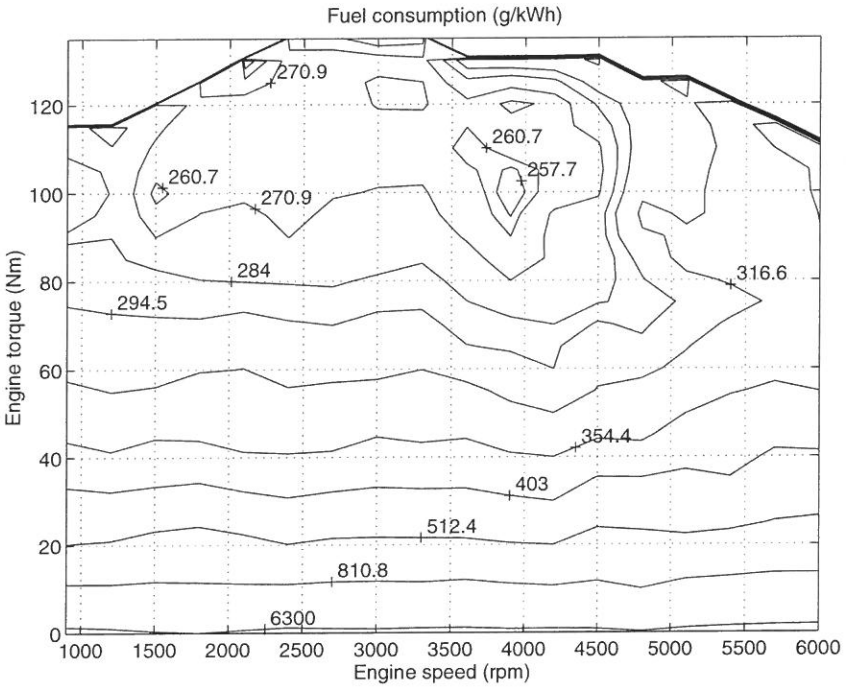

Figure 3.2 *Experimentally determined fuel consumption curves (engine B18U). Lines of constant specific fuel consumption are shown (g/kWh) (Source: VCST).*

of different manufacturers (Rover, Volvo, Chrysler) for CVT-equipped cars exhibited similarity, we organized the indices in a single benchmark test for CVT-equipped passenger cars. Within VCST, this benchmark test is now used to tune transmissions towards applications ([Van 96b]).

Table 3.1 shows the benchmark test. Nineteen different indices are included. Typical values for a specific application are added also. Once the car, the drive train and the control unit are modelled, these indices are easily computed from time-domain simulations.

3.2.2 Dynamic performance

Dynamic performance of a car is expressed by times, distances and accelerations. Four different tests (simulation or test-ride) must be conducted to obtain values

Index	Description	Objective	Units
$G_{kd,1}$	5 sec. distance at kick-down from rest	45	m
$G_{kd,2}$	Delay (0-1 km/h) at kick-down from rest	0.15	s
$G_{kd,3}$	Peak acc. at kick-down from rest	5.4	m/s^2
$G_{kd,4}$	Time to peak acc. at kick-down from rest	0.8	s
$G_{kd,5}$	0-60 mph time at kick-down from rest	8.7	s
$G_{kd,6}$	Attainable car speed (top speed)	210	km/h
$G_{kd,7}$	Max. allowed sec. speed at top speed	12000	rpm
G_{im}	40-60 mph time at kick-down from 40 mph	5.0	s
$G_{sl,1}$	Initial acceleration on a 12 % slope	0.6	m/s^2
$G_{sl,2}$	Attainable speed on a 12 % slope	85	km/h
G_{no}	Peak acc., no throttle, no brake from 60 mph	-0.3	m/s^2
$G_{fs,1}$	Consumed fuel at 40 mph	5.7	ltr/100 km
$G_{fs,2}$	Consumed fuel at 50 mph	6.3	ltr/100 km
$G_{fs,3}$	Consumed fuel at 60 mph	7.1	ltr/100 km
$G_{fs,4}$	Consumed fuel at 70 mph	8.1	ltr/100 km
$G_{fs,5}$	Consumed fuel at 80 mph	10.1	ltr/100 km
$G_{fc,1}$	Consumed fuel Urban cycle	9.5	ltr/100 km
$G_{fc,2}$	Consumed fuel Highway cycle	6.5	ltr/100 km
$G_{fc,3}$	Consumed fuel ECE cycle	11.5	ltr/100 km

Table 3.1 *A design benchmark for a CVT-equipped passenger car (Volvo 850, engine N2-P20, variator VT1-E). Speeds are given in miles per hour (mph, 1 mile = 1609,23 m).*

for all indices related to car performance:

- Kick-down starting from rest (indices $G_{kd,i}$)

  Before $t = 0$, full throttle and full brake are applied. The selector lever is in D-position. The engine is controlled at stall speed. At $t = 0$, the brake is released. The indices can be computed from car position, car speed, secondary speed and car acceleration.

- Kick-down starting from 40 MPH (index G_{im})

  Before $t = 0$, the car speed is constant and equal to 40 MPH. At $t = 0$, full throttle is applied. The index can be computed from car speed.

- Performance on a 12 % slope (indices $G_{sl,i}$)

  At $t = 0$, the road slope is 12 % and full throttle is applied. The initial acceleration and the final car speed are observed.

- Peak acceleration at no throttle, no brake, from 60 MPH (index G_{no})

  Before $t = 0$, the car speed is constant and equal to 60 MPH. At $t = 0$, the throttle is released. Shifting and engine braking will start. The index can be computed from car acceleration.

3.2.3 Fuel economy

Fuel economy is expressed by the consumed fuel per unit distance, in this case liters fuel per 100 kilometer (ltr/100 km). Basically, two types of tests (simulation or test-ride) are required to obtain values for all related indices:

- Five tests at constant car speed (indices $G_{fs,i}$)

  The car speed is held constant at the prescribed value. By combining the fuel consumption characteristic of the engine with the stationary values of the delivered engine torque and engine rotation speed, the corresponding index can be computed.

- Three tests while driving well-defined cycles (indices $G_{fc,i}$)

  A controller (the driver) forces the car to follow a prescribed speed profile (a cycle). By combining the fuel consumption characteristic of the engine with the values of the delivered engine torque and engine rotation speed, the corresponding index can be computed.

  Three different cycles are generally accepted in the automotive world. Detailed descriptions of these cycles (subcycles, handling instructions, prescribed car mass, allowed tracking error) are found in [Eur 91].

  - The Urban cycle is a good mix of city traffic and highway traffic (see figure 3.3).
  - The Highway cycle is used for highway traffic (see figure 3.4).
  - The ECE-cycle is used for city traffic (see figure 3.5).

The drive train model derived in Chapter 4 allows simulation of all required signals, under static and dynamic conditions, and is used for computation of performance and fuel economy indices.

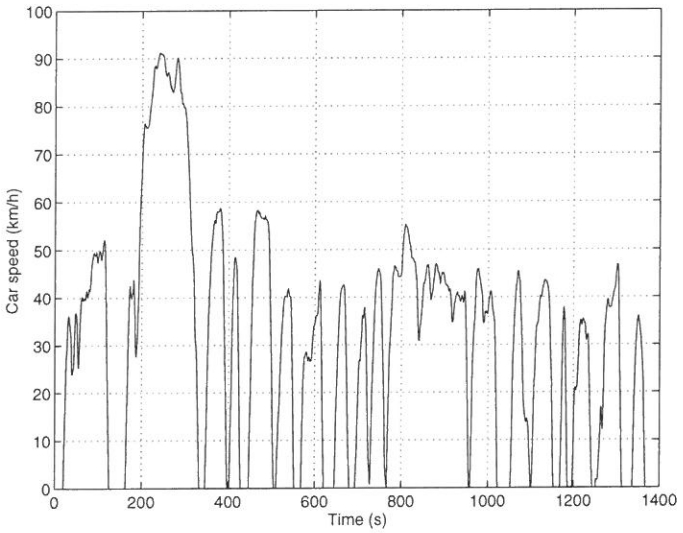

Figure 3.3 *The desired car speed profile for the Urban cycle (Source: VCST).*

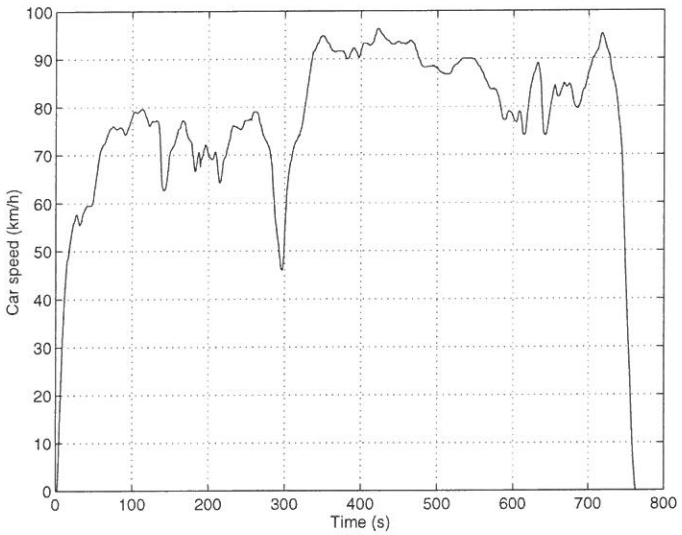

Figure 3.4 *The desired car speed profile for the Highway cycle (Source: VCST).*

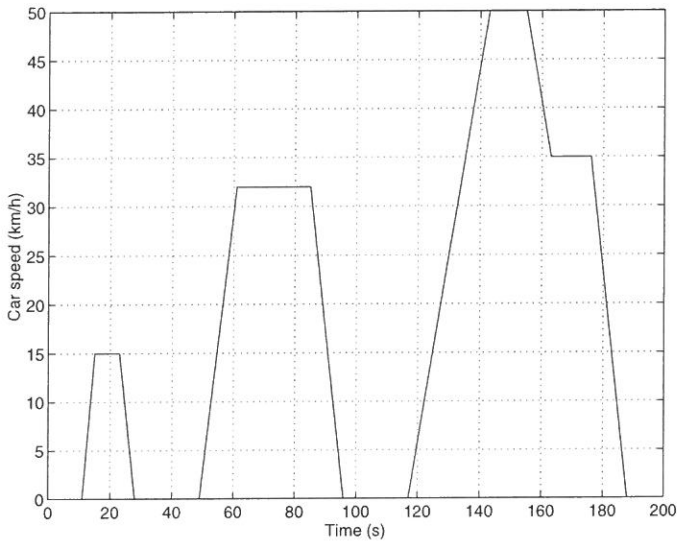

Figure 3.5 *The desired car speed profile for the ECE-cycle (Source: [Eur 91]).*

3.3 Drive comfort

Comfort is related to accelerations, caused by disturbances. The way the driver senses the accelerations determines the level of comfort in a car. In practice, two types of disturbances are distinguished:

- Stochastic disturbances: the road profile and the wind dynamics.
- Deterministic disturbances, e.g. step-alike changes in drive torque at kick down, braking or power shifting, and permanent drive torque oscillations due to drive axle compliance or CVT control.

Since comfort is related to accelerations, caused by stochastic or deterministic disturbances, acceleration signals are used for comfort evaluation. Much effort (see [ISO 86] and [VDI 87]) has been done to characterize the subjective human reactions on these accelerations. Five important factors are indicated:

- The direction of acceleration (transversal (z) versus longitudinal (x)).

- The point where the disturbance comes in (car body, suspension).
- The frequency contents of the acceleration (humans are most sensitive to accelerations within the frequency range from 1 to 80 Hz).
- The time that the disturbance works.
- The occurrence and height of peak accelerations.

From experimental data[1] of human sensitivity for harmonic longitudinal and transversal accelerations, two linear dynamic filters are constructed. These filters describe human sensitivity and are used to filter the computed or measured acceleration signals. The filtered accelerations are used to compute the comfort indices.

3.3.1 The human sensitivity filters

In the literature (see [ISO 86], [VDI 87], [Ket 91], [Mit 84], [KL 93]), most experimental results on human sensitivity are based on periodic excitations and are stated in terms of rms-values, so computation in the frequency domain is preferred. Longitudinal and transversal comfort appreciation is described by human sensitivity filters $H_{a_x}(\omega)$ and $H_{a_z}(\omega)$. The rms-values of the filtered acceleration signals $\underline{a}_x$ and $\underline{a}_z$ are computed from:

$$\underline{a}^2_{x,rms} = \int_0^\infty P_{a_x}(\omega) H^2_{a_x}(\omega) d\omega \tag{3.1}$$

$$\underline{a}^2_{z,rms} = \int_0^\infty P_{a_z}(\omega) H^2_{a_z}(\omega) d\omega \tag{3.2}$$

with $P_{a_x}(\omega)$ and $P_{a_z}(\omega)$ the spectra of the accelerations a_x and a_z. In the time domain, these human sensitivity filters take acceleration as an input, and compute the filtered accelerations.

Longitudinal sensitivity filter

A description of this filter is obtained from [ISO 86]. In the frequency range of interest (1 to 80 Hz), the filter amplitude $H_{a_x}(\omega)$ as a function of the frequency ω (rad/s) is specified as:

[1] The experimental data, found in [ISO 86] and [VDI 87], are used to construct the human sensitivity models.

$$2\pi \leq \omega \leq 4\pi \quad : \quad H_{a_x}(\omega) = 1 \tag{3.3}$$

$$4\pi \leq \omega \leq 160\pi \quad : \quad H_{a_x}(\omega) = \frac{4\pi}{\omega} \tag{3.4}$$

The non-linear filter $H_{a_x}(\omega)$ can easily be approximated by a linear filter (see figure 3.6) using a continuous-time frequency identification technique (see [VDM 96]). The filter is driven by a_x. The filtered acceleration is denoted as $\underline{a}_x$, and the state space equations of the approximating linear filter are given by:

$$\dot{\mathrm{X}}_{fx} = \mathrm{A}_{fx}\mathrm{X}_{fx} + \mathrm{B}_{fx}a_x \tag{3.5}$$

$$\underline{a}_x = \mathrm{C}_{fx}\mathrm{X}_{fx} \tag{3.6}$$

with

$$\mathrm{A}_{fx} = \begin{pmatrix} -14.30 & -111.884 \\ 1 & 0 \end{pmatrix}$$

$$\mathrm{B}_{fx} = \begin{pmatrix} 1 \\ 0 \end{pmatrix}$$

$$\mathrm{C}_{fx} = \begin{pmatrix} 12.3425 & 79.7614 \end{pmatrix}$$

Transversal sensitivity filter

A similar approach is used to describe a filter for transversal comfort evaluation. The description of the filter is also obtained from [ISO 86]. In the frequency range of 1 to 80 Hz, the filter amplitude $H_{a_z}(\omega)$ as a function of the frequency ω (rad/s) is specified as:

$$2\pi \leq \omega \leq 8\pi \quad : \quad H_{a_z}(\omega) = 0.5\sqrt{\frac{\omega}{2\pi}} \tag{3.7}$$

$$8\pi \leq \omega \leq 16\pi \quad : \quad H_{a_z}(\omega) = 1 \tag{3.8}$$

$$16\pi \leq \omega \leq 160\pi \quad : \quad H_{a_z}(\omega) = \frac{16\pi}{\omega} \tag{3.9}$$

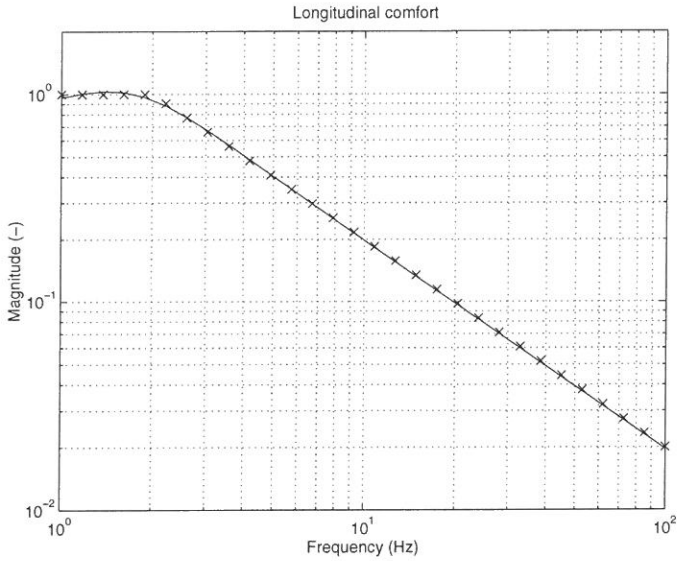

Figure 3.6 *The human sensitivity filter for longitudinal comfort (x) and its linear approximation (solid).*

This non-linear filter can easily be approximated by a linear filter (see figure 3.7) using a continuous-time frequency domain identification technique ([VDM 96]). The filter is driven by a_z. The filtered acceleration is denoted as $\underline{a}_z$ and the state space equations of the approximating linear filter are given by:

$$\dot{\mathrm{X}}_{fz} = \mathrm{A}_{cz}\mathrm{X}_{fz} + \mathrm{B}_{cz}a_z \tag{3.10}$$

$$\underline{a}_z = \mathrm{C}_{cz}\mathrm{X}_{fz} \tag{3.11}$$

with

$$\mathrm{A}_{fz} = \begin{pmatrix} -52.73 & -1240.5 \\ 1 & 0 \end{pmatrix}$$

$$\mathrm{B}_{fz} = \begin{pmatrix} 1 \\ 0 \end{pmatrix}$$

$$\mathrm{C}_{fz} = \begin{pmatrix} 52.5907 & 571.167 \end{pmatrix}$$

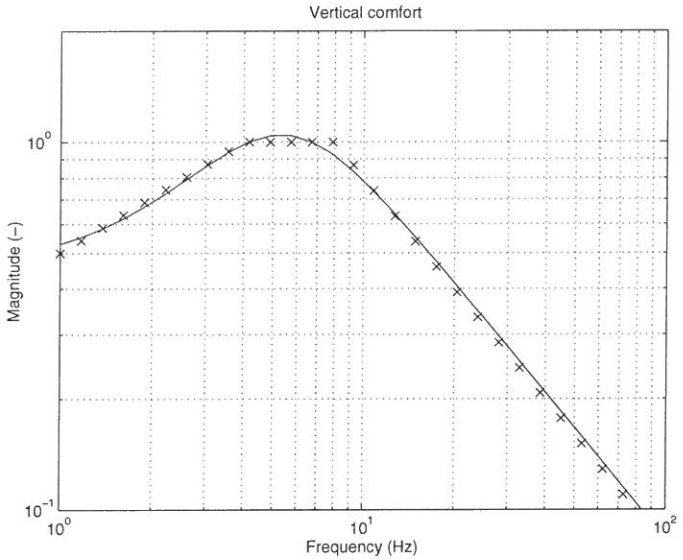

Figure 3.7 *The human sensitivity filter for transversal comfort (x) and its linear approximation (solid).*

3.3.2 Comfort indices

Although most results in the literature are stated in terms of rms-values of the filtered accelerations, practice has shown that peak values in the unfiltered acceleration signals are of similar importance, especially when evaluating the influence of step-wise throttle changes (kick-down (full throttle), tip-in (small positive throttle step at 20 km/h), tip-out (small negative throttle step at 20 km/h)) and braking actions (see [VCST 95]).

Therefore, four comfort measures are defined:

$$G_{x,rms} = 28\, \underline{a}_{x,rms} \tag{3.12}$$

$$G_{x,max} = \max_{t_1<t<t_2} \underline{a}_x(t) \tag{3.13}$$

$$G_{z,rms} = 20\, \underline{a}_{z,rms} \tag{3.14}$$

$$G_{z,max} = \max_{t_1<t<t_2} \underline{a}_z(t) \tag{3.15}$$

where t_1 and t_2 are well-defined times for each peak value test (see [VCST 95]).

From the definitions, it follows that smaller index-values correspond to higher comfort levels.

3.3.3 An integrated car-comfort model

The linearized car model derived in Chapter 2, can be combined with the human sensitivity filters, to construct an integrated car-comfort model[2].

The longitudinal comfort in a car is determined by the longitudinal acceleration a_x at the car's center of gravity (cog), while the vertical comfort at a position λ in the car is determined by the vertical acceleration a_z at that point. Both accelerations are linear combinations of the model states (see equation 2.36):

$$a_x = \ddot{x}_c \tag{3.16}$$
$$a_z = \ddot{z}_c + \lambda\ddot{\theta}_c \tag{3.17}$$

With the car's state vector denoted by X_c and the acceleration vector $\mathrm{V} = (a_x, a_z)'$, equations 3.16 and 3.17 can be combined as:

$$\mathrm{V} = \mathrm{C}_c\mathrm{X}_c \tag{3.18}$$

with the output vector C_c equal to:

$$\mathrm{C}_c = \begin{pmatrix} 0 & 0 & 0 & 0 & 0 & 0 & 0 & 0 & 0 & 0 & 1 & 0 & 0 & 0 & 0 & 0 & 0 & 0 \\ 0 & 0 & 0 & 0 & 0 & 0 & 0 & 0 & 0 & \lambda & 0 & 1 & 0 & 0 & 0 & 0 & 0 & 0 \end{pmatrix}$$

The system matrices A_{cf}, B_{cf} and C_{cf} of the combined system (car and human sensitivity filters) are given by:

$$\mathrm{A}_{cf} = \begin{pmatrix} \mathrm{A}_c & 0 \\ \mathrm{B}_f\mathrm{C}_c & \mathrm{A}_f \end{pmatrix}$$

$$\mathrm{B}_{cf} = \begin{pmatrix} \mathrm{B}_c \\ 0 \end{pmatrix}$$

[2]Note that the filters can also be combined with the non-linear model (in Matlab/Simulink, it can be done via block diagrams). In that case, the accelerations and the filtered accelerations are obtained by numerical integration

$$C_{cf} = \begin{pmatrix} 0 & C_f \end{pmatrix}$$

with the matrices A_f, B_f and C_f given by:

$$A_f = \begin{pmatrix} A_{fx} & 0 \\ 0 & A_{fz} \end{pmatrix}$$

$$B_f = \begin{pmatrix} B_{fx} & 0 \\ 0 & B_{fz} \end{pmatrix}$$

$$C_f = \begin{pmatrix} C_{fx} & 0 \\ 0 & C_{fz} \end{pmatrix}$$

This model uses the car inputs U_c to compute the filtered acceleration vector $(\underline{a}_x, \underline{a}_z)'$, required for comfort analysis. This model can be used for different purposes:

- To analyze the influence of drive torque variations, braking actions and wind dynamics on longitudinal comfort.
- To analyze the influence of drive train control on longitudinal comfort.
- To analyze the influence of road profile noise and drive torque variations on transversal comfort.
- For suspension analysis and optimization.

3.4 A sample of results and conclusions

This Section contains a sample of results that have been obtained when doing practical computations and experiments.

- Kick-down test: VT1-H versus VT1-E (simulation)

  Figure 3.8 shows the influence of the control unit and control strategy on car motion for a Rover 216, with engine 1.6K16MPI, equipped with

a VT1 variator and a wet multi-plate clutch (P811). When applying hydraulic control (VT1-H), the realized variogram is fixed and determined by the hydro-mechanical control hardware (see Chapters 5 and 6). When applying electronic control (VT1-E), the realized variogram depends on the user's specifications (economy, sport, mixed) and is determined by a look-up table in the control software (see Chapters 5 and 6). By adapting the look-up table, the performance of a car with an electronically controlled variator can be changed easily. In this simulation, an economy variogram was used, which resulted in minimal fuel consumption, high comfort (smooth acceleration, minimal two-stage engagement (see Chapter 4)) and moderate dynamic performance (compared to the potentials of a sport variogram).

- VT1-H versus VT1-F (experiments)

  Figures 3.9 and 3.10 and table 3.2 show the influence of the control unit and control strategy on car motion for a Rover 216, with engine 1.6K16MPI, equipped with a VT1 variator and a wet multi-plate clutch (P811). When applying hydraulic control (VT1-H), the realized variogram is fixed and determined by the hydro-mechanical control hardware (see Chapters 5 and 6). When applying electronic control (VT1-F), the realized variogram depends on the user's specifications (economy, sport, mixed) and is determined by a look-up table in the control software (see Chapters 5 and 6). In these experiments, a mixed variogram was used, to obtain a good trade-off in fuel consumption, comfort (smooth acceleration, minimal two-stage engagement (see Chapter 4)) and dynamic performance. With respect to comfort and dynamic performance, it follows from the acceleration and speed profiles that the electronically controlled CVT performs better than the hydraulically controlled CVT.

Throttle (%)	Car speed (km/h)	VT1-H (s)	VT1-F (s)
10	20	6.76	5.77
25	50	10.1	8.93
50	50	4.79	5.26
100	100	10.21	9.64

Table 3.2 *Dynamic performance VT1-H versus VT1-F (Rover 216, engine 1.6K16MPI). For different throttle positions, the time to reach a reference car speed was measured.*

- Variator optimization: influence of OD and FD (simulation)

  Figure 3.11 shows the influence of the variator geometry (minimal variator ratio OVERDRIVE (OD) and final drive reduction (FD), see Chapter 4) on

the consumed fuel at constant car speeds (indices $G_{fs,i}$), for a Volvo 850, with engine N2-P20, equipped with a VT1-E variator and a wet multi-plate clutch (P811). Reduced fuel consumption can be obtained by minimizing overdrive (OD) and the final drive reduction (FD). In practice, OD will be minimized, since FD must be maximized to guarantee good dynamic performance (see figure 3.12, for indices $G_{kd,1}$, $G_{kd,3}$ and $G_{kd,5}$).

- Plate clutch versus torque converter (simulation)

  Figures 3.12 and 3.13 show the influence of the coupling device (plate clutch P811 versus torque converter Daikin YT 220) on dynamic car performance. The torque converter shows higher dynamic performance (due to torque multiplication) and increased comfort (limited two-stage engagement).

- Benchmark test: plate clutch versus torque converter (simulation)

  Table 3.3 shows the simulation results of a partial CVT-benchmark test for a Rover 216, with engine 1.6K16MPI, equipped with a VT1-E variator and a wet multi-plate clutch (P811) or a torque converter (Daikin YT220). These simulations were done to analyze the influence of the coupling device on the car performance and to quantify the expected potentials of a torque converter. The test shows that the torque converter is advantageous with respect to dynamic car performance (due to torque multiplication, see Chapter 4) and that fuel consumption at constant car speeds is not affected if a converter lock-up facility is present (as we assumed here).

Index	Plate clutch	Torque converter	Units
$G_{kd,1}$	36	39	m
$G_{kd,2}$	0.12	0.05	s
$G_{kd,3}$	3.4	4.2	m/s^2
$G_{kd,4}$	0.67	0.5	s
$G_{kd,5}$	11.6	11.4	s
$G_{kd,6}$	185	185	km/h
$G_{kd,7}$	10100	10100	rpm
G_{im}	6	6	s
$G_{fs,1}$	5.92	5.92	ltr/100 km
$G_{fs,2}$	6.80	6.80	ltr/100 km
$G_{fs,3}$	7.25	7.25	ltr/100 km
$G_{fs,4}$	8.24	8.24	ltr/100 km
$G_{fs,5}$	9.18	9.18	ltr/100 km

Table 3.3 *CVT benchmark test (Rover 216, engine 1.6K16MPI, variator VT1-E): wet multi-plate clutch (P811) versus torque converter (Daikin YT220).*

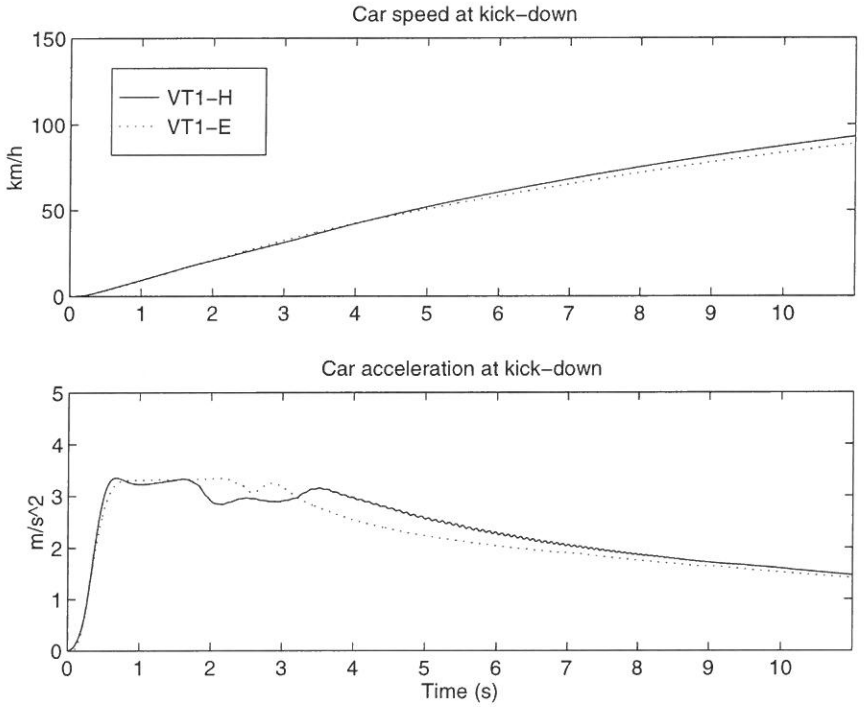

Figure 3.8 *Car acceleration and speed at kick-down from rest: influence of the control unit and control strategy on car motion for a Rover 216, with engine 1.6K16MPI, equipped with a VT1 variator and a wet multi-plate clutch (P811) (simulation).*

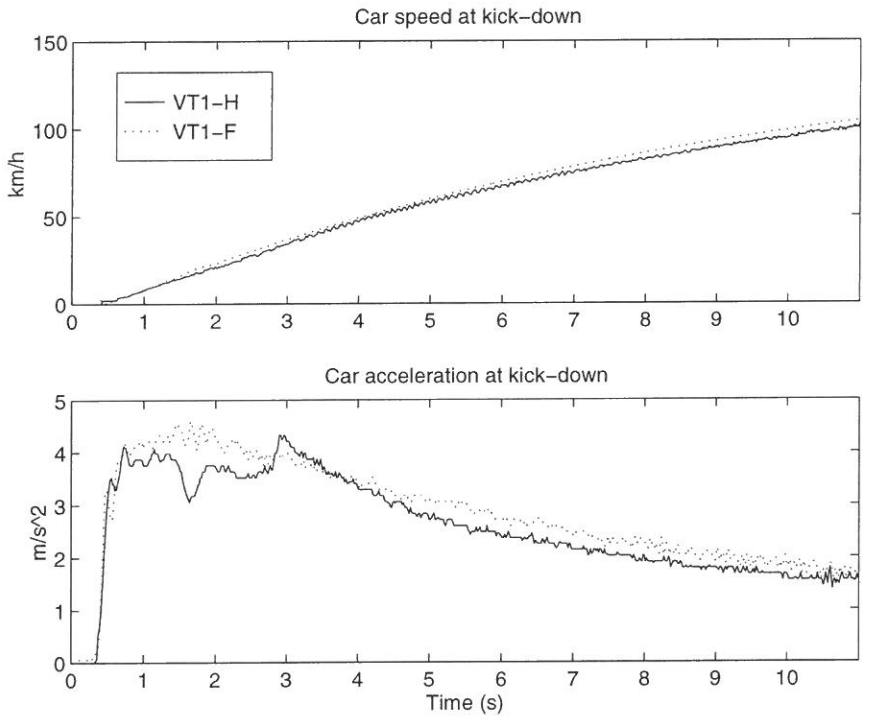

Figure 3.9 *Car acceleration and speed at kick-down from rest: influence of the control unit and control strategy on car motion for a Rover 216, with engine 1.6K16MPI, equipped with a VT1 variator and a wet multi-plate clutch (P811) (experiment).*

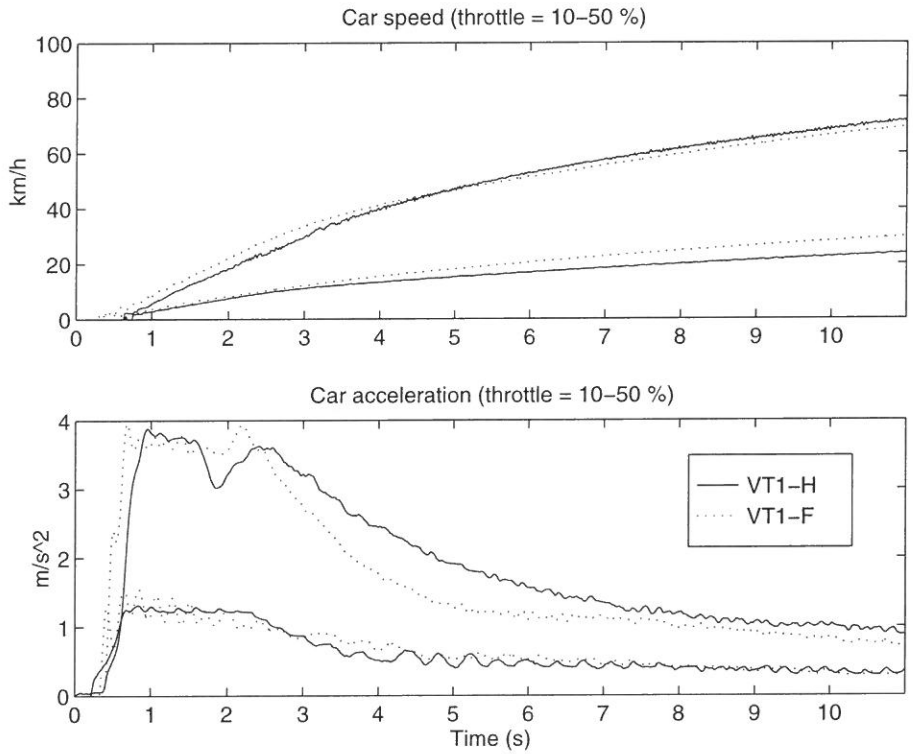

Figure 3.10 *Car acceleration and speed at intermediate throttle positions: influence of the control unit and control strategy on car motion for a Rover 216, with engine 1.6K16MPI, equipped with a VT1 variator and a wet multi-plate clutch (P811) (experiment).*

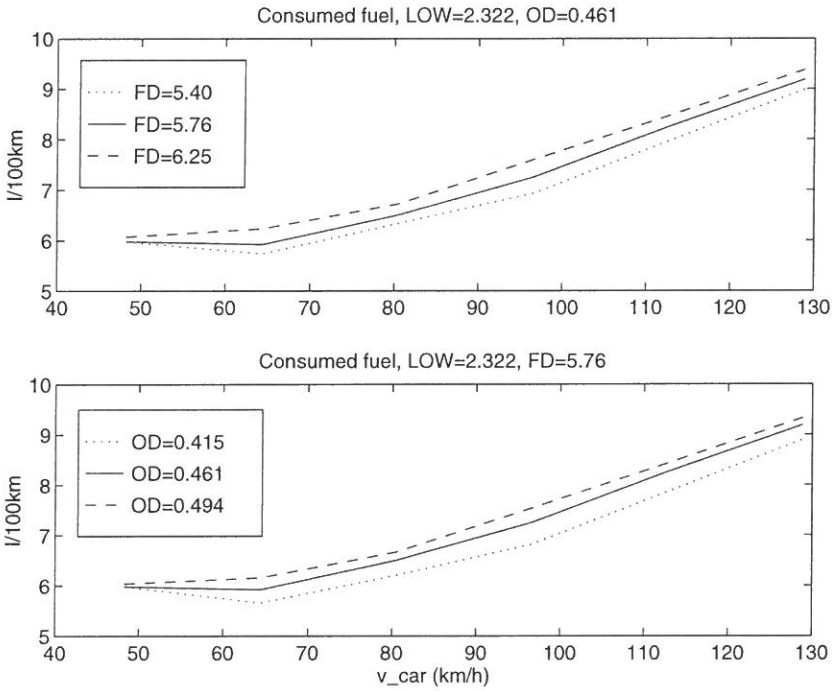

Figure 3.11 *Influence of the variator geometry (minimal variator ratio OVERDRIVE (OD) and final drive reduction (FD)) on the consumed fuel at constant car speeds (indices $G_{fs,i}$), for a Volvo 850, with engine N2-P20, equipped with a VT1-E variator and a wet multi-plate clutch (P811) (simulation).*

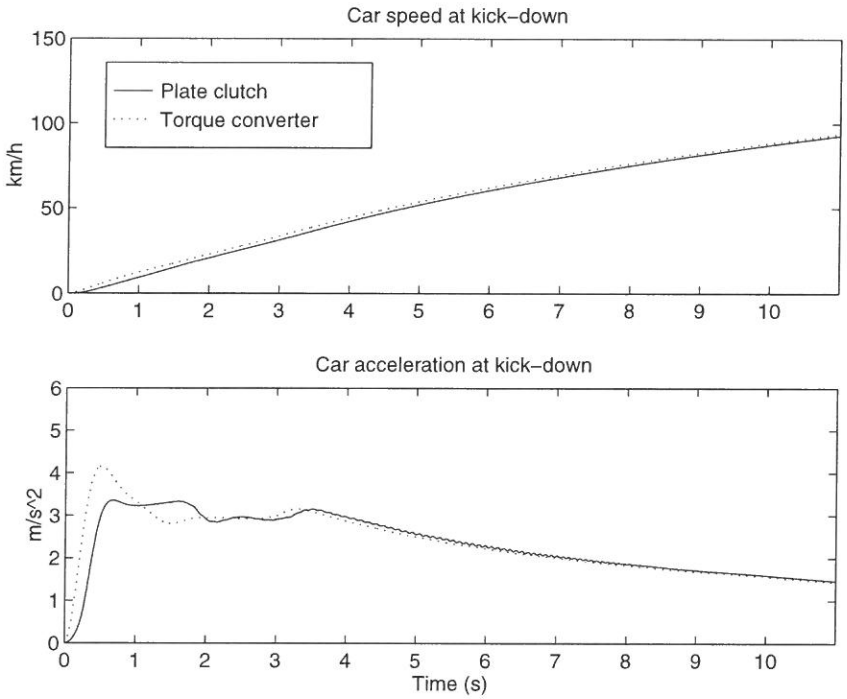

Figure 3.12 *Acceleration and speed at kickdown from rest: influence of the coupling device (plate clutch P811 versus torque converter Daikin YT 220) on dynamic car performance, for a Rover 216, with engine 1.6K16MPI, equipped with a VT1-H variator (simulation).*

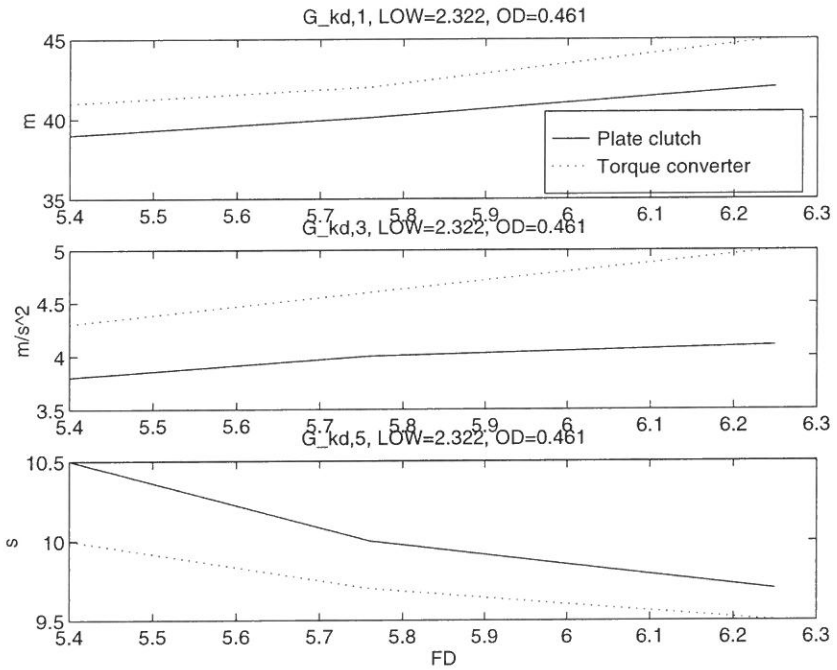

Figure 3.13 *Influence of the coupling device (plate clutch P811 versus torque converter Daikin YT 220) and the final drive reduction (FD) on dynamic car performance, for a Volvo 850, with engine N2-P20 and a VT1-E variator (simulation).*

Chapter 4

Drive Train Modeling and Control

In this Chapter, we analyze and describe a drive train with a Continuously Variable Transmission. In Section 4.2, the operation and the characteristics of all important drive train components are analyzed in detail. In order to estimate performance, fuel economy and comfort accurately, all relevant static and dynamic characteristics of the drive train and its components are considered. First, the combustion engine is treated. In the ideal case, the static characteristics are sufficient to describe the combustion engine accurately. In practice, experimental results on a B18U engine show that the delivered engine torque is delayed, inversely proportional to engine speed. Next, the wet multi-plate clutch is discussed. In the ideal case, the maximum torque that can be transmitted is only determined by the pressure in the clutch piston. Dynamic experiments with a P811 wet multi-plate clutch indicate that this torque depends on both the clutch pressure and the piston position. As an alternative for a wet multi-plate clutch, a torque converter is discussed. Two experimental characteristics are used to describe the Daikin YT220 torque converter. Afterwards, the variator is discussed. In the ideal case, it is a power transformer with a variable ratio i_v and a constant torque efficiency η_v. Experiments on a VT1-transmission indicate that efficiency varies with the operating point, and that the rate of ratio change is limited by oil flow requirements. These practical issues will be discussed in detail in Chapter 5. Finally, the gear pump, the pinion gear and the drive axle are described. In Section 4.3, the component equations derived in Section 4.1 are combined with the torque balances of the different inertias, to obtain a generic nonlinear physical model of the drive train. Physically reduced control models

for clutch mode (the variator ratio remains constant (LOW)) and variator mode (the clutch is locked, no clutch slip occurs) are derived also. In Section 4.4, we introduce the concept of variogram control and we use it for optimal drive train management. Finally, we use the idea of output feedback linearization to design optimal controllers for clutch mode and variator mode. Section 4.5 shows a sample of results and conclusions.

4.1 Description of the drive train

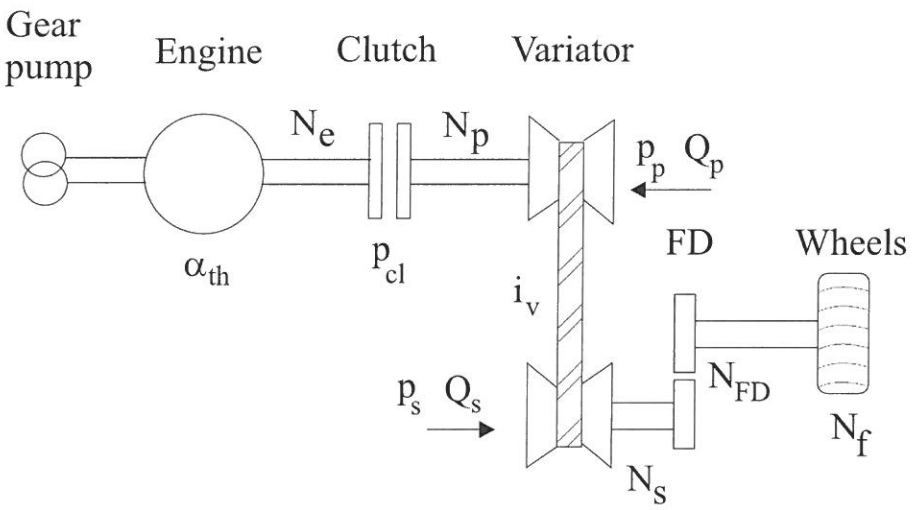

Figure 4.1 *Functional model of the drive train. The characteristics of the drive train depend on the coupling element, the metal push-belt variator, the pinion gear, the drive axle, the gear pump and the car and tire characteristics. The driver varies the throttle position α_{th} and the brake torque T_{brake}. The control unit of the transmission generates the control inputs required for drive train management. The control inputs are the variator ratio i_v and the clutch pressure p_{cl}.*

Although parameter estimation techniques are succesfully applied in car and drive train modelling (see [Lju 87], [SM 93], [MD 93]), we use physical models to describe the drive train components and their interactions (see [Mit 84], [KL 93], [Fun 95], [Granda 90], [Granda 91], [Rau 92]).

This allows us to create generic models, with physical parameters that depend on the application. The model parameters are obtained from data-sheets and dedicated experiments. In a context of tuning transmission characteristics to-

wards car and engine characteristics, it is advantageous that only data-sheets and a few experiments are required to tune the generic drive train for a new application.

Within the frequency range of interest (below 5 Hz), a lumped parameter approach is sufficient (see [Spijk 94], [GS 95], [NSS 90], [IUK 95]) to describe the drive train shown in figure 4.1). Therefore, the drive train has been considered as a system of discrete physical components that are interacting with each other:

- The combustion engine delivers the necessary power. Only the driver is allowed to change the throttle position α_{th} (i.e. ignition control is not considered).
- The wet multi-plate clutch transmits power from the engine to the variator, and is required for starting from rest. The pressure p_{cl} in the clutch piston is determined by the transmission control unit.
- The torque converter serves as an alternative for the wet multi-plate clutch. In a control context, its flexibility is rather low, because it has no control input. Only geometrical changes can be used to adapt the characteristics.
- The gear pump, driven by the engine, provides the hydraulic actuation unit with oil.
- The pinion gear, also referred to as the final drive reduction, is a gear-box that transmits power from the variator to the drive axle.
- The drive axle brings the power to the front wheels.
- The load torque is determined by the car and tire characteristics (R_{tot}), by environmental conditions (T_{ext}) and by the brake torque T_{brake}, that is applied by the driver.

Before deriving the equations of the drive train, a functional model of the drive train is discussed (see figure 4.2). Although the model is derived for a drive train with a wet multi-plate clutch, it can easily be adapted for a drive train with a torque converter. The following phenomena are taken into account:

- The engine is described as a nonlinear torque source, modulated by the engine speed and the throttle position. Internal friction is taken into account implicitly, in the static torque characteristic. The pump torque, required to drive the gear pump, mainly depends on pump pressure and pump speed.

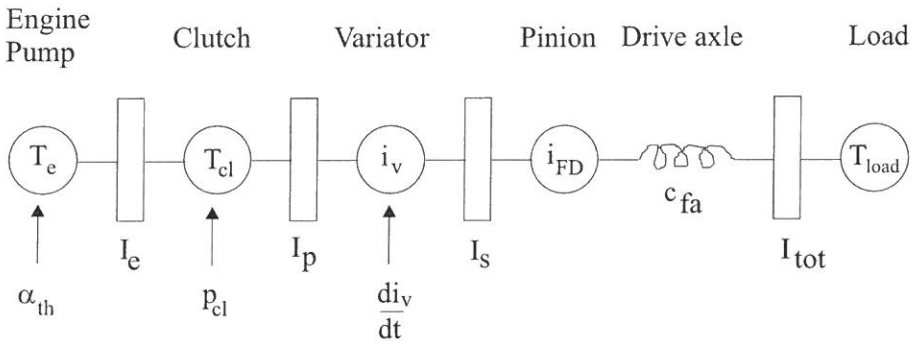

Figure 4.2 *A functional model of the drive train.*

- The flywheel inertia, the pump inertia, half of the clutch inertia and the inertia of the torsion damper are combined in a single rotational inertia, that rotates at engine speed.
- The clutch is described as a nonlinear friction element, modulated by the clutch pressure and the clutch slip.
- Half of the clutch inertia, the inertia of the primary axle and the inertia of the primary pulley are combined in a single rotational inertia, that rotates at primary speed.
- The variator is described as a variable transformer with a fixed torque efficiency (to take into account friction losses in the belt-pulley system and in all bearings. In practice, the torque efficiency is not constant, but strongly determined by the operating point of the variator (see Chapter 5)).
- The inertia of the secondary pulley, the inertia of the secondary axle and half of the pinion gears inertia is combined in a single rotational inertia, that rotates at secondary speed.
- The pinion gear-box is described as a fixed transformer with no torque losses.
- The drive axle is modeled as a linear torsional spring. The damping of the axle material is neglected.
- The total car inertia, reduced to the wheels, half of the pinion gear inertia and the drive shaft inertia are combined in a single rotational inertia I_{tot}, that rotates at wheel speed.

- The total load torque is reduced to the wheels and contains roll and air resistances, load due to road slope and brake torque.

In the following sections, the static and/or dynamic characteristics of all drive train components are discussed. Next, the system's torque balances and the drive train component characteristics are combined, to derive a generic (static and dynamic) drive train model. Inertia effects are modelled by discrete inertances, related to the different independent rotation speeds in the drive train (engine speed, primary speed, secondary speed, wheel speed). Internal friction (e.g. in bearings) is taken into account implicitly (e.g. in the engine characteristic) or explicitly via experimental component efficiency maps (e.g. torque efficiency of the variator).

4.2 Drive train component models

4.2.1 The combustion engine

The delivered static engine torque $T_e(\dot{\theta}_e, \alpha_{th})$ depends on the engine rotation speed $\dot{\theta}_e$ and the throttle position α_{th}, while the consumed fuel $\Phi_e(T_e, \dot{\theta}_e)$ depends on the delivered engine torque T_e and the engine rotation speed $\dot{\theta}_e$ (see [CA 94], [Hey 88]):

$$T_e = T_e(\dot{\theta}_e, \alpha_{th}) \tag{4.1}$$

$$\Phi_e = \Phi_e(T_e, \dot{\theta}_e) \tag{4.2}$$

In the ideal case, these static characteristics are sufficient to describe the engine. However, in practice, when evaluating clutch engagement, the torque time constant needs to be taken into account. An experimental curve from the literature and experiments on a B18U engine (see figure 4.3) show that the torque time constant $\tau_e(\dot{\theta}_e)$ strongly depends on the engine speed $\dot{\theta}_e$ (see [DH 95], [VCST 92]).

This is taken into account by embedding the static engine model in the following non-linear state-space system:

$$\dot{x_T} = \frac{1}{\tau_e} x_T + \frac{1}{\tau_e} T_e(\dot{\theta}_e, \alpha_t) \tag{4.3}$$

$$T_{e,dyn} = x_T \tag{4.4}$$

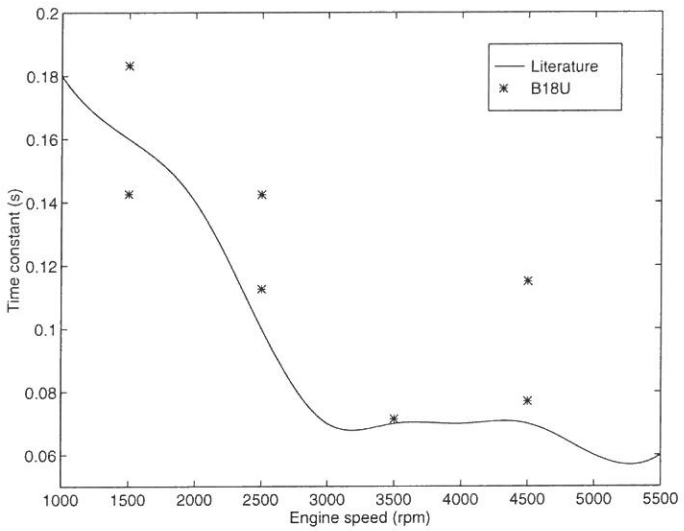

Figure 4.3 *Experimental torque time constant $\tau_e(\dot{\theta}_e)$ as a function of engine speed $\dot{\theta}_e$ (literature (see [DH 95]) and B18U (see [VCST 92])). Deviations of 40 ms were measured, due to changes in temperature, internal friction and instantaneous torque.*

The dynamic torque $T_{e,dyn}$ represents the instantaneously delivered torque and is used to compute instantaneous fuel consumption. This approximation of reality is sufficiently accurate for most operating conditions.

The engine and flywheel inertia are included in the engine inertia I_e, that rotates at engine speed.

4.2.2 The wet multi-plate clutch

The wet multi-plate clutch exists of axially slidable friction plates that are connected either to the engine shaft or to the primary shaft by a cottering (see figures 4.4 and 4.5). A piping in the primary shaft brings oil in the clutch piston. The clutch can transmit torque as soon as the plates make contact. By varying the pressure p_{cl} in the clutch piston, the distance between the plates and the torque to be transmitted is varied. The oil is also used for lubrication and cooling of the clutch plates, via small grooves in the plate surfaces (see [BW 91], [Bak 92]). A linear spring ensures that the clutch opens when zero pressure is applied.

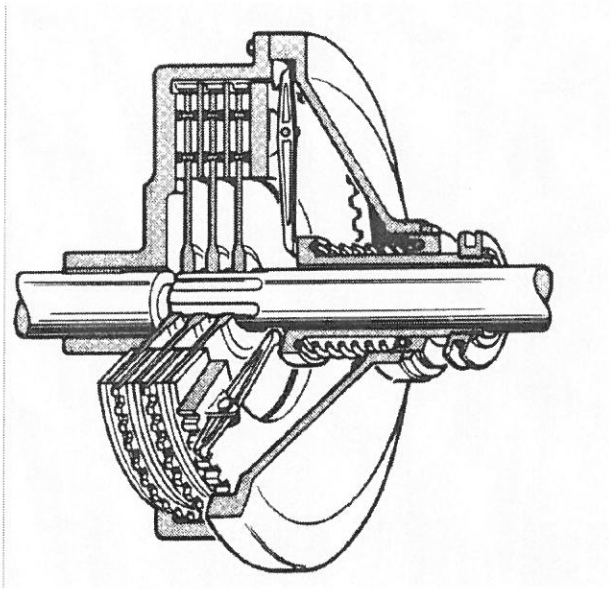

Figure 4.4 *An example of a wet multi-plate clutch. The clutch exists of axially slidable friction plates which are connected either to the engine shaft or to the primary shaft by a cottering. A piping in the primary shaft brings oil in the clutch piston. The clutch can transmit torque as soon as the plates make contact (Source: [Hur 94]).*

The clutch is described as a modulated friction element. If the clutch plates are infinitely stiff (with respect to compression) and never loose contact, the clutch is considered to be ideal. For an ideal clutch, the maximal torque T_{max} that can be transmitted is determined by the applied clutch pressure p_{cl} and equal to:

$$T_{max} = n_{cl}\mu_{cl}A_{cl}R_{cl}\eta_{cl}(p_{cl} - p_{cl,0}) \tag{4.5}$$

Table 4.1 explains the meaning of the parameters. The friction coefficient μ_{cl} is determined by the absolute clutch slip $s_{N,cl} = \dot{\theta}_e - \dot{\theta}_p$ (the difference between the engine speed and the primary speed), by the oil temperature T_{oil} and by the used oil and plate material. Experiments with different oil types (Esso EZL 799 and Lubrizol, see [Van 96c]) show that the friction coefficient can be described by the following equation:

$$\mu_{cl} = (\mu_{dyn} - \mu_{stat})\text{tgh}(\nu_{cl}s_{N,cl}) + \mu_{stat}\text{sign}(s_{N,cl}) \tag{4.6}$$

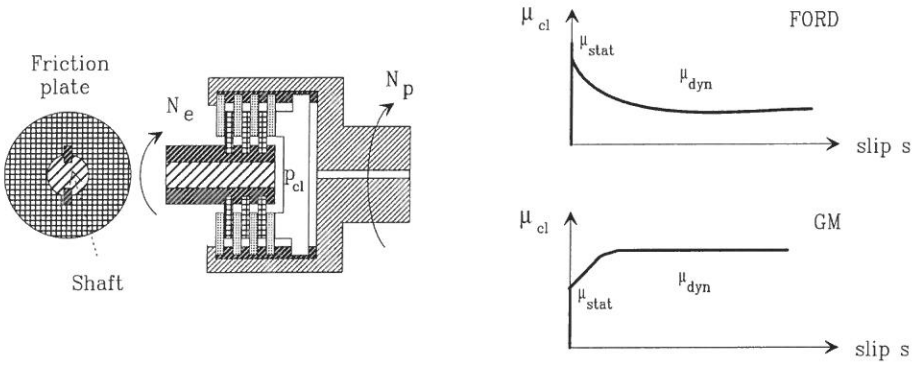

Figure 4.5 *A cross section and a longitudinal section of the wet multi-plate clutch. For reasons of clarity, only the engine shaft and a connected friction plate are shown in the cross section. For the same reasons, the spring is not shown in the longitudinal section. To guarantee smooth lock and un-lock transitions, the friction coefficient μ_{cl} must be well-designed. It seems that no optimal curve exists, since Ford asks for $\mu_{dyn} \leq \mu_{stat}$, while General Motors asks for $\mu_{dyn} \geq \mu_{stat}$ (Source: [MS 92]).*

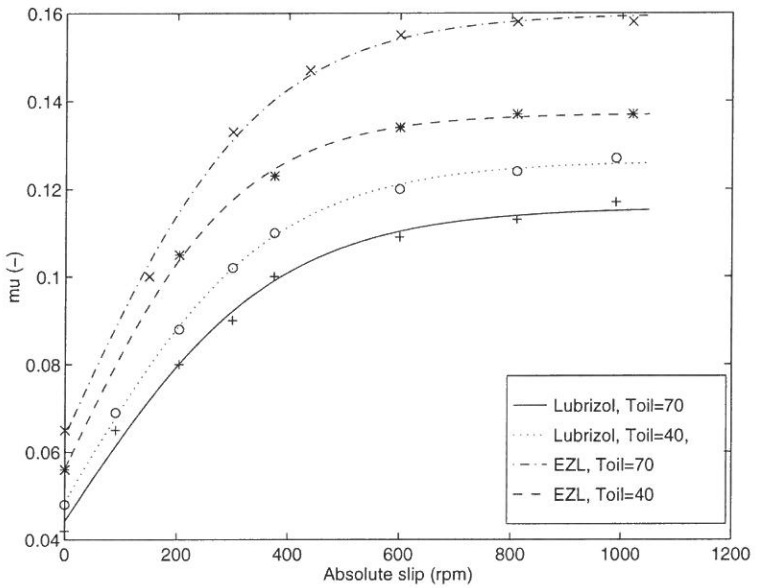

Figure 4.6 *Experimentally determined clutch friction coefficient μ_{cl} as a function of absolute clutch slip, for Esso EZL 799 and Lubrizol oil, at different temperatures (Source: [Van 96c]).*

Parameter	Meaning
$p_{cl,0}$	Minimal clutch pressure required for plate contact
A_{cl}	Pressure surface of the clutch piston
R_{cl}	Mean friction radius of a plate
n_{cl}	Number of active friction surface pairs
η_{cl}	Pressure efficiency (2.5 % loss per surface pair (see [Bak 92]))

Table 4.1 *Parameters to describe an ideal clutch.*

Parameter	EZL, 40°	EZL, 70°	Lubrizol, 40°	Lubrizol, 70°
μ_{stat}	0.0563	0.0638	0.0486	0.0443
μ_{dyn}	0.1371	0.1598	0.1263	0.1157
ν_{cl}	0.0033	0.0029	0.0028	0.0027

Table 4.2 *Friction coefficient parameters, for different types of oil (Esso EZL 799 and Lubrizol) and operating conditions ($T_{oil} = 40°$ and $T_{oil} = 70°$). EZL has positive temperature gradients, while Lubrizol has negative gradients.*

The parameters μ_{stat}, μ_{dyn} and ν_{cl} are found by solving a non linear least squares problem with the Matlab optimization toolbox (see [Mlab]). Table 4.2 shows the parameters of the two types of oil at different temperatures.

Until here, it is assumed that the clutch plates never loose contact. In practice, due to an additional clutch spring (to open the clutch at rest) and due to the finite stiffness of the clutch plate package, the clutch opens if insufficient clutch pressure is applied ($p_{cl} < p_{cl,0}$). Since the plate distance is not observed by the control unit, controlled timing of clutch engagement is difficult.

From figure 4.7, the force equation of the slidable part of the clutch is obtained, to compute the displacement x_{cl} of the clutch piston:

$$m_{cl}\ddot{x}_{cl} + b_{cl}\dot{x}_{cl} + (k_{pl}(x_{cl}) + k_{cl})x_{cl} = (p_{cl} - p_{cl,0})A_{cl} \tag{4.7}$$

The meaning of the parameters is explained in table 4.3. Note that $x_{cl} \geq 0$ implies plate contact, while $x_{cl} < 0$ implies lost contact. The force-position characteristic $F_{pl} = k_{pl}(x_{cl})x_{cl}$ of the VT1 clutch package has been determined experimentally (see [Van 96d] and figure 4.8). The other parameters are obtained

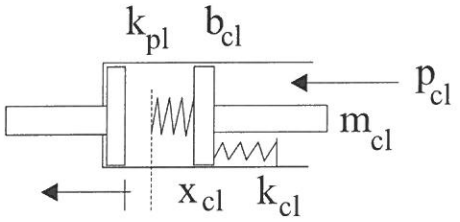

Figure 4.7 *A functional model for clutch piston displacement. The non-contact spring represents the stiffness of the clutch plate package. The make-contact situation is the reference position for the displacement x_{cl} of the clutch piston. For $x_{cl} \geq 0$, the clutch plates are in contact and compressed. For $x_{cl} < 0$, the clutch plates loose contact and no torque is transmitted.*

Parameter	Meaning
m_{cl}	Mass of the slidable clutch part
b_{cl}	Viscous damping between piston and housing
k_{cl}	Stiffness of the additional clutch spring

Table 4.3 *Additional parameters of a non-ideal clutch.*

from technical drawings and clutch engagement experiments and are included in table 4.4.

If this effect is taken into account, the instantaneous maximal torque that is transmitted equals:

$$T_{max} = n_{cl}\mu_{cl}R_{cl}\eta_{cl}k_{pl}(x_{cl})x_{cl} \tag{4.8}$$

with x_{cl} computed from the force equation.

The clutch inertia is equally distributed to the engine rotation inertia I_e and to the primary rotation inertia I_p.

4.2.3 The torque converter

A torque converter (see figure 4.9) exists of an impeller, a turbine and a stator, mounted in the same housing. In most conditions, the driving member (impeller) rotates faster than the driven member (turbine). At start-up, large differences exist between the kinetic energy of the fluid in the driving and driven members.

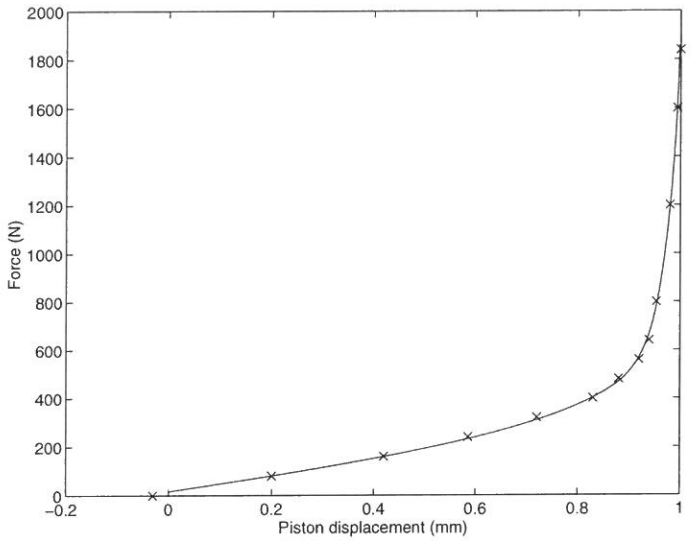

Figure 4.8 *The experimentally determined force-displacement characteristic of the VT1 clutch plate package relates the force $k_{pl}(x_{cl})x_{cl}$ to the clutch piston displacement x_{cl}. The test has been repeated 10 times, to check for hysteresis. No significant hysteresis has been detected (Source: [Van 96d])*

This difference is given as an input to the turbine. The fluid exits the impeller due to centrifugal forces, enters the turbine near its outer circumference and forces liquid from the turbine into the impeller near the inner circumference. The circulation continues as long as there is a difference in speed between the impeller and the turbine. The stator consists of a set of vanes, fixed in the housing, that redirect fluid flow from the turbine back against the impeller. This helps to turn the impeller (the engine) which in turn pushes the turbine, effectively multiplying the engine torque (see [Hur 94], [Got 91]).

Define the speed ratio $s_{N,tc}$ as $s_{N,tc} = \frac{\dot{\theta}_p}{\dot{\theta}_e}$. In practice, two static characteristics are sufficient to describe the torque converter (see [Hur 94]). Experimental data of a Daikin YT220 torque converter are taken from [Hel 94].

- The torque ratio $M_{tc}(s_{N,tc})$ is determined by the speed ratio (see figure 4.10). It relates the delivered output torque $T_{tc,out}$ to the applied input torque $T_{tc,in}$:

$$T_{tc,out} = T_{tc,in} M_{tc}(s_{N,tc}) \tag{4.9}$$

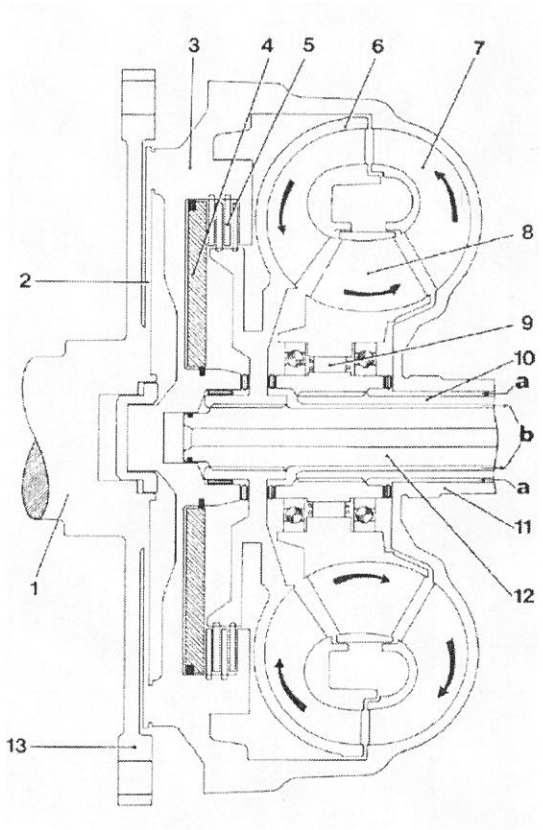

Figure 4.9 *Cross section of a modern torque converter. Different components can be observed: driving shaft (1), lock-up clutch (5), turbine (6), pump (7), stator (8) and driven shaft (10,12) (Source: [Got 91]).*

- The capacity factor $S_{tc}(s_{N,tc})$ is also determined by the speed ratio (see figure 4.11). It relates the applied input torque $T_{tc,in}$ to the engine rotation speed $\dot{\theta}_e$:

$$T_{tc,in} = \dot{\theta}_e^2 S_{tc}(s_{N,tc}) \tag{4.10}$$

Except for the lockup facility, this type of coupling has no true control input and the characteristics can only be changed by changing the geometry.

As for the multi-plate clutch, the inertia of the torque converter is distributed to the engine inertia I_e and the primary inertia I_p.

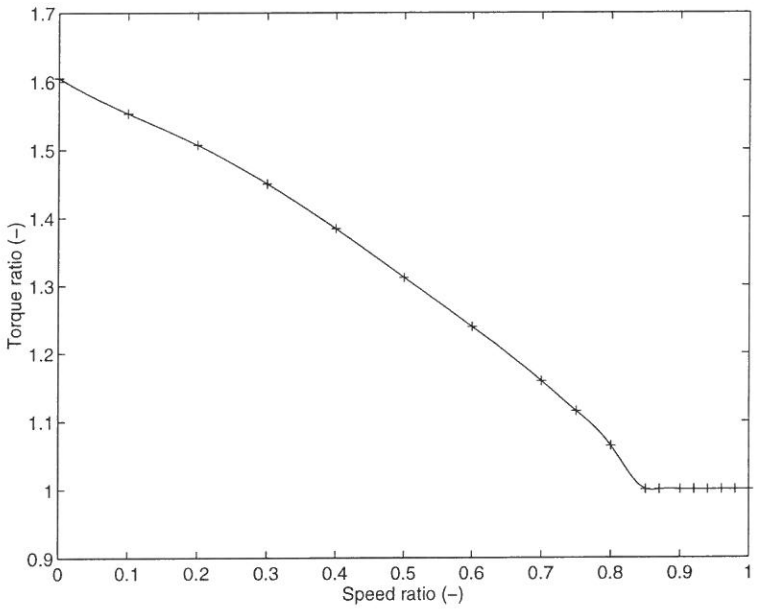

Figure 4.10 *Experimentally determined torque ratio $M_{tc}(s_{N,tc})$ as a function of speed ratio $s_{N,tc}$, for a Daikin YT220 torque converter. Only at low slip ratios, the effect of torque multiplication is present (maximal 1.6 at zero slip ratio). Due to the torque multiplication effect, high initial car acceleration is guaranteed (Source: [Hel 94]).*

4.2.4 The gear pump

In a CVT, the gear pump is driven by the combustion engine. The load torque T_{gp} of the pump is proportional to pump speed and pump pressure difference (see [Mer 67]). Experiments on a 12 mm pump show the presence of an additional static friction torque (see [Van 96e]). Therefore, the gear pump is modelled as:

$$T_{gp} = K_{T,N}\dot{\theta}_e + K_{T,p}p_{gp} + K_{T,0} \tag{4.11}$$

Linear total least squares are used to compute the coefficients $K_{T,N}$, $K_{T,p}$ and $K_{T,0}$ from experimental data of a 12 mm gear pump (see [VHV 91], [Van 96e]). The estimated parameters are included in table 4.4

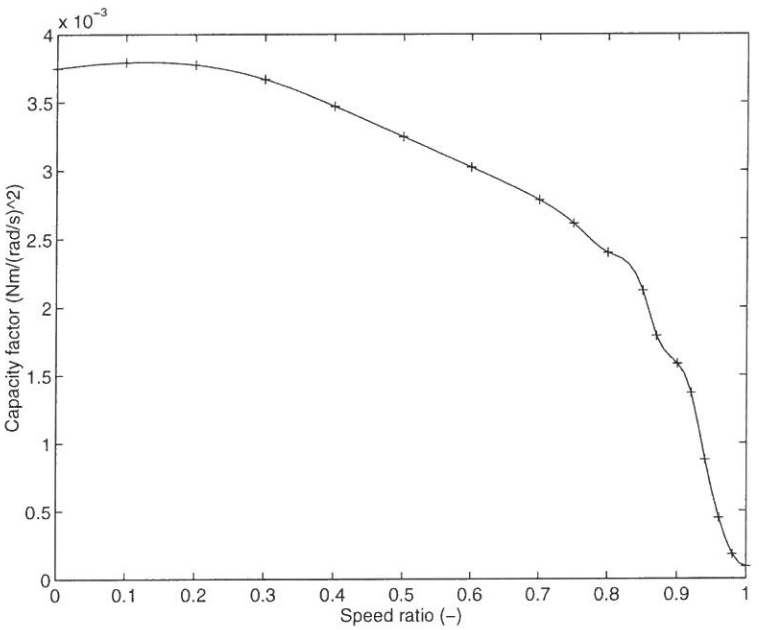

Figure 4.11 *The experimentally determined capacity factor $S_{tc}(s_{N,tc})$ as a function of the speed ratio $s_{N,tc}$, for a Daikin YT220 torque converter. At higher slip ratios, the capacity factor reduces drastically, which guarantees small slip speeds (and thus low inherent power losses) when no lockup facility is available (Source: [Hel 94]).*

The pump inertia is included in the engine inertia I_e, while the internal friction is included in the pump coefficient $K_{T,N}$.

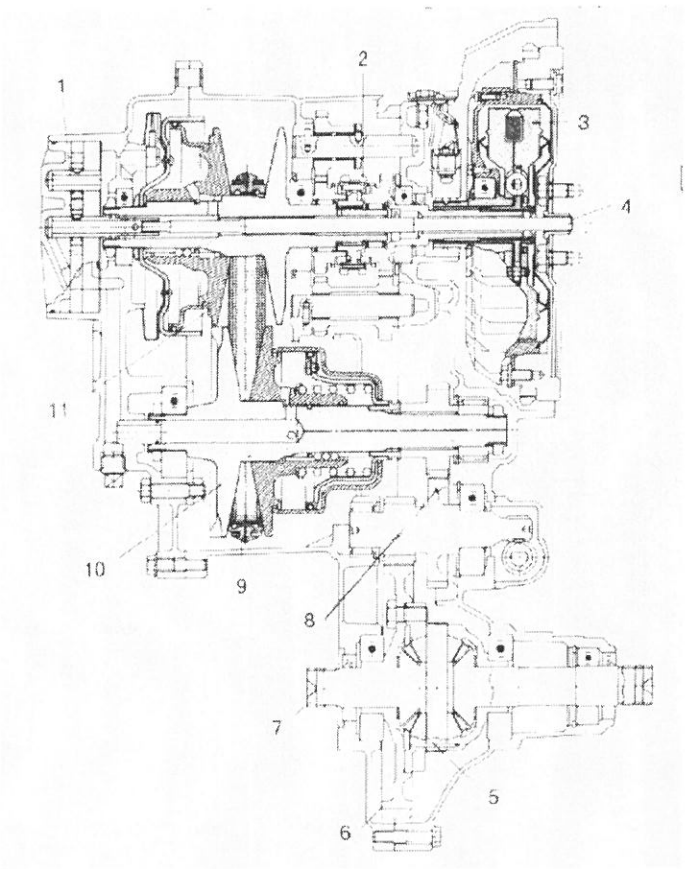

Figure 4.12 *A modern push-belt variator. Different components can be observed: oil pump (1), forward-backward selector (2), powder clutch (3), engine shaft (4), differential gears (5), final drive reduction (6,8), driven shaft (7), push-belt (9), secondary pulleys (10) and primary pulleys (11) (Source: [MS 92]).*

4.2.5 The push-belt variator

The push-belt variator (see figure 4.12) is the heart of the CVT. The circumferential force of the driving torque T_p at the primary pulley is transmitted by a flexible medium (a steel V-belt) to the secondary pulley. The metal belt exists of strings and links. To obtain flexibility, the links can rotate relatively to each other. Force is transmitted from one link to another, through the line contact of neighbouring links. Strings are used to connect the links and to avoid nodding of the belt. Compactness, efficiency, a longer life time and the possibility to transmit higher torques are the major advantages over the classical rubber-belt variator.

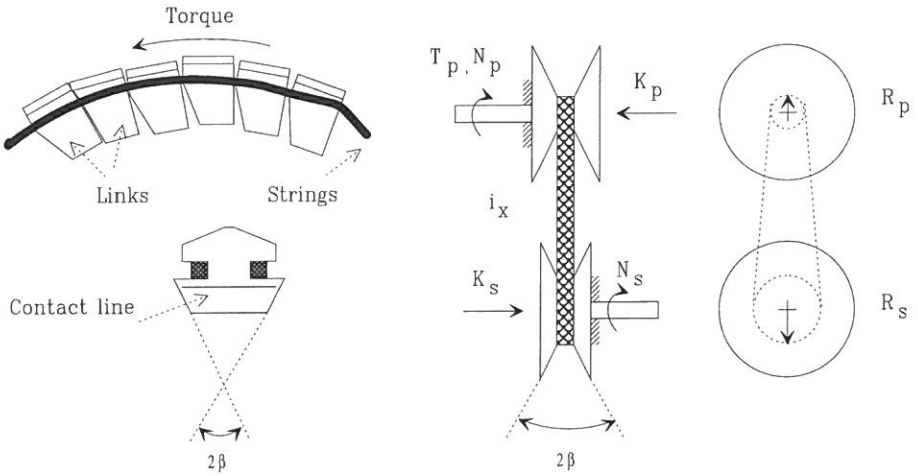

Figure 4.13 *To transmit power, a push-belt variator uses a belt that exists of metal links and metal strings. Power is transmitted by pushing, through the line contact of neighboring links. The variator ratio $i_v = R_s/R_p$ can be changed by the axial forces K_p and/or K_s.*

The ratio between the secondary running radius R_s and the primary running radius R_p is equal to the variator ratio i_v. This ratio is adjusted by axial shifting of the movable half of one of both conical pulley sheaves. Reducing the primary axial force K_p has the same effect as increasing the secondary axial force K_s, and vice versa (see 4.13).

The variator is modeled as a modulated transformer with a variable transformation ratio i_v. The ratio i_v varies between a minimal ratio (OD) and a maximal ratio (LOW), which depend on the geometry of the variator and the belt. A constant torque efficiency η_v might be assumed when electronic control is applied

(see [Gie 89], [Spijk 94], [Dev 93], [Rek 90], [SVR 92]). It holds that:

$$T_s = \eta_v i_v T_p \tag{4.12}$$
$$\dot{\theta}_p = i_v \dot{\theta}_s \tag{4.13}$$

with T_p being the applied primary torque and T_s the torque that is delivered to the secondary side. Experiments on a VT1-transmission indicate that efficiency varies with the operating point and that the rate of ratio change is limited by oil flow requirements. These practical issues will be discussed in detail in Chapter 5.

The inertia of the primary axle and the inertia of the primary pulley are included in the rotational inertia I_p, that rotates at primary speed, while the inertia of the secondary pulley, the inertia of the secondary axle and half of the pinion gears inertia are combined in a single rotational inertia I_s, that rotates at secondary speed. All friction losses (bearings, belt-pulley contact, string-link contact) are taken into account by the torque efficiency η_v.

4.2.6 The pinion gear

The pinion gear, also referred to as the final drive reduction, is a gear-box with a fixed ratio, mounted between the secondary side of the CVT and the drive axle. It is described as a transformer with a fixed ratio i_{FD}:

$$T_{FD,out} = i_{FD} T_{FD,in} \tag{4.14}$$
$$\dot{\theta}_s = i_{FD} \dot{\theta}_{FD} \tag{4.15}$$

with $T_{FD,in}$ the input torque of the gear-box, $T_{FD,out}$ the output torque of the gear-box and $\dot{\theta}_{FD}$ the output speed of the gear-box. The inertia of the gears is distributed to the secondary inertia I_s and the car inertia I_{tot}.

4.2.7 The drive axle

The compliance of the drive axle is modeled by a linear torsion spring with a stiffness c_{fa}. The drive torque M_{fw} applied at the front wheel is computed from:

$$M_{fw} = c_{fa}(\theta_{FD} - \theta_f) \tag{4.16}$$

The inertia of the shaft is added to the car inertia I_{tot}. Material damping is neglected.

4.3 Drive train modeling

As discussed in the previous section, the following phenomena have been taken into account:

- The engine is described as a nonlinear torque source, modulated by the engine speed and the throttle position.
- The flywheel inertia, the pump inertia, half of the clutch inertia and the inertia of the torsion damper are combined in a single rotational inertia I_e, that rotates at engine speed.
- The clutch is described as a nonlinear friction element, modulated by the clutch pressure and the clutch slip.
- Half of the clutch inertia, the inertia of the primary axle and the inertia of the primary pulley are combined in a single rotational inertia I_p, that rotates at primary speed.
- The variator is described as a variable transformer with a fixed torque efficiency.
- The inertia of the secondary pulley, the inertia of the secondary axle and half of the pinion gears inertia is combined in a single rotational inertia I_s, that rotates at secondary speed.
- The pinion gear-box is described as a fixed transformer with no torque losses.
- The drive axle is modeled as a linear torsional spring.
- The total car inertia, reduced to the wheels, half of the pinion gear inertia and the drive axle inertia are combined in a single rotational inertia I_{tot}, that rotates at wheel speed.
- The total load torque is reduced to the wheels and contains roll and air resistances, load due to road slope and brake torque.

An overview and typical parameter values for Volvo 480, equipped with a VT1H transmission (oil, pump, clutch, variator and pinion), are given in table 4.4.

	Meaning	Value	Units
c_{fa}	Torsion stiffness of driving axle	50000	Nm/rad
I_e	Inertia of engine and flywheel	0.1584	kgm^2
I_p	Inertia of primary system	0.0355	kgm^2
I_s	Inertia of secondary system	0.0186	kgm^2
μ_{stat}	Static friction coefficient	0.0638	-
μ_{dyn}	Dynamic friction coefficient	0.1598	-
ν_{cl}	Clutch slip coefficient	0.0029	s/rad
η_v	Torque efficiency of the variator	0.95	-
i_{FD}	Final drive reduction	5.76	-
$K_{T,N}$	Speed coefficient of gear pump	2.356e-3	s/rad
$K_{T,p}$	Pressure coefficient of gear pump	0.141e5	1/Pa
$K_{T,0}$	Offset torque of gear pump	0.350	Nm
η_{cl}	Torque efficiency of clutch	0.85	-
n_{cl}	Number of surface pairs	6	-
R_{cl}	Effective radius of the clutch	0.074	m
A_{cl}	Effective surface of the clutch	4.488e-3	m^2
$p_{cl,0}$	Offset pressure of the clutch	2e4	Pa
m_{cl}	Mass of the slidable clutch part	1	kg
b_{cl}	Viscous damping between piston and housing	1125	Ns/m
k_{cl}	Stiffness of the additional clutch spring	90000	N/m
LOW	Variator ratio in low	2.47	-
OD	Variator ratio in overdrive	0.445	-

Table 4.4 *Drive train parameters of a Volvo 480, equipped with a VT1-H transmission (Esso EZL 799 oil (T_{oil} = 70°), 12 mm gear pump, wet multi-plate clutch, variator and pinion).*

4.3.1 A physical model of the drive train

Writing the torque balances of the four inertias (see figure ??) leads to the following equations:

$$I_e\ddot{\theta}_e = T_{e,dyn} - T_{gp} - T_{cl} \quad (4.17)$$

$$I_p\ddot{\theta}_p = T_{cl} - T_p \quad (4.18)$$

$$I_s\ddot{\theta}_s = T_s - T_{FD,in} \quad (4.19)$$

$$I_{tot}\ddot{\theta}_f = T_{FD,out} - R_{tot}\dot{\theta}_f^2 - T_{ext} - T_{brake} \quad (4.20)$$

T_{brake} is the braking torque, applied by the driver and T_{cl} is the torque that is effectively transmitted through the clutch[1]. Combining the component equations 4.1 till 4.16 with the torque balances leads to a set of coupled algebraic and differential equations, which implies that elimination of variables is required to prevent simulation problems. Define the front wheel axle deformation ϵ_{fa} as the relative deformation over the torsional spring:

$$\epsilon_{fa} = \theta_{FD} - \theta_f \tag{4.21}$$

By taking the time derivative of the speed equation 4.13 of the variator, it follows that:

$$\ddot{\theta}_s = \frac{\ddot{\theta}_p}{i_v} - \frac{\dot{\theta}_p}{i_v^2}\frac{di_v}{dt} \tag{4.22}$$

Combining this equation with the torque equation 4.12 of the variator and the torque balances 4.18 and 4.19 of the primary and secondary inertias finally gives:

$$(I_p + \frac{I_s}{\eta_v i_v^2})\ddot{\theta}_p = T_{cl} - \frac{c_{fa}\epsilon_{fa}}{\eta_v i_{FD} i_v} + \frac{\dot{\theta}_p I_s}{\eta_v i_v^3}\frac{di_v}{dt} \tag{4.23}$$

$$T_s = \frac{I_s}{i_v}\ddot{\theta}_p - \frac{I_s\dot{\theta}_p}{i_v^2}\frac{di_v}{dt} + \frac{c_{fa}}{i_{FD}}\epsilon_{fa} \tag{4.24}$$

By combining the drive axle equation 4.16 with the torque balances 4.18 and 4.20 of the secondary inertia and the car inertia, the following equation is obtained:

$$\ddot{\epsilon}_{fa} = \frac{T_s}{i_{FD} I_s} - c_{fa}(\frac{1}{I_s i_{FD}^2} + \frac{1}{I_{tot}})\epsilon_{fa} + \frac{R_{tot}}{I_{tot}}(\frac{\dot{\theta}_p}{i_v i_{FD}} - \dot{\epsilon}_{fa})^2 + \frac{T_{ext} + T_{brake}}{I_{tot}}$$

[1]To compute the torque T_{cl}, two clutch operation modes must be considered (stick and slip). When the clutch is unlocked (slip), T_{cl} equals T_{max} which is computed from the earlier derived clutch equations. When the clutch is locked (stick), T_{cl} is computed as the minimum of the maximal clutch torque T_{max} and the lockup torque T_{lockup} (the torque that is required to keep the engine speed and the primary speed equal). For more details, we refer to [Sim 96] and [GM 89].

Elimination of the secondary torque T_s gives:

$$\begin{aligned} I_{p,eq}\ddot{\epsilon}_{fa} &= \frac{T_{cl}}{i_v i_{FD}} - c_{fa}\left(\frac{1}{\eta_v i_v^2 i_{FD}^2} + \frac{I_{p,eq}}{I_{tot}}\right)\epsilon_{fa} - \left(\frac{I_p \dot{\theta}_p}{i_{FD} i_v^2}\right)\frac{di_v}{dt} \\ &\quad + \frac{I_{p.eq} R_{tot}}{I_{tot}}\left(\frac{\dot{\theta}_p}{i_v i_{FD}} - \dot{\epsilon}_{fa}\right)^2 + \frac{I_{p,eq}}{I_{tot}}(T_{ext} + T_{brake}) \end{aligned}$$

with the equivalent primary inertia $I_{p,eq}$ given by:

$$I_{p,eq} = I_p + \frac{I_s}{\eta_v i_v^2}$$

The non linear differential equations that describe the drive train are summarized below:

$$I_e \ddot{\theta}_e = T_{e,dyn} - T_{gp} - T_{cl} \tag{4.25}$$

$$I_{p,eq}\ddot{\theta}_p = T_{cl} - \frac{c_{fa}\epsilon_{fa}}{\eta_v i_{FD} i_v} + \frac{\dot{\theta}_p I_s}{\eta_v i_v^3}\frac{di_v}{dt} \tag{4.26}$$

$$\begin{aligned} I_{p,eq}\ddot{\epsilon}_{fa} &= \frac{T_{cl}}{i_v i_{FD}} - c_{fa}\left(\frac{1}{\eta_v i_v^2 i_{FD}^2} + \frac{I_{p,eq}}{I_{tot}}\right)\epsilon_{fa} - \left(\frac{I_p \dot{\theta}_p}{i_{FD} i_v^2}\right)\frac{di_v}{dt} \\ &\quad + \frac{I_{p,eq}}{I_{tot}}\left(R_{tot}\left(\frac{\dot{\theta}_p}{i_v i_{FD}} - \dot{\epsilon}_{fa}\right)^2 + T_{ext} + T_{brake}\right) \end{aligned} \tag{4.27}$$

The clutch pressure p_{cl} (that determines the clutch torque T_{cl}) and the rate of ratio change $\frac{di_v}{dt}$ of the variator are considered as control inputs and are elements of the control input vector $\mathrm{U} = (u_1, u_2)'$.

The slope and brake torques and the throttle position (that partially determines the delivered engine torque) act as disturbances and are elements of the disturbance vector $\mathrm{W} = (w_1, w_2)'$:

$$\begin{aligned} u_1 &= p_{cl} \\ u_2 &= \frac{di_v}{dt} \\ w_1 &= T_{ext} + T_{brake} \\ w_2 &= \alpha_{th} \end{aligned}$$

The state vector X_{dt} of the drive train is given by:

$$X_{dt} = \begin{pmatrix} \dot{\theta}_e & \dot{\theta}_p & \epsilon_{fa} & \dot{\epsilon}_{fa} & i_v \end{pmatrix}'$$

The engine torque $T_{e,dyn}$, the gear pump torque T_{gp} and the transmitted clutch torque T_{cl} are non linear functions of the system states. When a torque converter is used instead of a wet multi-plate clutch, the following adaptations are required:

- In the engine equation, T_{cl} must be replaced with $T_{tc,in}$.
- In the equivalent primary equation, T_{cl} must be replaced with $T_{tc,out}$.
- The characteristics of the torque converter (torque ratio and capacity factor) must be used to compute $T_{tc,in}$ and $T_{tc,out}$.
- Only u_2 remains as a control input.

The generic drive train model described by equations 4.25, 4.26 and 4.27 is implemented in Matlab/Simulink and tuned for a wide variety of applications, to compute fuel economy, dynamic performance and comfort for the various customers and potential customers of VCST. Actually, 9 engines, 2 coupling devices, 6 variators, 10 cars, 2 gear pump and 2 transmission oils are included in the VIRTUES database (see [Van 96a]).

To develop advanced model-based control strategies, reduced control models for clutch mode and variator mode are derived in the next subsections.

4.3.2 A reduced model for clutch control

In clutch mode, it is assumed that the variator is not shifting (i_v remains LOW). Assuming that the drive axle is infinitely stiff, the model reduces to:

$$I_e \ddot{\theta}_e = T_{e,dyn} - T_{gp} - T_{cl} \tag{4.28}$$

$$I_{p,eqr} \ddot{\theta}_p = T_{cl} - \frac{R_{tot}}{\eta_v i_v^3 i_{FD}^3} \dot{\theta}_p^2 - \frac{T_{ext} + T_{brake}}{\eta_v i_v i_{FD}} \tag{4.29}$$

with

$$I_{p,eqr} = I_p + \frac{I_s}{\eta_v i_v^2} + \frac{I_{tot}}{\eta_v i_v^2 i_{FD}^2}$$

In Section 4.4, this model is used to derive an advanced model-based clutch controller.

4.3.3 A reduced model for variator control

In variator mode, it is assumed that the clutch is locked (no clutch slip). Assuming that the drive axle is infinitely stiff, the model reduces to:

$$\begin{aligned} I_{e,eqr}\ddot{\theta}_e &= T_{e,dyn} - T_{gp} + \frac{I_s i_{FD}^2 + I_{tot}}{\eta_v i_v^3 i_{FD}^3}\frac{di_v}{dt}\dot{\theta}_e \\ &\quad - \frac{R_{tot}}{\eta_v i_v^3 i_{FD}^3}\dot{\theta}_e^2 - \frac{T_{ext} + T_{brake}}{\eta_v i_v i_{FD}} \end{aligned} \tag{4.30}$$

with

$$I_{e,eqr} = I_e + I_p + \frac{I_s i_{FD}^2 + I_{tot}}{\eta_v 1_v^2 i_{FD}^2}$$

In Section 4.4, this model is used to derive an advanced model-based variator controller.

4.4 Drive train control

In the literature, a wide variety of control concepts for CVTs is proposed (see [Spijk 94], [COYVBJF 84], [FM 92], [GS 95], [LRWK 93]). Although advantageous from multiple points of view, the proposed strategies also have some disadvantages for transmission suppliers:

- The strategies can only be implemented using digital control techniques and require a huge amount of computations. For being effective, sampling frequencies of at least 250 Hz are required. This requires dedicated ECUs, sensors and actuators, too expensive for series production.
- The drive torque needs to be measured (vulnerable) or estimated.
- An ideal hydraulic actuation unit is assumed (no interactions with the drive train, decoupled steering outputs).

In this thesis, the concept of variogram control is introduced. It is rather easy to implement (either hydraulically or digitally) and needs no expensive ECU nor drive torque information when implemented in a digital way. In practice, only speed and pressure measurements are required.

4.4.1 Drive train management via variogram control

From the engine characteristics, optimal engine rotation speeds with respect to power production or fuel consumption can be derived for each throttle position α_{th}:

$\dot{\theta}_{e,P}(\alpha_{th})$: optimal engine speed w.r.t. power production
$\dot{\theta}_{e,\Phi}(\alpha_{th})$: optimal engine speed w.r.t. fuel consumption

These optimal speeds form optimal operating lines for the engine (see [NSS 90]). Notice that only a CVT is able to track these operating lines, since continuous shifting capabilities are required to do so (see figures 4.14 and 4.15).

In theory, these engine speeds can be realized independent from vehicle speed. In practice, smoothing is required to meet comfort specifications. In the variogram, the desired engine speed is shown as a function of vehicle speed and throttle position. An economy variogram for a B18U engine is shown in figure 4.16. For a given application (engine-variator-car and specifications), the variogram is treated as a control parameter that must be tuned. Once the optimal variogram is designed, it is the task of the drive train control unit to realize variogram tracking.

For a drive train with an electronically controlled CVT, the proposed control configuration for variogram tracking is shown in figure 4.17. Table 4.5 summarizes the proposed strategy. In theory, the feedback controllers are formed by simple linear controllers, followed by linearizing controllers obtained from feedback linearization. In practice, gain scheduled PI-controllers are implemented due to cost constraints. At this moment, advanced feedback linearization controllers are being implemented on the power test rig at VCST.

In clutch mode, the clutch is controlled, to realize the desired shifting traject, while the variator remains in LOW. Throttle dependent stall speeds (engine speed control at zero car speed) and smooth acceleration/deceleration at low vehicle speeds are the major goals. In variator mode, the variator is controlled to realize variogram tracking. Reduced fuel consumption and increased dynamic performance are the major goals.

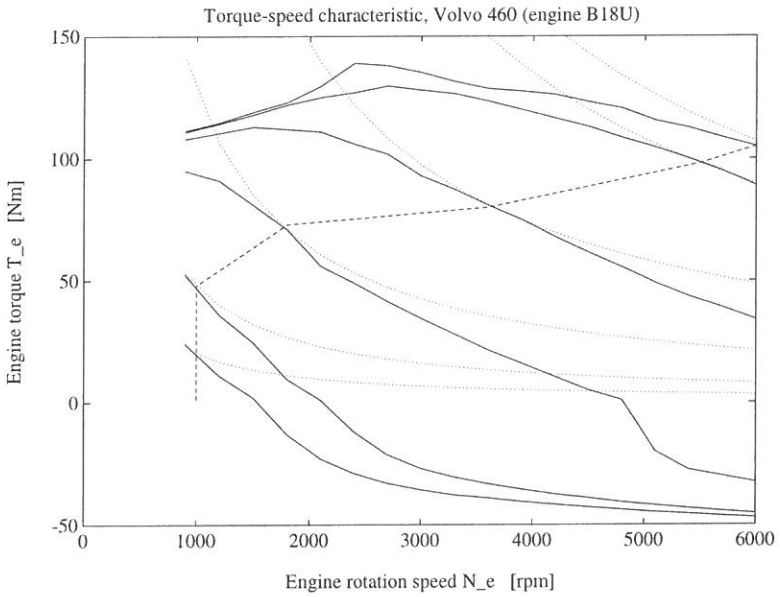

Figure 4.14 *The experimentally determined torque-speed characteristic* $T_e(\theta_e, \alpha_{th})$ *(solid, different throttle positions) and the optimal operating line for sport mode, i.e. maximal power production, for a B18U engine (dashed). Lines of constant power production are shown also (dotted). In sport mode, high engine speeds are required to increase dynamic performance. (Source: VCST)*

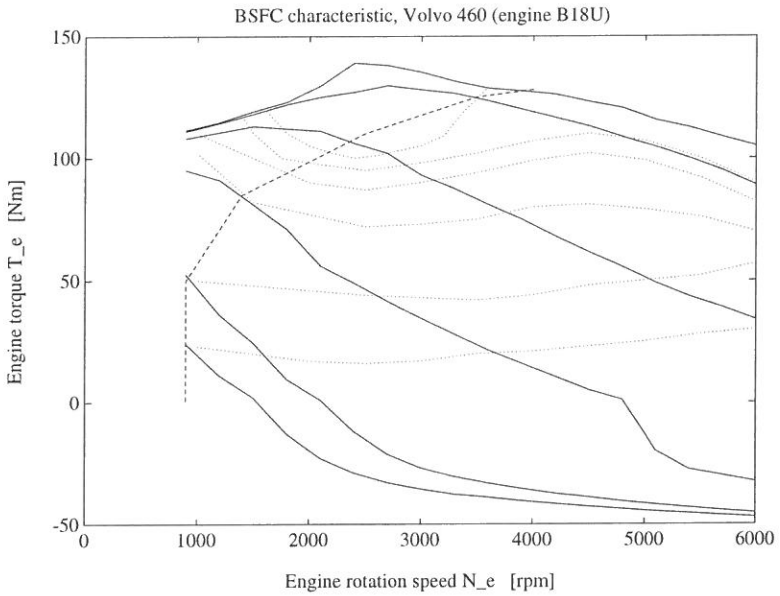

Figure 4.15 *The experimentally determined fuel consumption characteristic $\Phi_e(T_e, \dot{\theta}_e)$ (dotted, lines of constant specific fuel consumption) and the optimal operating line for economy mode, i.e. minimal fuel consumption, for a B18U engine (dashed). Lines of constant throttle position are shown also (solid). In economy mode, low engine speeds are required to decrease fuel consumption (Source: VCST).*

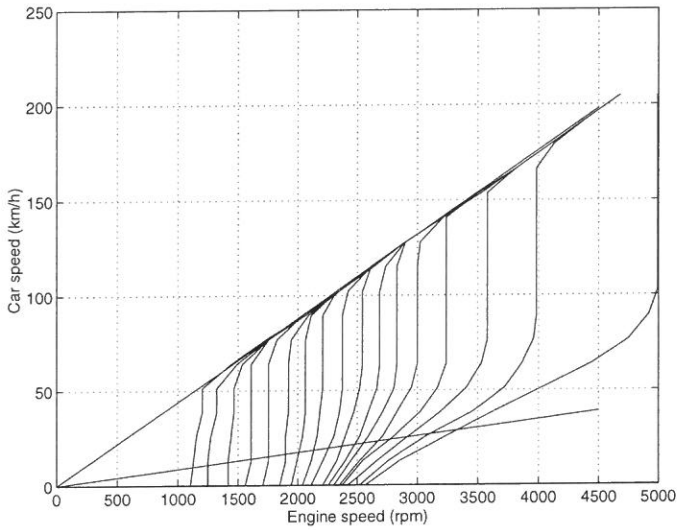

Figure 4.16 *An economy variogram for a B18U engine. The straight lines from the origin represent LOW (lowest line) and OD (highest line) and form the boundaries of the CVT's operation region. The other lines show how the desired engine speed varies with car speed, for different throttle positions. Smoothing near LOW and OD is required for drive comfort. Two-stage engagement is minimized due to throttle dependent stall speeds (Source: VCST).*

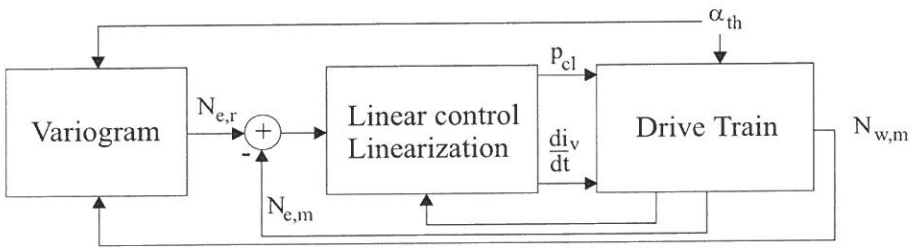

Figure 4.17 *Variogram control: the reference engine rotation speed $N_{e,r}$ is obtained from the measured wheel speed $N_{w,m}$, the measured throttle position α_{th} and the variogram. This reference speed is compared with the measured engine rotation speed $N_{e,m}$. Linear controllers, followed by output feedback linearization controllers can be used to compute the clutch control signal p_{cl} and the variator control signal i_v.*

Mode	Computation of p_{cl}	Computation of i_v
Clutch mode $\frac{\dot{\theta}_{p,m}}{\dot{\theta}_{f,m}} >$ LOW	From $\dot{\theta}_{e,r} - \dot{\theta}_{e,m}$ Linear control and feedback linearization	Keep $i =$ LOW
Variator mode $\frac{\dot{\theta}_{p,m}}{\dot{\theta}_{f,m}} <$ LOW	Sufficiently high to lock	From $\dot{\theta}_{e,r} - \dot{\theta}_{e,m}$ Linear control and feedback linearization

Table 4.5 *The proposed control strategy for drive train control. The subscripts m and r refer to measured and reference values.*

4.4.2 An algorithm for control in clutch mode

In clutch mode, the variator remains in LOW, while the clutch pressure p_{cl} is varied to control the engine speed $\dot{\theta}_e$ as required by the reference variogram. The control model for clutch mode looks like:

$$I_e \ddot{\theta}_e = T_{e,dyn} - T_{gp} - T_{cl} \tag{4.31}$$

$$I_{p,eqr} \ddot{\theta}_p = T_{cl} - \frac{R_{tot}}{\eta_v i_v^3 i_{FD}^3} \dot{\theta}_p^2 - \frac{T_{ext} + T_{brake}}{\eta_v i_v i_{FD}} \tag{4.32}$$

with

$$I_{p,eqr} = I_p + \frac{I_s}{\eta_v i_v^2} + \frac{I_{tot}}{\eta_v i_v^2 i_{FD}^2}$$

This model is used to design a clutch controller. Equation 4.5 relates the clutch torque T_cl to the clutch pressure p_{cl}. By applying output feedback linearization (see [SL 91]), the control signal $u_1 = p_{cl}$ can finally be computed as:

$$u_1 = p_{cl} = p_{cl,0} + \frac{-I_e v_1 + T_{e,dyn} - T_{gp}}{n_{cl}\mu_{cl}A_{cl}R_{cl}\eta cl}$$

with v_1 being the signal from a linear controller, designed for the linearized system given by:

$$\begin{aligned} \dot{x} &= v_1 \\ y &= x \end{aligned}$$

By applying feedback linearization, the system reduces to a simple integrator, with input $\ddot{\theta}_e$ and state $\dot{\theta}_e$.

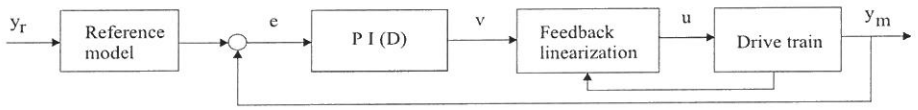

Figure 4.18 Feedback linearization and model reference CVT control: the reference engine speed $y_r = \dot{\theta}_{e,r}$ is applied to the closed loop reference model. The output of the reference model is compared with the measured engine speed $y_m = \dot{\theta}_{e,m}$ and fed to a PI-controller (in practice, there is a PI-controller for clutch mode and one for variator mode). The output v of the PI-controller(s) ($v = v_1$ for clutch mode, $v = v_2$ for variator mode) is applied to the feedback linearization block, to obtain the drive train control signal u ($u = u_1 = p_{cl}$ for clutch mode and $u = u_2 = \frac{di_v}{dt}$ for variator mode).

Although a wide variety of techniques is available to design the linear controller, we propose a model-reference controller for simplicity. The required engine speed, obtained from the variogram, is fed into a second order reference model (characterized by ζ_1 and ω_{n1}). This (internal) reference speed is compared to the measured engine speed and fed into a PI-controller. The parameters ζ_1, ω_{n1} and the PI-controller parameters are obtained from the specifications and the linear dynamics (see [Ack 93], [AW 84], [Jus 92], [Orl 94], [Per 92], [ZA 93] and [ZN 42] for model-based tuning methods for this type of controllers).

An advantage of the proposed approach is the simplicity of the controller (see figure 4.18). A disadvantage is the requirement for clutch slip measurement, to estimate μ_{cl}. The clutch slip is estimated from the difference between the measured engine speed and the measured primary speed. The engine torque $T_{e,dyn}$ and the pump torque T_{gp} are estimated from the engine and pump characteristics, since $\dot{\theta}_e$, α_{th} and p_{gp} are easily measured.

4.4.3 An algorithm for control in variator mode

In variator mode, the clutch is locked (no clutch slip). The control model for variator mode looks like:

$$I_{e,eqr}\ddot{\theta}_e = T_{e,dyn} - T_{gp} + \frac{I_s i_{FD}^2 + I_{tot}}{\eta_v i_v^3 i_{FD}^3}\frac{di_v}{dt}\dot{\theta}_e - \frac{R_{tot}}{\eta_v i_v^3 i_{FD}^3}\dot{\theta}_e^2 - \frac{T_{ext} + T_{brake}}{\eta_v i_v i_{FD}}$$

with

$$I_{e,eqr} = I_e + I_p + \frac{I_s i_{FD}^2 + I_{tot}}{\eta_v 1_v^2 i_{FD}^2}$$

This model is used to design a variator controller. By applying output feedback linearization, the control signal $u_2 = \frac{di_v}{dt}$ can now be computed as:

$$u_2 = \frac{di_v}{dt} = \frac{I_{e,eqr} v_2 + \frac{R_{tot}\dot{\theta}_e^2}{\eta_v i_v^3 i_{FD}^3} + \frac{T_{ext}+T_{brake}}{\eta_v i_v^3 i_{FD}^3} - T_{e,dyn} + T_{gp}}{\frac{I_{tot}+I_s i_{FD}^2}{\eta_v i_v^3 i_{FD}^2}\dot{\theta}_e}$$

with v_2 being the signal from the linear controller, designed for the linearized system given by:

$$\begin{aligned} \dot{x} &= v_2 \\ y &= x \end{aligned}$$

In practice, a model-reference controller is used. The required engine speed, obtained from the variogram, is fed into a second order reference model (characterized by ζ_2 and ω_{n2}). This (internal) reference speed is compared to the measured engine speed and fed into a PI-controller.

All terms in the linearization equation can be estimated from measurements and system characteristics. To estimate the torque T_{ext}, the road slope is measured and a nominal car mass m_t is assumed. The brake torque T_{brake} is easily measured on the experimental power test rig or estimated from the measured brake pedal position and the static brake characteristics. An important advantage of this controller is the absence of vulnerable torque measurements[2].

[2]Robust performance is said to become critical when dealing with output feedback linearization. In fact, the error dynamics need to be analyzed carefully ([SL 91]). This issue will be investigated in the near future, when the proposed controllers will be implemented and validated on the power test rig of VCST and in several demo cars.

4.5 A sample of results and conclusions

This Section contains a sample of results and conclusions that were obtained when doing practical computations and experiments.

- Kick-down test: VT1-H versus VT1-E (simulation)

  Figure 4.19 shows the influence of the control unit and control strategy on car motion for a Rover 216, with engine 1.6K16MPI, equipped with a VT1 variator and a wet multi-plate clutch (P811). When applying hydraulic control (VT1-H), the realized variogram is fixed and determined by the hydro-mechanical control hardware (see Chapters 5 and 6). Two stage-engagement (piece-wise linear shifting trajectory that follows LOW for a while) is important and limits drive comfort. When applying electronic control (VT1-E), the realized variogram depends on the user's specifications (economy, sport, mixed) and is determined by a look-up table in the control software (see Chapters 5 and 6). By adapting the look-up table, the performance of a car with an electronically controlled CVT can be changed easily. In this simulation, an economy variogram was used, which resulted in minimal fuel consumption, high comfort (smooth acceleration, minimal two-stage engagement) and moderate dynamic performance (compared to the potentials of a sport variogram).

- VT1-H versus VT1-F (experiments)

  Figures 4.20 and 4.21 show the influence of the control unit and control strategy on car motion for a Rover 216, with engine 1.6K16MPI, equipped with a VT1 variator and a wet multi-plate clutch (P811). When applying hydraulic control (VT1-H), the realized variogram is fixed and determined by the hydro-mechanical control hardware (see Chapters 5 and 6). Two stage-engagement (piece-wise linear shifting trajectories that follow LOW for a while) is important and limits drive comfort. When applying electronic control (VT1-F), the realized variogram depends on the user's specifications (economy, sport, mixed) and is determined by a look-up table in the control software (see Chapters 5 and 6). In these experiments, a mixed variogram was used, to obtain a good trade-off in fuel consumption, comfort (smooth acceleration, minimal two-stage engagement) and dynamic performance.

- Plate clutch versus torque converter (simulation)

  Figure 4.22 shows the influence of the coupling device (plate clutch P811 versus torque converter Daikin YT 220) on dynamic car performance. The torque converter shows higher dynamic performance (due to torque multiplication) and increased comfort (limited two-stage engagement).

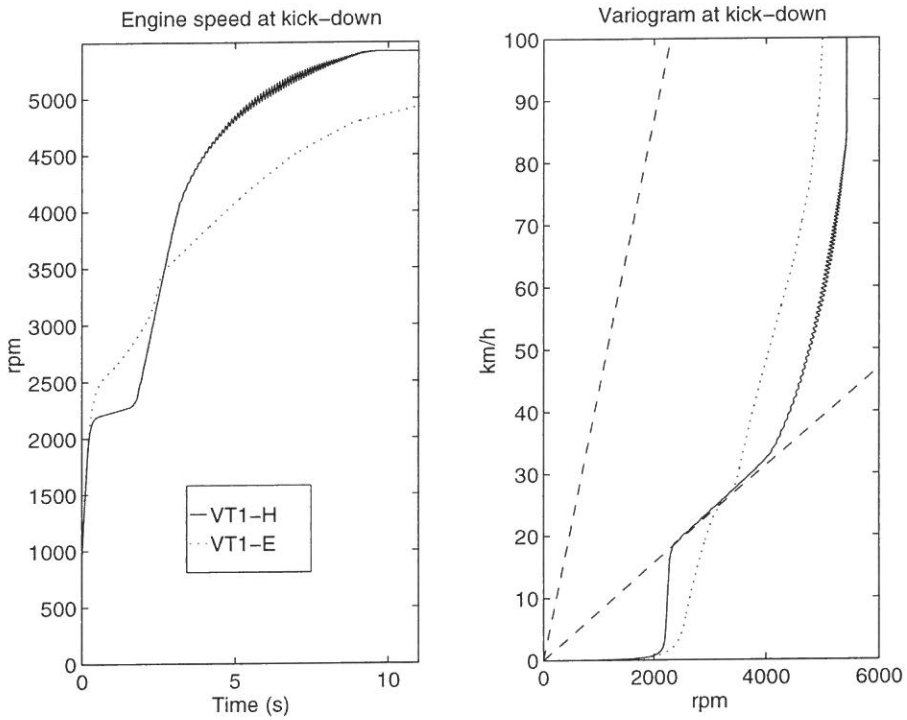

Figure 4.19 *Engine speed and realized variogram at kick-down from rest: influence of the control unit and control strategy on car motion for a Rover 216, with engine 1.6K16MPI, equipped with a VT1 variator and a wet multi-plate clutch (P811) (simulation). The oscillations in engine speed are introduced by the simulator and are absent in practical situations. By reducing the time-step for integration, these oscillations can be made arbitrarely small, at the cost of simulation time.*

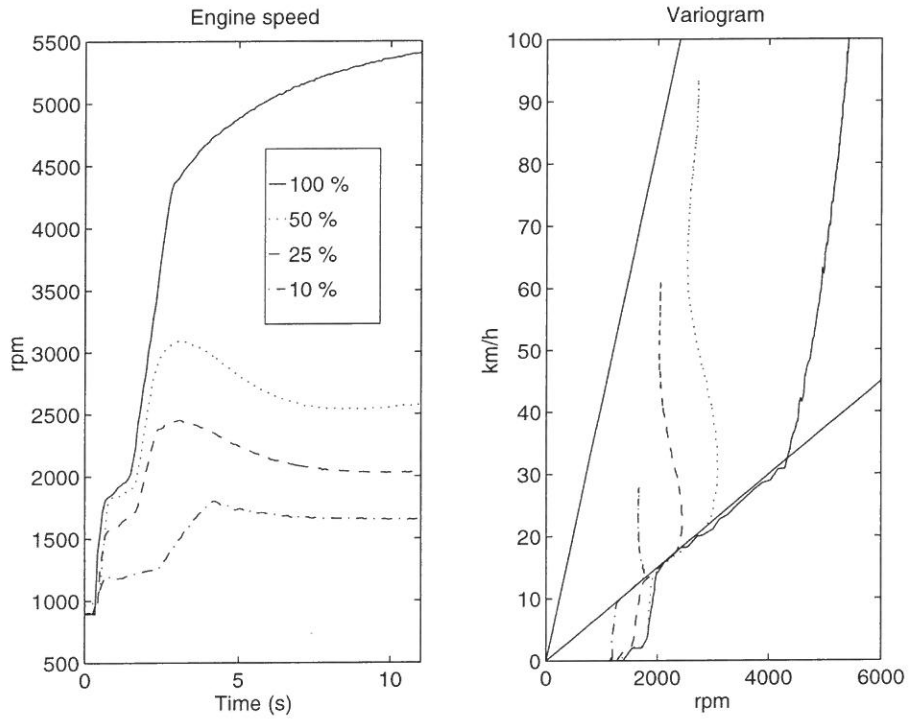

Figure 4.20 *Engine speeds and the realized variogram for different throttle positions: influence of the control unit and control strategy on car motion for a Rover 216, with engine 1.6K16MPI, equipped with a VT1-H variator and a wet multi-plate clutch (P811) (experiment).*

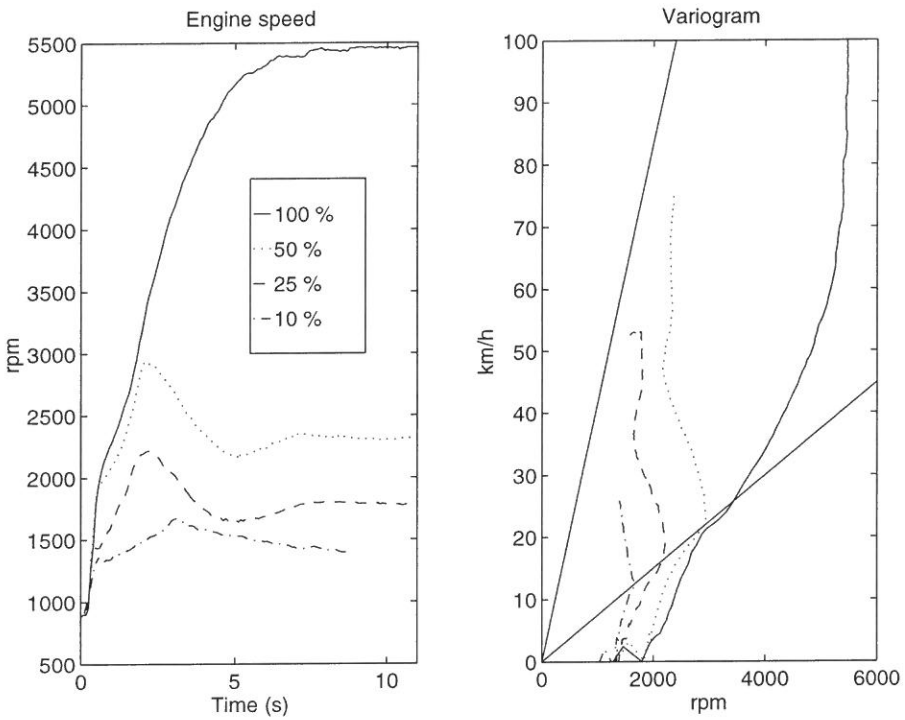

Figure 4.21 *Engine speeds and the realized variogram for different throttle positions: influence of the control unit and control strategy on car motion for a Rover 216, with engine 1.6K16MPI, equipped with a VT1-F variator and a wet multi-plate clutch (P811) (experiment).*

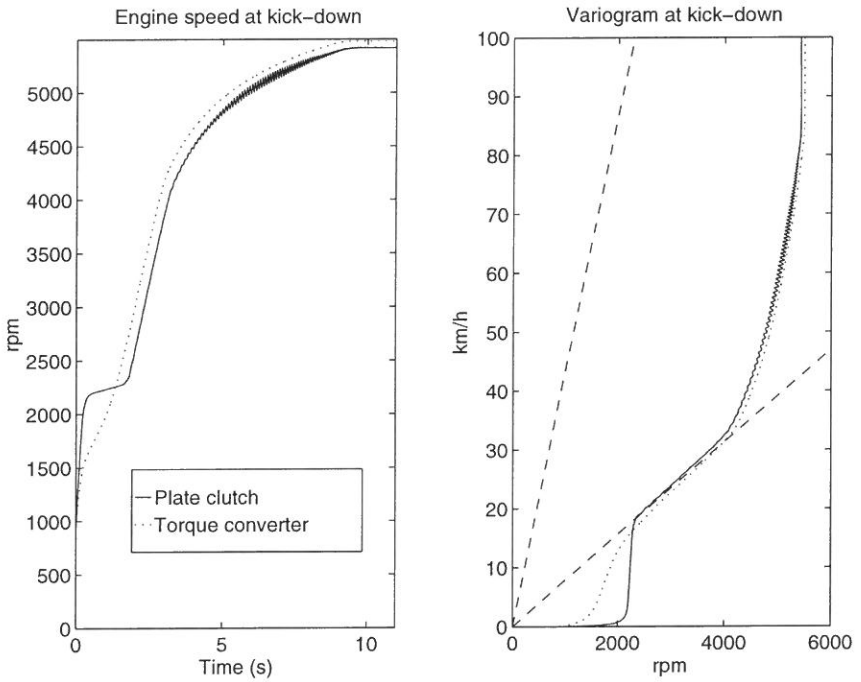

Figure 4.22 *Engine speed and the realized variogram at kickdown from rest: influence of the coupling device (plate clutch P811 versus torque converter Daikin YT 220) on dynamic car performance, for a Rover 216, with engine 1.6K16MPI, equipped with a VT1-H variator (simulation). The oscillations in engine speed are introduced by the simulator and are absent in practical situations. By reducing the time-step for integration, these oscillations can be made arbitrarely small, at the cost of simulation time.*